

**PALLADIUM COMPLEXES OF DIPHOSPHAZANE
AND
RELATED LIGANDS**

by

**ANU PRAVA SHARMA B.Sc, (CHITTAGONG)
BANGLADESH**

**A thesis submitted in partial fulfilment of the requirements for the degree of
Master of Science in the Faculty of Science and Agriculture, University of
Natal,
Pietermaritzburg**

School of Chemical and Physical Sciences
University of Natal
Pietermaritzburg
January 2001

DECLARATION

I hereby certify that this research is the result of my own investigation which has not already been accepted for any other degree and is not being submitted in candidature for any other degree.

Signed.....

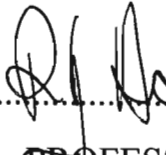
A. P. SHARMA

I hereby certify that this statement is correct.

Signed.....

PROFESSOR J. S. FIELD

(SUPERVISOR)

Signed.....

PROFESSOR R. J. HAINES

(CO-SUPERVISOR)

School of Chemical and Physical Sciences
University of Natal
Pietermaritzburg
January 2001

to my dearest mum and dad.....

CONTENTS

Acknowledgements.....	i
Abbreviations.....	ii
Abstract.....	iv

CHAPTER 1

BIS(DIPHOSPHINO)AMINE LIGAND DERIVATIVES OF THE GROUP 10 METALS.....1

1.1 Complexes of Nickel.....	2
1.1.1 Monodentate Mode(I).....	2
1.1.2 Chelating Mode(II).....	2
1.1.3 Bridging Mode(II).....	4
1.2 Complexes of Palladium.....	5
1.2.1 Chelating Mode(II).....	6
1.2.2 Bridging Mode(III).....	10
1.3 Complexes of Platinum.....	17
1.3.1 Monodentate Mode(I).....	17
1.3.2 Chelating Mode(II).....	18
1.3.3 Bridging Mode(III).....	28
1.4 Conclusion.....	29
1.4.1 ^{31}P NMR Chemical Shifts.....	29
1.4.2 Structural parameters.....	33
1.5 Aims of this work.....	36

Chapter 2

BIS(DIPHENYLPHOSPHINO)ETHYLAMINE (DPPEA) LIGAND DERIVATIVES OF PALLADIUM(II) AND PALLADIUM(0).....38

2.1 Introduction.....	38
-----------------------	----

2.2 Results and discussion.....	40
2.2.1 Synthesis of bis(diphenylphosphino)ethylamine	40
2.2.2 Reaction of dppea ligand with $[PdCl_2(PhCN)_2]$	40
2.2.3 Reaction of dppea ligand with $[PdCl_2(PhCN)_2$ and $[Pd_2(dbu)_3]$	44
2.2.4 Addition of I_2 to $[Pd_2Cl_2\{\mu\text{-}Ph_2PN(Et)PPh_2\}_2]$ 2	48
2.2.5 Reaction of dppea ligand with $[Pd_2(dbu)_3]$	55
2.4 Experimental.....	64
2.4.1 Synthesis.....	64
2.4.1.1 $Ph_2PN(Et)PPh_2$	64
2.4.1.2 $[PdCl_2\{\eta^2\text{-}Ph_2PN(Et)PPh_2\}]$ 1	65
2.4.1.3 $[Pd_2Cl_2\{\mu\text{-}Ph_2PN(Et)PPh_2\}_2]$ 2	65
2.4.1.4 $[PdI_2\{\eta^2\text{-}Ph_2N(Et)PPh_2\}]$ 3	65
2.4.1.5 $[Pd_2\{\mu\text{-}Ph_2PN(Et)PPh_2\}_3]$ 5 and $Ph_2P(O)N(Et)P(O)Ph_2$. dba. H_2O	66
2.4.2 Crystal Structure Determination.....	70

Chapter 3

PALLADIUM(II) AND DIPALLADIUM(I) COMPLEXES OF THE PHENYLBIS(2-PYRIDYL)PHOSPHINE LIGAND.....105

3.1 Introduction.....	105
3.2 Results and discussion.....	106
3.2.1 Synthesis of phenylbis(2-pyridyl)phosphine.....	106
3.2.2 Reaction of $PhP(py)_2$ with $[PdCl_2(PhCN)_2]$	107
3.2.3 Reaction of <i>cis</i> - $[PdCl_2\{\eta^1\text{-}PhP(py)_2\}_2]$ 6 with $Pd_2(dbu)_3$	111
3.3 Conclusion.....	113
3.4 Experimental.....	114
3.4.1 Synthesis.....	114
3.4.1.1 $PhP(py)_2$	114

3.4.1.2 <i>cis</i> -[PdCl ₂ {η ¹ -PhP(py) ₂ } ₂] 6	114
3.4.1.3 [Pd ₂ Cl ₂ {μ-PhP(py) ₂ } ₂] 7	115
3.4.2 Crystal Structure Determination.....	118
 Chapter 4	
2,5-BIS(DIPHENYLPHOSPHINO)THIOPHENE AS A BRIDGING LIGAND IN PLANAR COMPLEXES OF PALLADIUM(II).....	136
4.1 Introduction.....	136
4.2 Results and Discussion.....	139
4.2.1 Synthesis of 2,5-bis(diphenylphosphino)thiophene.....	139
4.2.2 Reaction of Ph ₂ P(C ₄ H ₂ S)PPh ₂ with [PdCl ₂ (PhCN) ₂].....	140
4.2.3 Reaction of [Pd ₂ Cl ₄ {μ-Ph ₂ P(C ₄ H ₂ S)PPh ₂ } ₂] 8 with AgPF ₆	141
4.3 Experimental.....	143
4.3.1 Synthesis.....	143
4.3.1.1 Ph ₂ P(C ₄ H ₂ S).....	144
4.3.1.2 Ph ₂ P(C ₄ H ₂ S)PPh ₂	144
4.3.1.3 [Pd ₂ Cl ₄ {μ-Ph ₂ P(C ₄ H ₂ S)PPh ₂ } ₂] 8	145
4.3.1.4 [Pd ₂ Cl ₃ {μ-Ph ₂ P(C ₄ H ₂ S)PPh ₂ } ₂ (MeCN)](PF ₆) ₂ 9	145
 APPENDIX A.....	148
General Experimental Details.....	148
A.1. INSTRUMENTATION.....	148
A.2. EXPERIMENTAL TECHNIQUES.....	148
A.3. Crystal Structure Determinations.....	149
 APPENDIX B.....	151
SOURCES OF CHEMICALS.....	151
 REFERENCES.....	152

ACKNOWLEDGEMENTS

I wish to thank of Professors J. S. Field and R. J. Haines for their expert guidance and input through the course of this investigation and for allowing me the opportunity on this course of study.

I am also grateful to the persons:

Dr O Q Munro for his patient contribution to the X-ray crystal structure determinations especially with regard to data collection and computation. His unselfish assistance at all times is greatly appreciated.

Mrs Niyum Rampersadh for her support, advice and encouragement through my initial work.

Mrs Elena Lakoba, Garth Cripps and Jan Gertenbach for their support.

Mr Martin Watson for his tireless recording of NMR spectra, the running of GCMS samples and for his assistance and training in the operation of these instruments.

Mr James Ryan for elemental analysis.

Mr Raj Somaru and Mr Shawn Ball for technical assistance.

Mr Paul Forder for the construction and repair of glassware.

The Faculty of Science Mechanical instrument workshop for the repair of mechanical instrumentation.

Dr J Perils for her advice and her support at proofreading in the final stage of this work.

A special thank you to my father for his continuous encouragement and financial support and my husband Goutam for encouraging me and also his financial support, standing by me throughout; your patience is appreciated.

ABBREVIATIONS

Å	angstrom
cod	1,5-cyclooctadiene
cm	centimetre
cm ⁻¹	reciprocal centimetre
dba	dibenzylideneacetone
dppaH	bis(diphenylphosphino)amine
dppa	bis(diphenylphosphino)amido
dppma	bis(diphenylphosphino)methylamine
dppm	bis(diphenylphosphino)methane
dppea	bis(diphenylphosphino)ethylamine
dppe	bis(diphenylphosphino)ethane
PSP	bis(diphenylphosphino)thiophene
δ	chemical shift in parts per million
v	frequency
g	gram
{ ¹ H}	proton noise decoupled
IR	infrared
L	ligand
λ	wavelength
M	molar
mg	milligram
mm	millimetre
ml	millilitre
mmol	millimole
mol	mole
nm	nanometre
NMR	nucleair magnetic resonance
Ph	phenyl

py	pyridine
(Ph ₂ P) ₂ py	2,6-bis(diphenylphosphino)pyridine
Ph ₂ Ppy	2-(diphenylphosphino)pyridine
PhP(py) ₂	phenylbis(2-pyridyl)phosphine
PhCN	benzonitrile
THF	tetrahydrofuran

ABSTRACT

The synthesis, characterisation and X-ray structure determinations of homonuclear nickel, palladium and platinum complexes with bis(phosphino)amine ligands is reviewed in Chapter 1. Particular attention is given to the mode of coordination that these ligands may adopt when coordinating to a transition metal *i.e.*, as a monodentate (η^1 -), chelating (η^2 -) or bridging (μ -) ligand. The Chapter is concluded with a brief summary of (i) The dependence of the ^{31}P chemical shift for the bonded phosphorus atom(s) on the mode of coordination and (ii) The dependence of key, ligand-based, structural parameters on the mode of coordination.

The synthesis and characterisation of the bis(diphenylphosphino)-ethylamine, $\text{Ph}_2\text{PN}(\text{Et})\text{PPh}_2$, ligand and its subsequent reactions with various palladium precursors is described in Chapter 2. Reaction with the Pd(II) precursor, $[\text{PdCl}_2(\text{PhCN})_2]$, afforded the mononuclear complex *cis*- $[\text{PdCl}_2\{\eta^2\text{-Ph}_2\text{PN}(\text{Et})\text{PPh}_2\}]$ **1**; when the same reaction was carried-out in the presence of the Pd(0) species $[\text{Pd}_2(\text{dba})_3]$ (dba = dibenzylideneacetone) the dinuclear ligand-bridged complex $[\text{Pd}_2\text{Cl}_2\{\mu\text{-Ph}_2\text{PN}(\text{Et})\text{PPh}_2\}_2]$ **2** was formed. Reaction of **2** with I_2 afforded **1**, as well as the mononuclear di-iodo species *cis*- $[\text{PdI}_2\{\eta^2\text{-Ph}_2\text{PN}(\text{Et})\text{PPh}_2\}]$ **3**, and the mixed-halogeno complex $[\text{PdClI}\{\eta^2\text{-Ph}_2\text{PN}(\text{Et})\text{PPh}_2\}]$ **4**. Direct reaction of the ligand with $[\text{Pd}_2(\text{dba})_3]$ afforded, in the first instance, $[\text{Pd}_2\{\mu\text{-Ph}_2\text{PN}(\text{Et})\text{PPh}_2\}_3]$ **5**, an extremely air-sensitive red compound, that readily reacted with oxygen in the solution to afford palladium metal and a yellow clathrate species that contained the oxidised ligand *i.e.*, $\text{Ph}_2\text{P(O)N(Et)P(O)PPh}_2 \cdot \text{dba} \cdot \text{H}_2\text{O}$. Apart from **4**, all compounds were characterised by means of elemental analysis, ^1H and $^{31}\text{P}\{^1\text{H}\}$ NMR spectroscopy and, in the case of **1**, **2**, **3** and $\text{Ph}_2\text{P(O)N(Et)P(O)PPh}_2 \cdot \text{dba} \cdot \text{H}_2\text{O}$, by means of single crystal X-ray structure determinations. The structures of the palladium complexes are, as expected, dominated by the requirement that the

coordination geometry at the Pd atom is square-planar. In the case of the dinuclear ligand-bridged complex **2**, this is achieved through formation of a Pd-Pd bond of length 2.600(1)Å. Of particular interest is the crystal structure of the clathrate, which has the oxidised ligand and dba molecules stacked in alternating lines approximately parallel to the [c]-axis of the unit cell.

The synthesis and characterisation of the bis(2-pyridyl)phenylphosphine, PhP(py)₂ ligand and its subsequent reaction with [PdCl₂(PhCN)₂] to afford the mononuclear complex *cis*-[PdCl₂{η¹-PhP(py)₂}₂] **6** is described in Chapter 3. The latter reacted with [Pd₂(dba)₃] to afford the dinuclear ligand-bridged species [Pd₂Cl₂{μ-PhP(py)₂}₂] **7**. The ¹H and ³¹P{¹H} NMR spectral data, as well the results of single crystal X-ray structure determinations are reported for **6** and **7**. The square-planar coordination at each palladium atom in **7** is achieved through the formation of a Pd-Pd bond of length 2.586(1)Å.

The synthesis and characterisation of the 2,5-(diphenylphosphino)thiophene, Ph₂P(C₄H₂S)PPh₂ ligand is described in Chapter 4. Reaction of the ligand with [PdCl₂(PhCN)₂] afforded the dinuclear ligand-bridged species [Pd₂Cl₄{μ-Ph₂P(C₄H₂S)PPh₂}₂] **8**. Characterisation of **8** was by means of elemental analysis, ¹H and ³¹P{¹H} NMR spectroscopy. Reaction of **8** with Ag⁺ in acetonitrile afforded a compound isolated as a yellow solid and formulated as [Pd₂Cl₃(MeCN){μ-Ph₂P(C₄H₂S)PPh₂}₂] **9**. Evidence for this formulation is based on the ³¹P{¹H} NMR spectrum which shows two closely-spaced singlets, consistent with two sets of phosphorus atoms in different chemical environments, and too far separated (by 4 bonds) for magnetic coupling. Unfortunately, single crystals of these thiienylphosphine ligand-bridged compounds could not be grown.

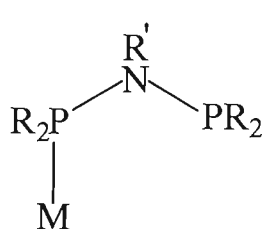
CHAPTER 1

BIS(PHOSPHINO)AMINE LIGAND DERIVATIVES OF THE GROUP 10 METALS

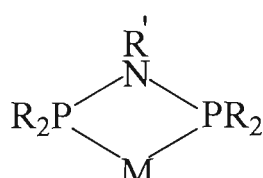
The focus of the work presented in this thesis is the synthesis, characterisation and where possible, the structure determination of palladium complexes of the bis(diphenylphosphino)ethylamine (dppea) ligand. Of particular interest is whether the dppea ligand chelates at one palladium atom in a mononuclear complex or whether it serves as a bridge between two palladium atoms in a dinuclear species. In order to provide background to this work, the literature on bis(phosphino)amine and bis(phosphino)amido ligand complexes of the Group 10 metals nickel, palladium and platinum is reviewed here that have been reported in the literature up to and including 1999.

It is noted that only homonuclear complexes of these metals are considered.

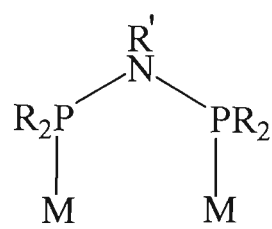
Emphasis is placed on the coordination mode of the ligand *i.e.*, whether it acts as a monodentate ligand (Mode I), chelating ligand (Mode II) or bridging ligand (Mode III).



(I)
(monodentate)



(II)
(chelating)



(III)
(bridging)

1.1 Complexes Of Nickel

In this section bis(phosphino)amine ligand complexes of nickel are reviewed according to the coordination mode of the ligand.

1.1.1 Monodentate Mode (I)

There is only one characterised complex that contains a bis(phosphino)amine ligand, in particular the bis(diphenylphosphino)methylamine (dppma) ligand, with one of the phosphorus atoms coordinated to a Ni atom in a monodentate fashion. This is the neutral complex $[\text{Ni}(\text{C}_5\text{H}_5)(\eta^1\text{-dppma})(\text{CN})]^{(1)}$ obtained through the following series of reactions.



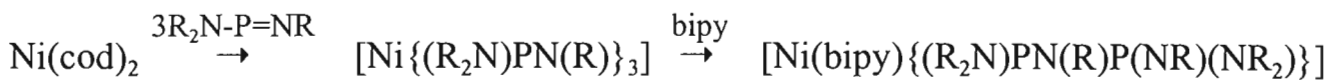
The monodentate coordination mode of the ligand in the latter complex was confirmed by means of $^{31}\text{P}\{\text{H}\}$ NMR spectroscopic analysis. The $^{31}\text{P}\{\text{H}\}$ NMR spectrum shows two singlets at δ 69.0 and δ 82.7 corresponding to the coordinated and uncoordinated phosphorus atoms respectively. The structure of the complex has not been verified X-ray crystallographically.

1.1.2 Chelating Mode(II)

There are three nickel complexes containing a bis(phosphino)amine ligand bonded in the chelating mode.

The $[\text{Ni}(\text{bipy})\{(R_2N)PN(R)P(NR)(NR_2)\}]^{(2)}$ ($R=\text{SiMe}_3$, bipy=2,2'-bipyridine) complex is the only structurally characterised example and is illustrated in **Fig. 1.1**. The

compound is obtained as a consequence of the coupling of two amino(imino)-phosphanes bonded to nickel, as illustrated in the following reaction sequence.



The P(1)-Ni(1)-P(2) and N(5)-Ni(1)-N(6) bond angles of 81.2(2) and 73.8(2) $^\circ$ respectively, are considerably lower than the idealised value of 90 $^\circ$ for a regular square-planar geometry at the Ni atom. Interestingly, there is a barely significant difference between the Ni-P(1) distance of 2.160(1) \AA and the Ni(1)-P(2) distance of 2.201(1) \AA , despite the two phosphorus atoms being in two different formal oxidation states of +5 and +3 respectively.

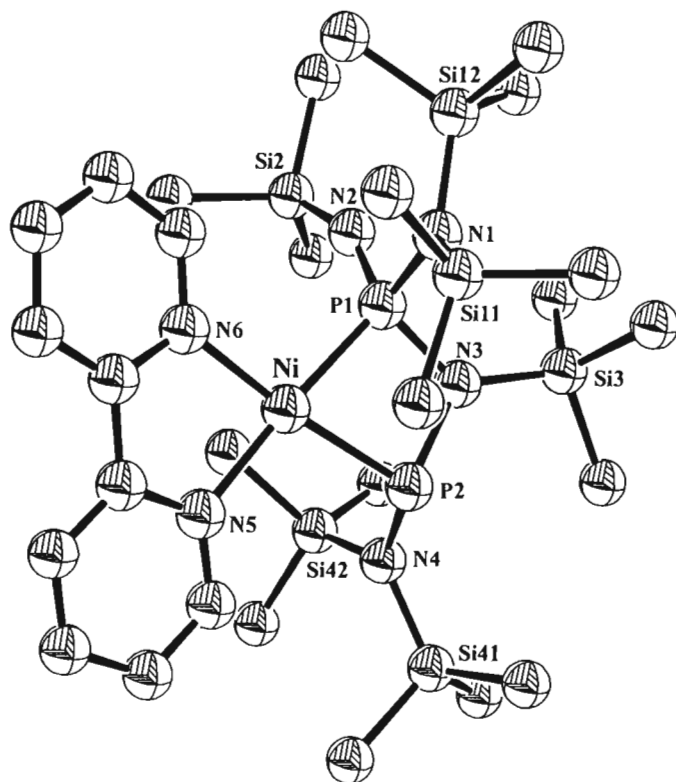


Fig. 1.1 : Structure of $[\text{Ni}(\text{bipy})\{(\text{R}_2\text{N})\text{PN}(\text{R})\text{P}(\text{NR})(\text{NR}_2)\}]$ ($\text{R}=\text{SiMe}_3$) (Redrawn from ref. 2.)

Reaction of lithiated bis(diphenylphosphino)amine, $[(C_6H_5)_2P]_2N^-Li^+$ with $NiCl_2/(CH_3)_3P$ afforded the chloro-bridged dinuclear complex bis[P,N,P-bis(diphenylphosphino)amido]- μ,μ -dichloronickel(II)⁽³⁾. This complex contains the anionic bis(diphenylphosphino)amido (dppa) ligand bonded to the nickel atom in the chelating mode, as confirmed by means of $^{31}P\{^1H\}$ NMR spectroscopy. No X-ray crystal structure of the compound was reported.

The $[NiBr(\eta^2\text{-dppa})(PEt_3)]^{(4)}$ complex also contains the dppa ligand coordinated to a nickel atom in a chelating fashion. This Ni(II) complex was obtained by reacting $[Ni(PEt_3)_2Br_2]$ with the lithium reagent $[(C_6H_5)_2P]_2N^-Li^+$ (prepared *in situ* by reaction of the amine with $LiBu^n$ at low temperature), in the presence of free phosphine PEt_3 , in order to prevent the formation of $[\{Ni(\mu\text{-Cl})(Ph_2PNPPh_2)_2\}]$, the dinuclear complex mentioned above. This complex also has been characterised by IR, 1H and ^{31}P NMR spectroscopy.

The cycloheptatriene ligand in the $[Ni(C_5H_5)(C_7H_8)]BF_4$ complex is easily replaced by the bis(diphenylphosphino)methylamine (dppma) ligand in the presence of CH_3CN to give $[Ni(C_5H_5)\{\eta^2\text{-Ph}_2PN(CH_3)PPh_2\}][BF_4]^{(1)}$. The ^{31}P NMR spectrum shows a singlet at δ 65.9. This complex was also characterised by IR, and 1H NMR spectroscopy.

1.1.3 Bridging Mode(III)

There is only one example of a nickel complex containing a bis(phosphino)amine ligand coordinated in the bridging mode that has had its structure confirmed X-ray crystallographically. This is the dinuclear Ni(0) complex $[Ni_2(\mu\text{-SO}_2)(CO)_2(\mu\text{-dppaH})_2]^{(5)}$ depicted in Fig. 1.2. The complex was prepared by the reaction of

$\text{Ni}(\text{CO})_4$ with bis(diphenylphosphino)amine (dppaH) followed by addition of SO_2 . This bimetallic $\text{Ni}(0)$ complex has a terminal CO ligand on each Ni atom, a bridging SO_2 ligand and two bridging dppaH ligands. The $\text{Ni}-\text{Ni}'$ distance is $2.633(3)\text{\AA}$. The bound SO_2 ligand in the $\text{Ni}(0)$ complex shows an increase in the $\text{S}-\text{O}$ bond length and a decrease in the $\text{O}-\text{S}-\text{O}$ angle compared to the free molecule⁽⁶⁾.

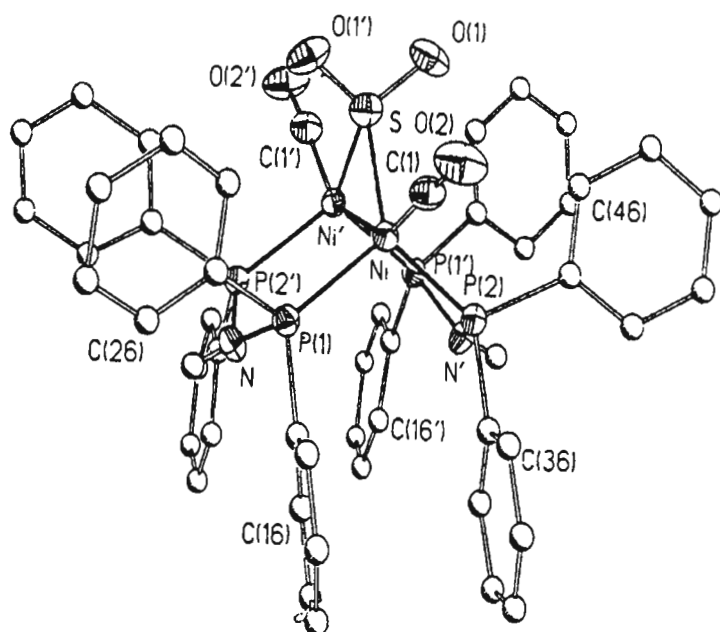


Fig. 1.2 : Structure of $[\text{Ni}_2(\mu-\text{SO}_2)(\text{CO})_2\{\mu\text{-Ph}_2\text{PN(H)PPh}_2\}_2]$

1.2 Complexes of Palladium

Bis(diphosphino)amine ligand complexes of palladium exhibit only two modes of coordination for the ligand: chelating and bridging. It is worth noting that much of the interest in the synthesis and structural characterisation of bis(diphosphino)-amine complexes of palladium(II), is their potential application as homogeneous catalysts for the oligomerisation and polymerisation of olefins.

1.2.1 Chelating Mode(II)

An example of a structurally characterised complex containing the anionic bis(diphenylphosphino)amido ligand [synthesised from $\text{Ph}_2\text{PNHPPPh}_2$ (dppaH)], coordinating in the chelating mode is $[\text{Pd}\{\eta^2\text{-Ph}_2\text{PNPPh}_2\}(\text{PEt})_3]$ ⁽⁴⁾ Fig. 1.3. The compound shows a distorted square-planar coordination at Pd: the angles Cl-Pd-P(3) and P(1)-Pd-P(2) are $90.8(1)$ and $65.2(1)^\circ$ respectively. The Pd-P(1) [$2.244(1)\text{\AA}$] bond is shorter than Pd-P(2) [$2.284(1)\text{\AA}$], consistent with the lower *trans*-influence of the chloro ligand as compared to a phosphine ligand. The distances P(1)-N and P(2)-N [$1.653(4)$ and $1.644(4)\text{\AA}$] are shorter than those found for complexes containing the chelated neutral diphosphazane $(\text{Ph}_2\text{P})_2\text{NH}$ typically *ca.* (1.74\AA)⁽⁷⁾. This is in accord with delocalisation of the negative charge of the anionic $(\text{Ph}_2\text{P})_2\text{N}^-$ ligand. A decrease is also observed in the bond angle P(1)-N-P(2) [$95.5(2)^\circ$] relative to that for the free ligand (122.8°)⁽³⁾, indicative of considerable strain in the four-membered metallocycle.

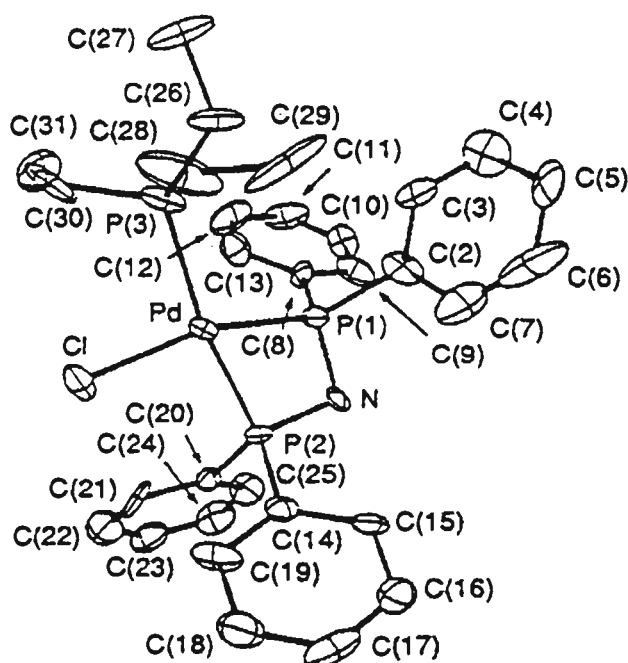


Fig. 1.3 : Structure of $[\text{Pd}\{\eta^2\text{-Ph}_2\text{PNPPh}_2\}\text{Cl}(\text{PEt})_3]$

The neutral bis(diphenylphosphino)methylamine (dppma) ligand also forms stable chelate complexes with palladium, despite the strain caused by the formation of a four-membered chelate ring. A structurally characterised example is $[\text{Pd}\{\eta^2\text{-Ph}_2\text{P}(\text{CH}_3)\text{PPh}_2\}\text{Cl}_2]$ ⁽⁸⁾ **Fig. 1.4**. This complex has two chloride ligands *trans* to the dppma ligand in a highly distorted, square-planar coordination geometry, as evidenced by a P(1)-N-P(2) angle of $100.4(2)^\circ$, which is significantly compressed from the value of $118.9(2)^\circ$ observed in the free dppma ligand⁽⁹⁾. The bond distances of $2.222(1)$ and $2.217(1)\text{\AA}$ for Pd-P(1) and Pd-P(2) respectively are, as expected, essentially the same.

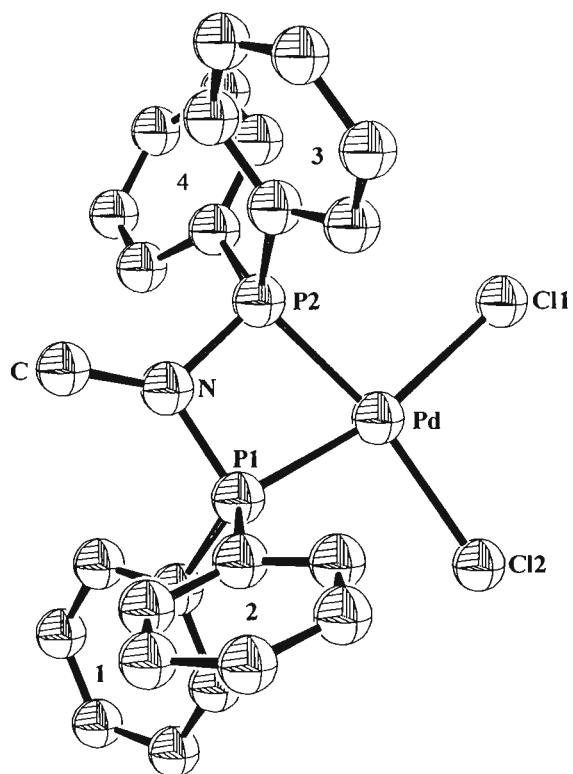


Fig. 1.4 : Structure of $[\text{Pd}\{\eta^2\text{-Ph}_2\text{PN}(\text{CH}_3)\text{PPh}_2\}\text{Cl}_2]$ (Redrawn from ref. 8.)

The reaction of $\text{Pd}_2(\text{dba})_3 \cdot \text{CHCl}_3$ with the diphosphazane ligand $\text{Ph}_2\text{PN}(\text{Pr}^i)\text{PPhY}'$ [$\text{Y}' = \text{OC}_6\text{H}_4\text{Me}-4$] in the presence of MeI yielded *cis*- $[\text{PdI}_2\{\eta^2\text{-Ph}_2\text{PN}(\text{Pr}^i)\text{PPhMe}\}]$ (**Fig. 1.5**), which contains the diphosphazane ligand coordinated in a chelating

fashion⁽¹⁰⁾. This palladium diiodo complex is structurally similar to that of other palladium(II) and platinum(II) diphosphazane complexes reported previously (see **Section 1.2.1 and 1.3.2**). The P(1)-N(1)-P(2) bond angle [100.1(3) $^{\circ}$] is considerably less than the idealised tetrahedral or trigonal angle, and indicates considerable strain in the four-membered PdP_2N ring. The related bond angle at the metal centre P(1)-Pd(1)-P(2), is 71.14(5) $^{\circ}$, which represents a considerable distortion from the 90 $^{\circ}$ expected for a square-planar configuration. The presence of a methyl instead of a phenyl group bonded to P(2) does not alter the adjacent P-N bond length, which is almost the same as the P(1)-N(1) distance of 1.694(5) \AA .

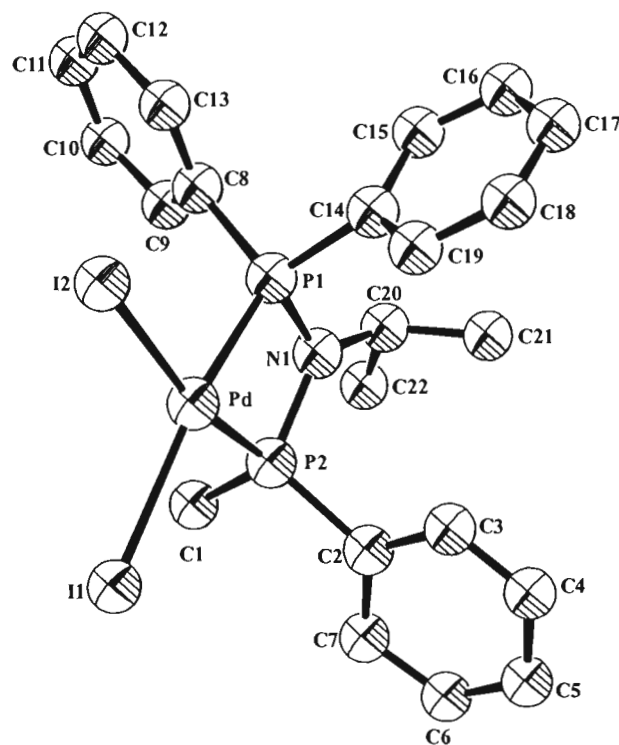


Fig. 1.5 : Structure of $[\text{PdI}_2\{\eta^2\text{-Ph}_2\text{PN}(\text{Pr})\text{PPhMe}\}]$ (Redrawn from ref. 10.)

Reaction of lithiated bis(diphenylphosphino)amine, $[(\text{C}_6\text{H}_5)_2\text{P}]^-\text{Li}^+$, with PdCl_2 in the presence of trimethylphosphine affords the homoleptic bis(diphenylphosphino)-amido complex $[\text{Pd}(\eta^2\text{-dppa})_2]$. Methylation of this species with $\text{CH}_3\text{OSO}_2\text{F}$ led

to the formation of the ionic compound $[\text{Pd}\{\eta^2\text{-Ph}_2\text{PN}(\text{CH}_3)\text{PPh}_2\}_2](\text{OSO}_2\text{F}^-)_2$ ⁽³⁾, the cation of which containing neutral chelating dppma ligands. This complex (**Fig. 1.6**) contains a planar $\text{CNP}_2\text{PdP}_2\text{NC}$ skeleton and is thus based on planar ligand arrays both at the Pd and at the two N atoms.

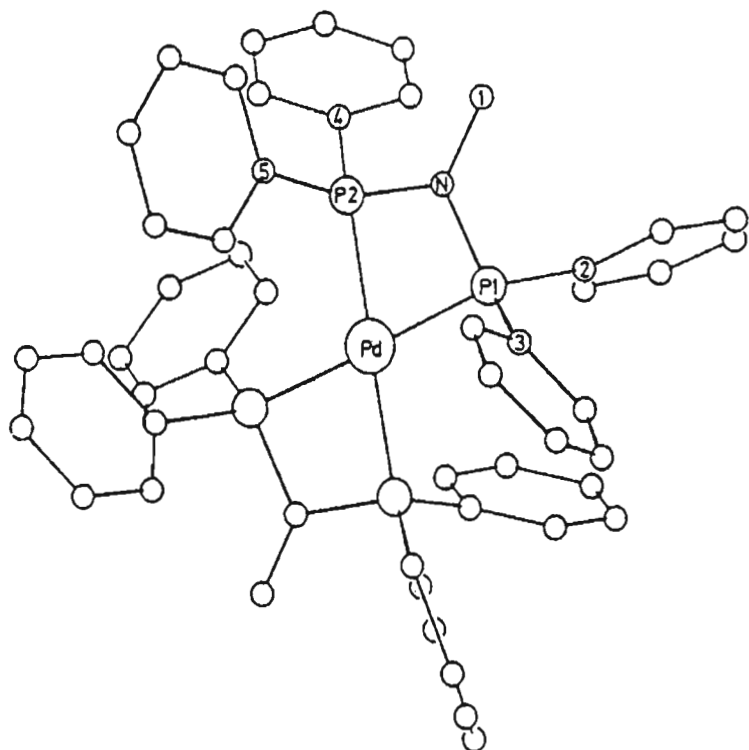


Fig. 1.6 : Structure of $[\text{Pd}\{\eta^2\text{-Ph}_2\text{PN}(\text{CH}_3)\text{PPh}_2\}_2]^{2+}$

The reaction of $[\text{PdCl}_2(\text{PhCN})_2]$ with $\text{Ph}_2\text{PN}(\text{S-}^*\text{CHMePh})\text{PPh}_2$ in dichloromethane afforded $[\text{PdCl}_2\{\eta^2\text{-(Ph}_2\text{P)}_2\text{N}(\text{S-}^*\text{CHMePh})\}]\text{CH}_2\text{Cl}_2$ ⁽¹¹⁾. As illustrated in **Fig. 1.7**, the diphosphazane ligand is coordinated in a chelating mode. The P(1)-N(1)-P(2) bond angle (98.2°) is considerably less than the idealised tetrahedral or trigonal value. The chelate bite angle [P(1)-Pd-P(2)= 71.5°] shows much distortion from the value

expected (90°) for a square-planar configuration. Indeed, this bite angle is much smaller than that observed in the case of $[\text{PdCl}_2\{\eta^2\text{-(R)-BINAP}\}]^{(12)}$ (92.7°) where a seven membered chelate ring is present.

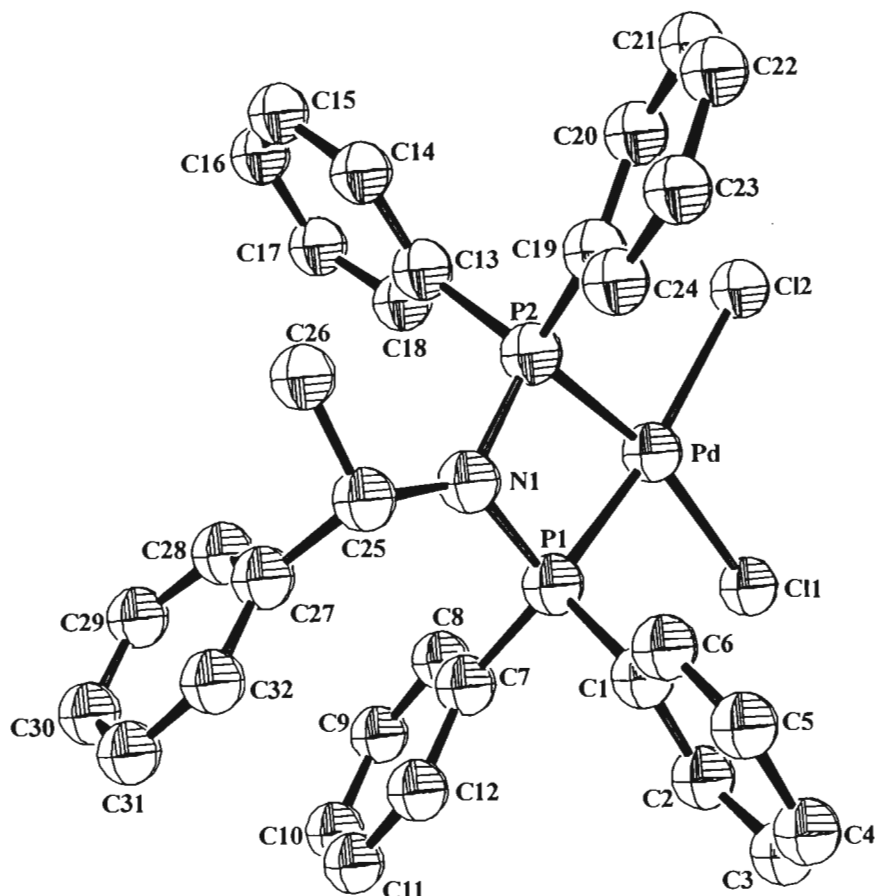


Fig. 1.7 : Structure of $[\text{PdCl}_2\{\eta^2\text{-(Ph}_2\text{P)}_2\text{N}(\text{S-CHMePh})\}]$ (Redrawn from ref. 11.)

1.2.2 Bridging Mode(III)

A structurally characterised neutral species containing the bis(diphenylphosphino)-amine (dppaH) ligand in a bridging coordination mode is $[\text{Pd}_2\text{Cl}_2\{\mu\text{-dppaH}\}_2]^{(13)}$. This compound was prepared by treating $\text{PdCl}_2(\text{NCPh})_2$ with a half molar amount of $\text{Pd}_2(\text{dba})_3 \cdot \text{CHCl}_3$ and a twice molar amount of dppaH in CH_2Cl_2 . As can be seen in **Fig. 1.8**, the structure contains two palladium centres with a Pd-Pd bond

distance of $2.637(6)\text{\AA}$; two dppaH ligands bridge the metal-metal bond and there is one Cl ligand per palladium atom. The geometry around each palladium is almost square-planar with small tetrahedral distortions (*e.g.*, the dihedral angles between the planes $\text{Cl}(1)\text{Pd}(1)\text{P}(2)$, $\text{P}(1)\text{Pd}(1)\text{Pd}(2)$ and $\text{Cl}(2)\text{Pd}(2)\text{P}(3)$, $\text{P}(4)\text{Pd}(2)\text{Pd}(1)$ are $4.93(4)$ and $3.03(4)^\circ$ respectively. The $\text{P}(1)\text{-N}(1)\text{-P}(4)$ and $\text{P}(2)\text{-N}(2)\text{-P}(3)$ angles of 112.7° and 116.1° are close to 120° , consistent with approximate sp^2 -hybridisation at the amine N-atom.

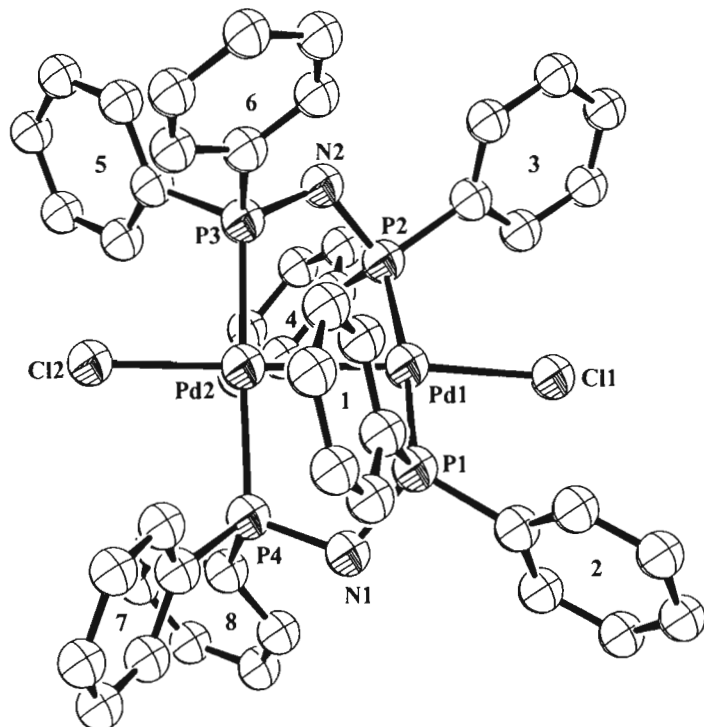


Fig. 1.8 : Structure of $[\text{Pd}_2\text{Cl}_2\{\mu\text{-Ph}_2\text{PN}(\text{H})\text{PPh}_2\}_2]$ (Redrawn from ref. 13.)

The dipalladium ligand-bridged species $[\text{Pd}_2(\mu\text{-dppaH})_2(\text{THF})(\text{PPh}_3)][\text{BF}_4]_2\cdot 4\text{THF}^{(14)}$ (**Fig. 1.9**) is a second example of a complex containing two bridging dppaH ligands. Distorted square-planar coordination geometries are observed about the Pd centres. The bridging dppaH ligands are clearly bent away from the terminal PPh_3 ligand, however, the planarity at the Pd centres is maintained. The planarity at the

Pd centres is evident in the sum of the four *cis*-angles, which is 362° . The Pd-Pd bond length is $2.6665(9)\text{\AA}$. The Pd(1) atom sits furthest at $0.112(1)\text{\AA}$, from the least squares plane defined by Pd(1) and the three P atoms bonded to it. The Pd(2) atom, which is bound to the THF O(1) atom shows much less distortion from a square-planar coordination geometry.

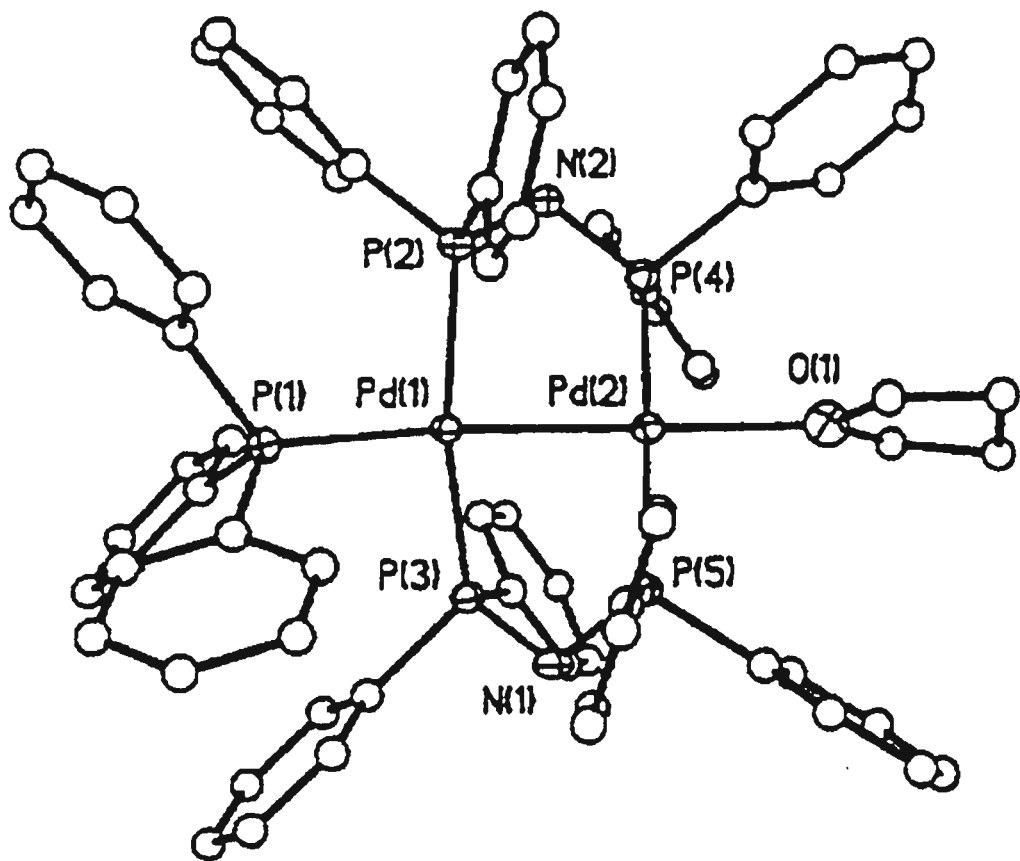


Fig. 1.9 : Structure of $[\text{Pd}_2\{\mu\text{-Ph}_2\text{PN}(\text{H})\text{PPh}_2\}_2(\text{THF})(\text{PPh}_3)]^{2+}$

The structure of the cation in the complex $[\text{Pd}_2(\mu\text{-dppaH})_2(\text{PPh}_3)_2][\text{BF}_4]_2 \cdot \text{THF} \cdot \text{H}_2\text{O}^{(14)}$ (**Fig. 1.10**) is similar to that of $[\text{Pd}_2(\mu\text{-dppaH})_2(\text{THF})(\text{PPh}_3)]^{2+}$ but there are differences. The Pd-Pd bond length [$2.812(2)\text{\AA}$] is considerably longer than that

of the THF derivative, and this lengthening may be another indication of the strain caused by the large PPh_3 ligands. The $\text{Pd-P}(\text{dppaH})$ distances are less at 2.294(4) and 2.309(4) \AA than those observed for the THF complex, which fall in the range 2.319(2) to 2.334(2) \AA . However, the geometry at each palladium atom remains essentially square-planar.

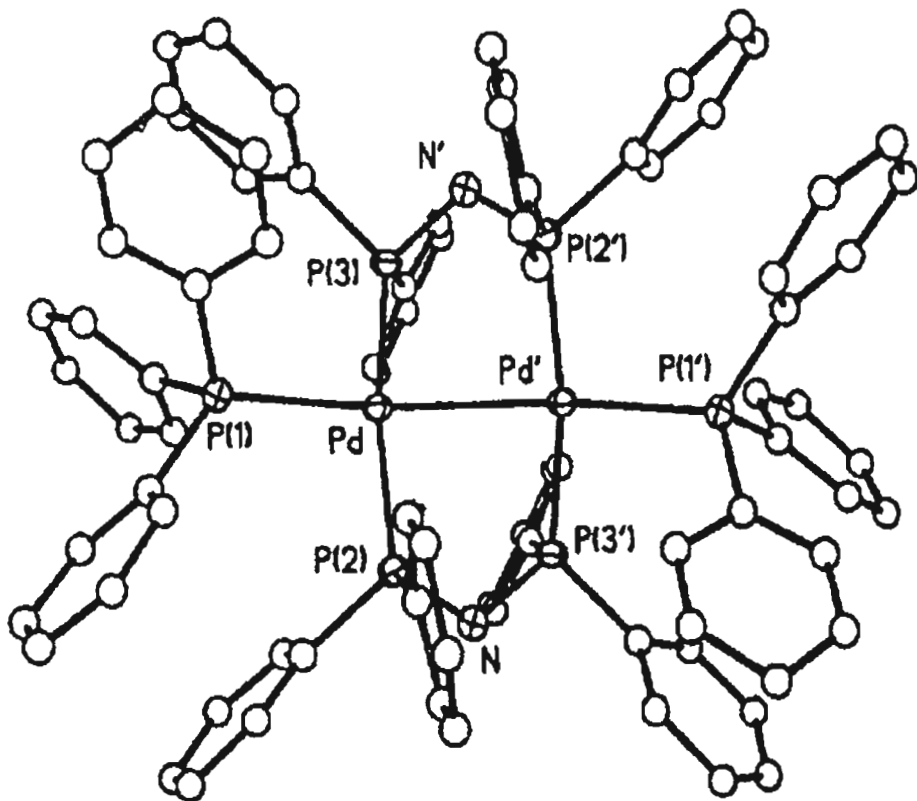


Fig. 1.10 : Structure of $[\text{Pd}_2\{\mu\text{-Ph}_2\text{PN}(\text{H})\text{PPh}_2\}_2(\text{PPh}_3)_2]^{2+}$

The reaction of $[\text{Pd}_2(\mu\text{-dppaH})_2(\text{CH}_3\text{CN})\text{Cl}]$ in 1:1 $\text{CH}_2\text{Cl}_2/\text{CH}_3\text{CN}$ with $[\text{NEt}_4]\text{Cl}$ produced a ligand-bridged complex characterised as $[\text{Pd}_2(\mu\text{-dppaH})_2\text{Cl}_2].3\text{CH}_3\text{CN}^{(14)}$ (**Fig. 1.11**). The $\text{Pd}(1)\text{-Pd}(2)$ bond distance is 2.635 \AA which is slightly shorter than that observed in $[\text{Pd}_2\{\mu\text{-Ph}_2\text{PN}(\text{H})\text{PPh}_2\}_2(\text{THF})(\text{PPh}_3)][\text{BF}_4].4\text{THF}$. However, the distance is comparable to values observed in other Pd(I) dinuclear complexes^(15,16,17).

The Pd(1)-P distances differ by 7σ while the Pd(2)-P distances are statistically equivalent. No chemical significance is attributed to this difference and the average value for the Pd-P bond lengths is 2.287(4)Å. The Pd-Cl distances are normal and their average is 2.398(3)Å. There is a considerable twist about the Pd-Pd bond as evidenced by a dihedral angle between the two distorted square-planar centres of 42.2(2)°.

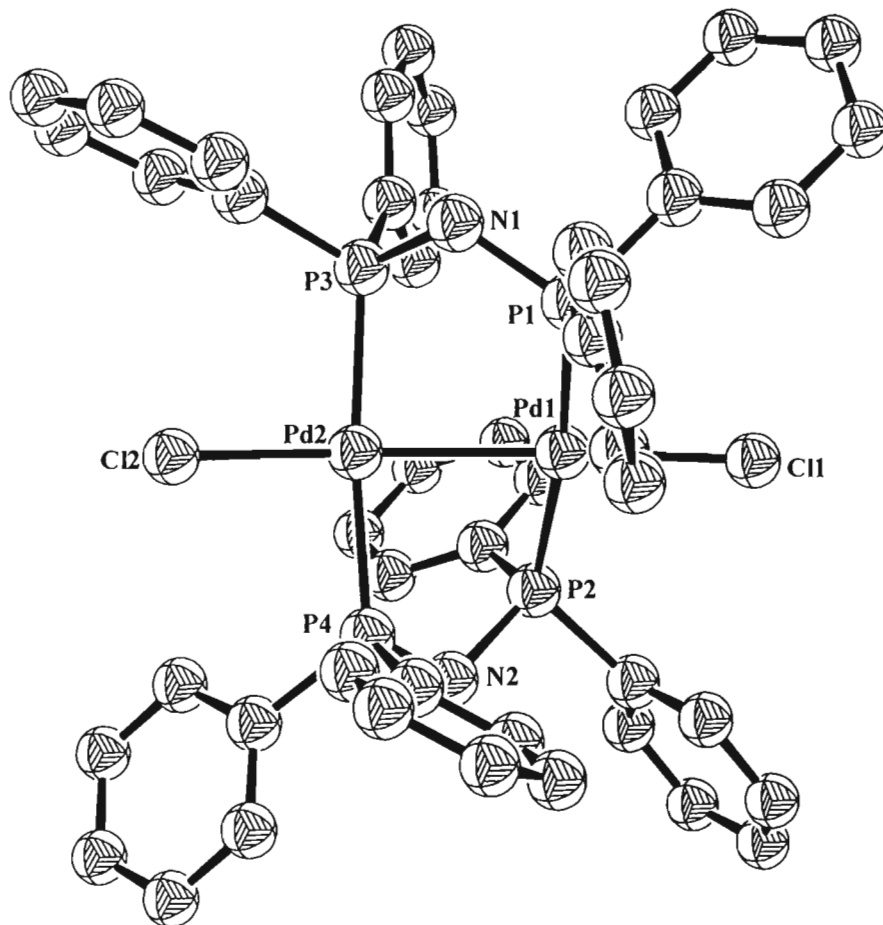


Fig. 1.11 : Structure of $[\text{Pd}_2\{\mu\text{-Ph}_2\text{PN}(\text{H})\text{PPh}_2\}_2\text{Cl}_2]$ (Redrawn from ref. 14.)

The reaction of $[\text{Pd}_2(\text{dba})_3]\cdot\text{CHCl}_3$ and $[\text{PdCl}_2(\text{PhCN})_2]$ in the presence of two equivalents of the ligand, $(\text{PhO})_2\text{PN}(\text{Ph})\text{P}(\text{OPh})_2$ gives the dinuclear palladium(I) complex $[\text{Pd}_2\text{Cl}_2\{\mu-(\text{PhO})_2\text{PN}(\text{Ph})\text{P}(\text{OPh})_2\}_2]^{(18)}$, **Fig. 1.12**. The geometry around each

palladium atom is square-planar and the nitrogen atom is co-planar with the atoms bonded to it. The Pd-Pd bond distance of 2.620(1)Å is shorter than those observed for analogous complexes with the metal in the same oxidation state (+1)⁽¹⁴⁾. There is also a corresponding decrease in the Pd-P distances to an averaged value of 2.259Å. The ³¹P chemical shift for this dipalladium(I) complex shows a singlet centred at δ 111.5, which is shifted upfield compared to its position in the spectrum of the free ligand (δ 127.7).

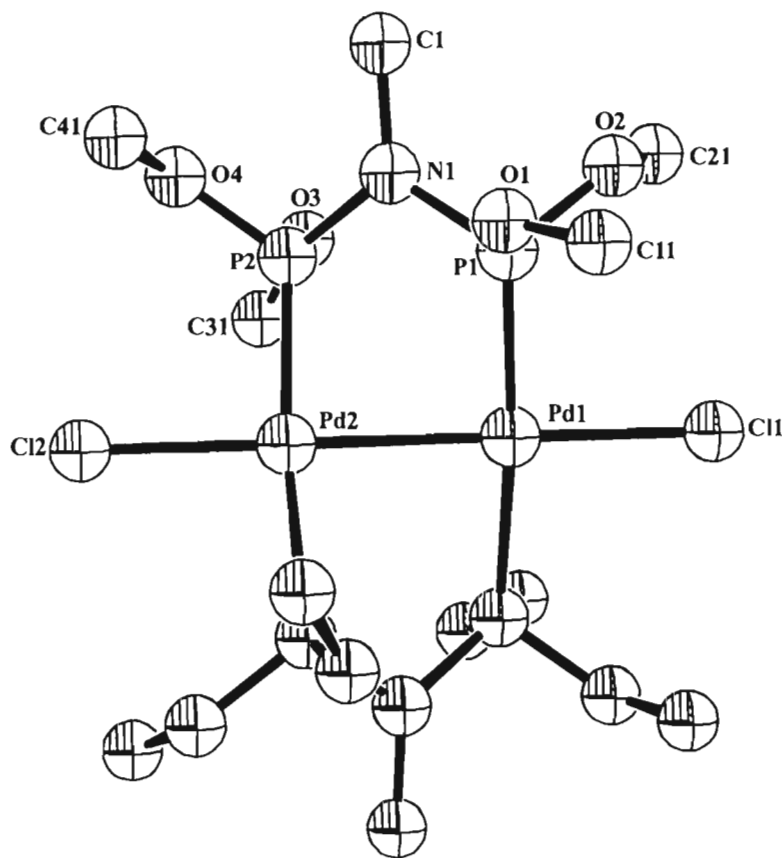


Fig. 1.12 : Structure of $[\text{Pd}_2\text{Cl}_2\{\mu\text{-(PhO)}_2\text{PN}(\text{Me})\text{P}(\text{OPh})_2\}_2]$ (Redrawn from ref. 18.)

In a related reaction, the Pd(0) derivative $\text{Pd}_2(\text{dba})_3 \cdot \text{CHCl}_3$, reacts with an excess of the diphosphazane ligand, $(\text{PhO})_2\text{PN}(\text{Me})\text{P}(\text{OPh})_2$ to give the dinuclear complex $[\text{Pd}_2\{\mu\text{-(PhO)}_2\text{PN}(\text{Me})\text{P}(\text{OPh})_2\}_3]^{(18)}$ (Fig. 1.13) containing three bridging

diphosphazane ligands. The coordination around each palladium atom is trigonal planar the displacement of the Pd atoms from their local P_3 planes being *ca.* 0.05 Å. The two P_3 planes are nearly parallel to one another (dihedral angle 2.0°) and the two PdP_3 moieties adopt an eclipsed configuration. The most interesting aspect of this structure is the short Pd-Pd separation of 2.855(2) Å. This value is significantly shorter than those observed for analogous complexes with the metal in the zero oxidation state⁽¹⁹⁾. There is also a decrease in Pd-P distance to an averaged value of 2.269 Å.

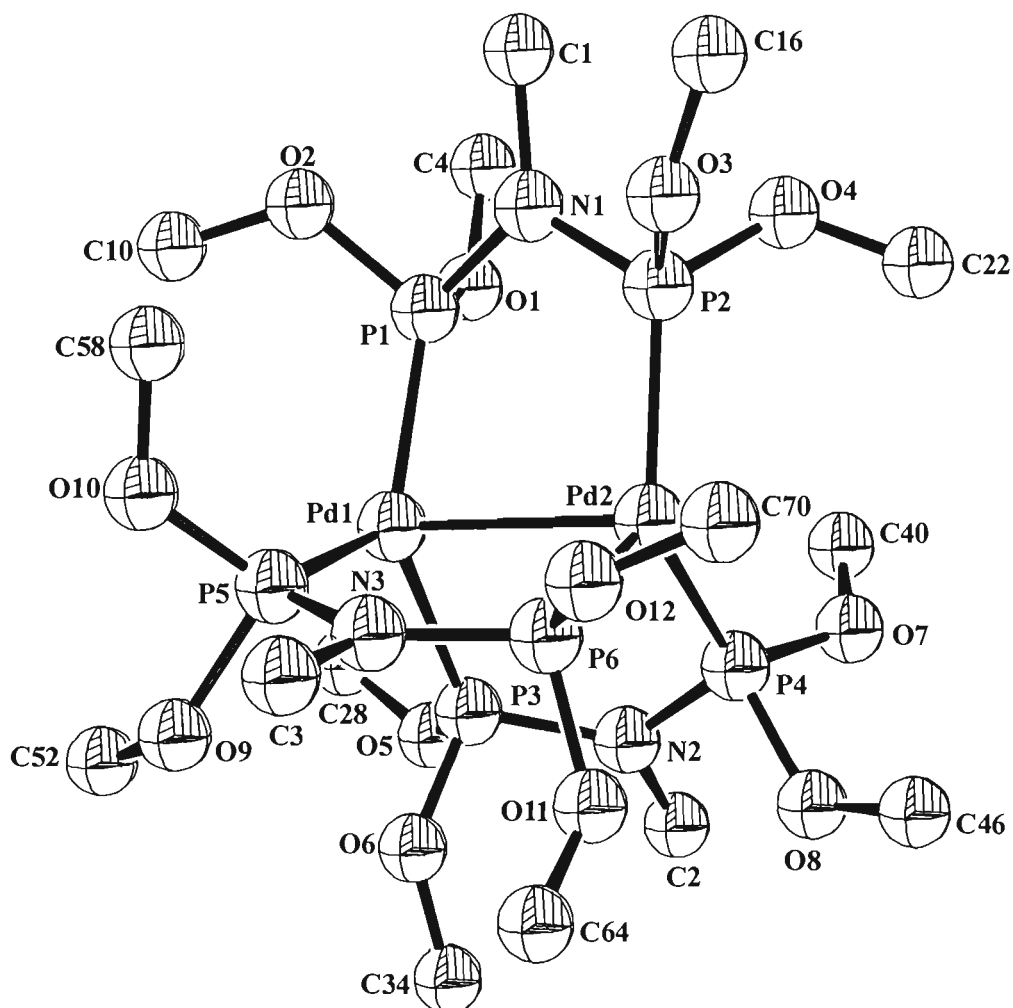


Fig. 1.13 : Structure of $[Pd_2\{\mu-(PhO)_2PN(Me)P(OPh)_2\}_3]$ (Redrawn from ref. 18.)

1.3 Complexes of Platinum

In practice it is found that bis(phosphino)amine ligands adopt all three different coordination modes namely monodentate, chelating and bridging, in their complexes of platinum.

1.3.1 Monodentate Mode(I)

The only example of a complex containing a bis(phosphino)amine ligand coordinated to platinum in a monodentate fashion is the neutral species, *trans*- $[\text{Pt}\{\eta^1\text{-Ph}_2\text{PN(H)PPh}_2\}_2(\text{CN})_2]$ ⁽²⁰⁾. The compound is obtained by the slow addition of 2 equivalents of NaCN to $[\text{Pt}(\text{dppaH})_2](\text{BF}_4)_2$, the product being isolated as a fine white solid. The $^{31}\text{P}\{\text{H}\}$ NMR spectrum exhibits two singlets at δ 43.6 and δ 27.3, the former resonance being assigned to the phosphorus bonded to the platinum and the latter to the uncoordinated phosphorus atom. The structure of the complex was confirmed X-ray crystallographically. As illustrated in **Fig. 1.14**, the two phosphorus ligands adopt positions *trans* to each other and the molecule possesses a crystallographically imposed centre of symmetry. The P(1)-Pt-C(1) bond angle of $91.0(2)^\circ$ is close to the idealised value of 90° and suggests that there is little steric crowding about the metal centre. On the other hand the angles between the substituents of the coordinated phosphorus atom are significantly greater than the corresponding angles within the uncoordinated diphenylphosphino group. This is expected given the greater steric crowding associated with the bonded phosphorus atom. Interestingly, the P(1)-N bond of $1.663(5)\text{\AA}$ is 0.063\AA shorter than the P(2)-N bond of $1.727(5)\text{\AA}$. The P(1)-N-P(2) angle of 125.2° is consistent with sp^2 -hybridisation at the nitrogen atom. This complex forms the platinum(I) dimer $[\text{Pt}_2\{\mu\text{-Ph}_2\text{PN(H)PPh}_2\}_2(\text{CN})_2]$ on addition of 1 equivalent of $[\text{Pt}(\text{cod})_2]$ (**see Section 1.3.3**).

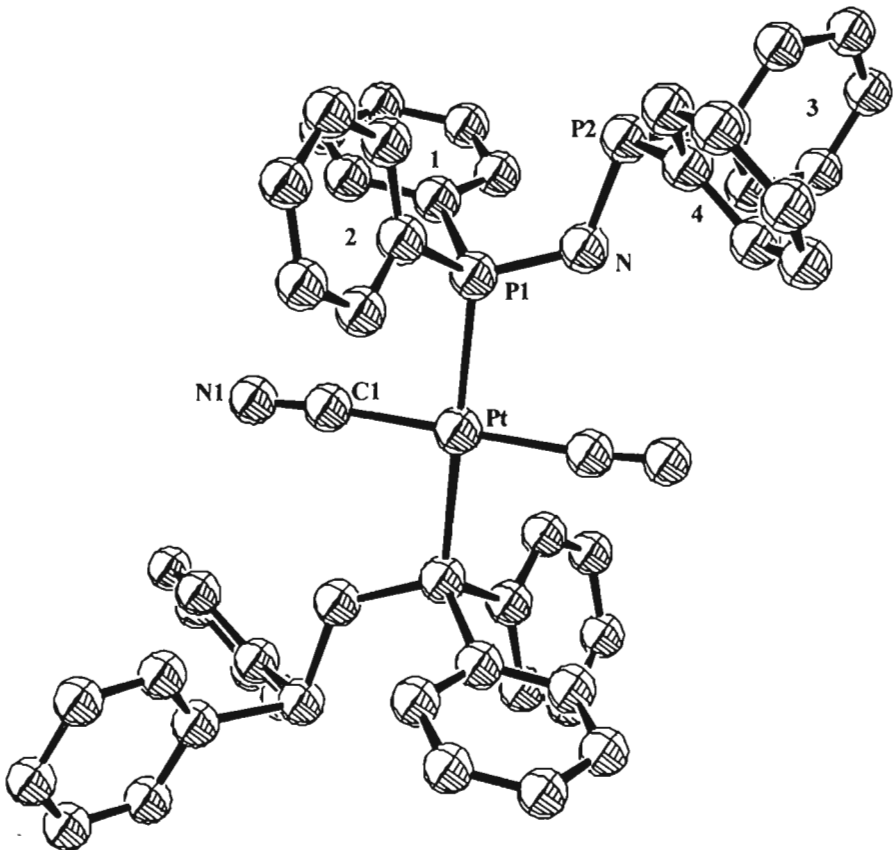


Fig. 1.14 : Structure of $\text{trans-}[\text{Pt}\{\eta^1\text{-Ph}_2\text{PN(H)PPh}_2\}_2(\text{CN})_2]$ (Redrawn from ref. 20.)

1.3.2 Chelating Mode(II)

Complexes of platinum containing a bis(phosphino)amine ligand bonded in the chelating mode are well characterised.

A well-documented example that contains only the dppaH ligand is $[\text{Pt}\{\eta^2\text{-Ph}_2\text{PN(H)PPh}_2\}_2][\text{BF}_4]_2^{(20)}$. The ${}^{31}\text{P}\{{}^1\text{H}\}$ NMR spectrum of this compound shows that the phosphorus nuclei are equivalent in solution. The structure of the cation, determined X-ray crystallographically, and which possesses a crystallographically imposed centre of symmetry is shown in **Fig. 1.15**. The square-planar geometry

expected at Pt(II) is significantly distorted because of the formation of the four-membered chelate rings, with a P(1)-Pt-P(2) bond angle of $69.90(7)^\circ$. However, in all other respects, the interatomic distances and angles are normal.

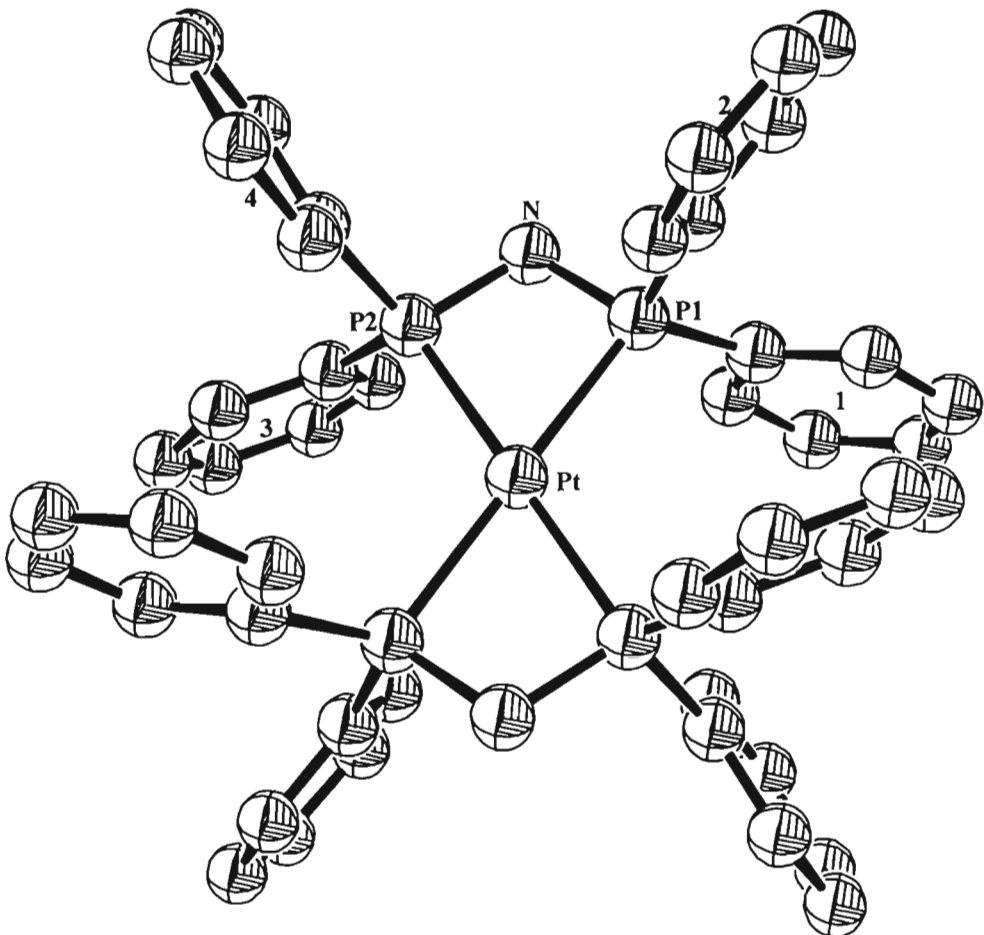


Fig. 1.15 : Structure of $[\text{Pt}\{\eta^2\text{-Ph}_2\text{PN(H)PPh}_2\}_2]^{2+}$ (Redrawn from ref. 20.)

Another closely-related and homoleptic complex is $[\text{Pt}\{\eta^2\text{-Ph}_2\text{PN(CH}_3\text{)PPh}_2\}_2][\text{BF}_4]_2^{(20)}$, the structure of the cation being illustrated in **Fig. 1.16**. The only difference with the former complex is the replacement of -NH group with a -NCH₃ group in the chelating bis(phosphino)amine ligand. This does not lead to any significant changes in the geometrical parameters for the complex, the same distortion from ideal square-planar geometry being seen *e.g.*, P(1)-Pt-P(2) = $69.76(7)^\circ$. As expected the

$^{31}\text{P}\{\text{H}\}$ NMR spectrum shows a singlet in this case at δ 39.6.

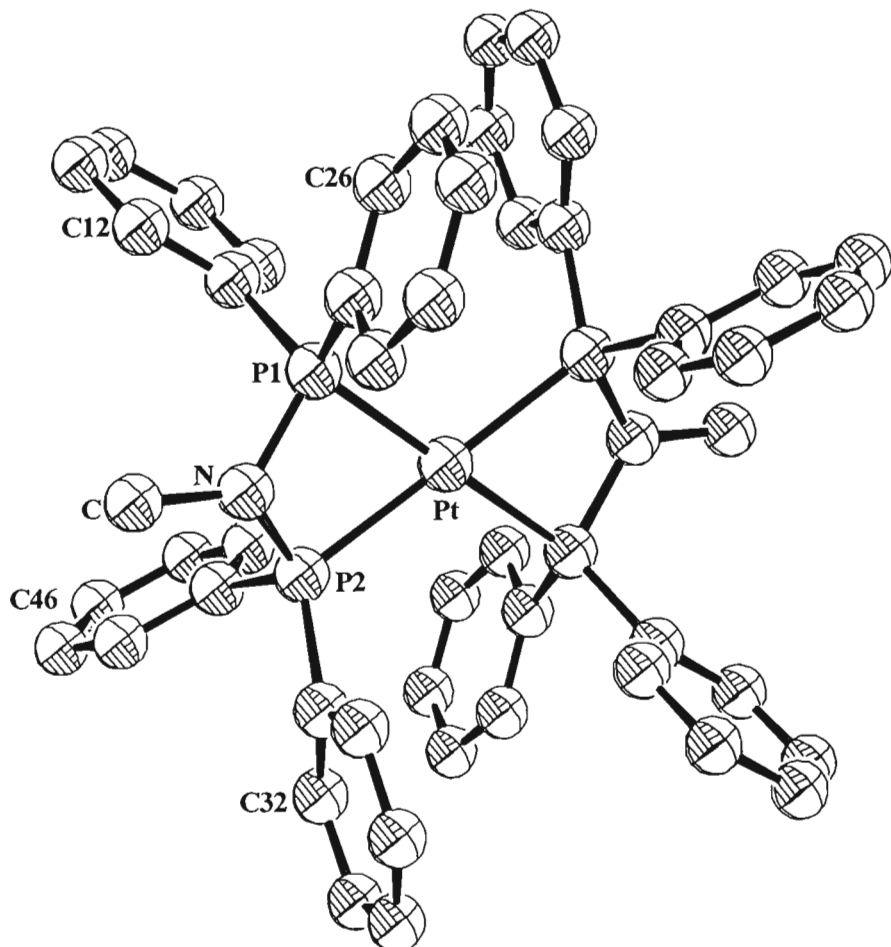


Fig. 1.16 : Structure of $[\text{Pt}\{\eta^2\text{-Ph}_2\text{PN}(\text{CH}_3)\text{PPh}_2\}_2]^{2+}$ (Redrawn from ref. 20.)

Reaction of the bis(diphenylphosphino)amine (dppaH) ligand with *cis*- $[\text{PtCl}_2(\text{PMe}_2\text{Ph})_2]$ produces the complex $[\text{PtCl}(\text{PMe}_2\text{Ph})\{\eta^2\text{-Ph}_2\text{PN}(\text{H})\text{PPh}_2\}]\text{Cl}^{(21)}$. The structure of the cation, determined X-ray crystallographically, is shown in **Fig. 1.17**. The central platinum atom adopts a distorted square-planar geometry defined by the bidentate dppaH ligand, the phosphine ligand and a chloro-group. The five atoms Pt, P(1), P(2), P(3) and Cl are essentially coplanar, with the maximum deviation of the position any one of these atoms from the plane being 0.065 Å (for Pt). The nitrogen atom lies 0.13 Å from this plane, the deviation being due to

folding along the P(1) . . . P(2) axis; the fold angle is 5°. The $^{31}\text{P}\{\text{H}\}$ NMR spectrum shows a first-order pattern consisting of three doublets of doublets, with satellites from coupling to ^{195}Pt .

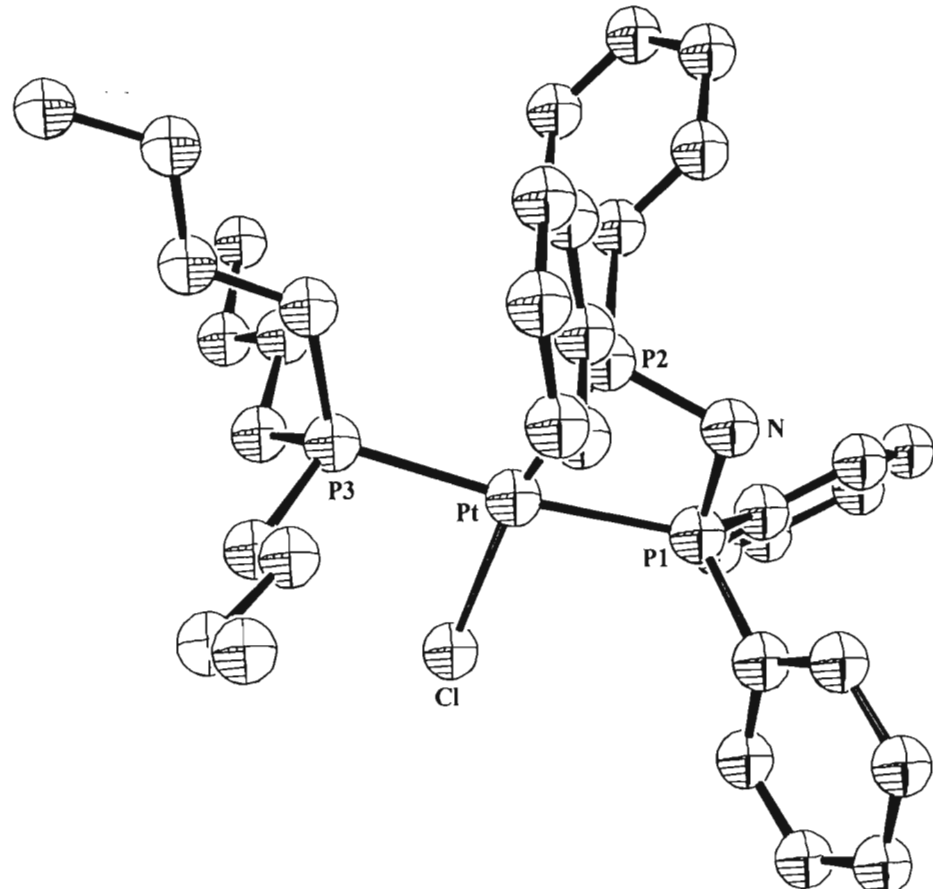


Fig. 1.17: Structure of $[\text{PtCl}\{\eta^2\text{-Ph}_2\text{PN}(\text{H})\text{PPh}_2\}(\text{PMe}_2\text{Ph})]^+$ (Redrawn from ref. 21.)

Reaction of dppaH with $[\text{PtCl}_2(\text{PBu}^n_3)_2]$ results in the displacement of a chloro-group and one monodentate phosphine ligand to give the ionic compound, $[\text{PtCl}\{\eta^2\text{-Ph}_2\text{PN}(\text{H})\text{PPh}_2\}(\text{PBu}^n_3)]\text{Cl}^{(21)}$. The crystal structure of this complex has been determined, a perspective view of the cation being illustrated in **Fig. 1.18**. As expected, the coordination geometry at the platinum atom is very similar to that observed for $[\text{PtCl}\{\eta^2\text{-Ph}_2\text{PN}(\text{H})\text{PPh}_2\}(\text{PMe}_2\text{Ph})]\text{Cl}$. The deviations of the positions platinum and nitrogen atoms from the mean plane through Pt, P(1), P(2), P(3) and

Cl are now 0.04 and 0.23 Å respectively.

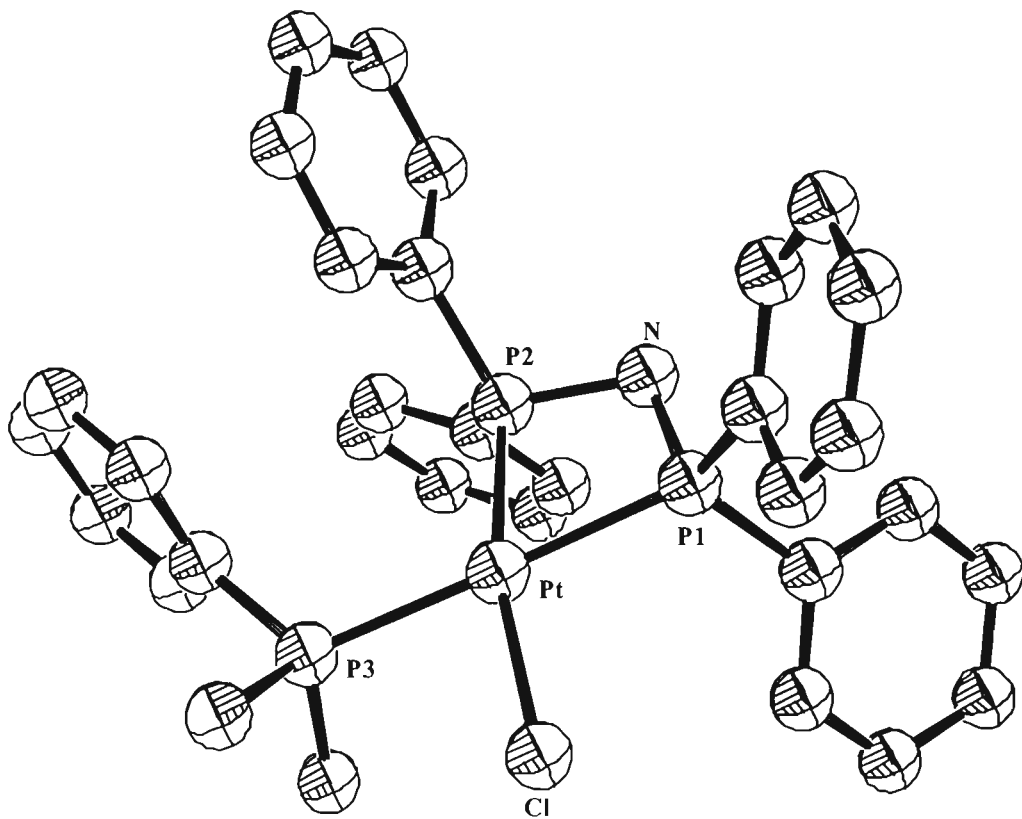


Fig. 1.18 : Structure of $[\text{PtCl}\{\eta^2\text{-Ph}_2\text{PN}(\text{H})\text{PPh}_2\}(\text{PBu}^n_3)]$ (Redrawn from ref. 21.)

The reaction of $[\text{PtCl}_2(\text{dppe})]$ with the bis(diphenylphosphino)amine (dppaH) ligand proceeds to give $[\text{Pt}\{\eta^2\text{-Ph}_2\text{PN}(\text{H})\text{PPh}_2\}(\text{dppe})]\text{Cl}_2^{(21)}$ (Fig. 1.19), an interesting complex that contains both a chelating bis(diphenylphosphino)amine and bis(diphenylphosphino)ethane (dppe) ligand. In view of the presence of the two different ligands the ${}^{31}\text{P}\{{}^1\text{H}\}$ NMR spectrum is of the AA'XX' type, where A,A' represent the dppaH phosphorus nuclei and X,X' the dppe phosphorus nuclei. The coordination plane of this compound is noticeably distorted with P(3) lying 0.46 Å from the Pt-P(1)-P(2)-P(4) plane. (These atoms are coplanar to within 0.03 Å.) The angles subtended at the platinum atom by the dppaH and dppe ligands are 69.5(1)

and $81.2(1)^\circ$ respectively, a further indication of the deviation from ideal square-planar geometry at the platinum atom. A comparison of these two angles shows that the angle strain associated with chelating dppaH is more severe than for chelating dppe.

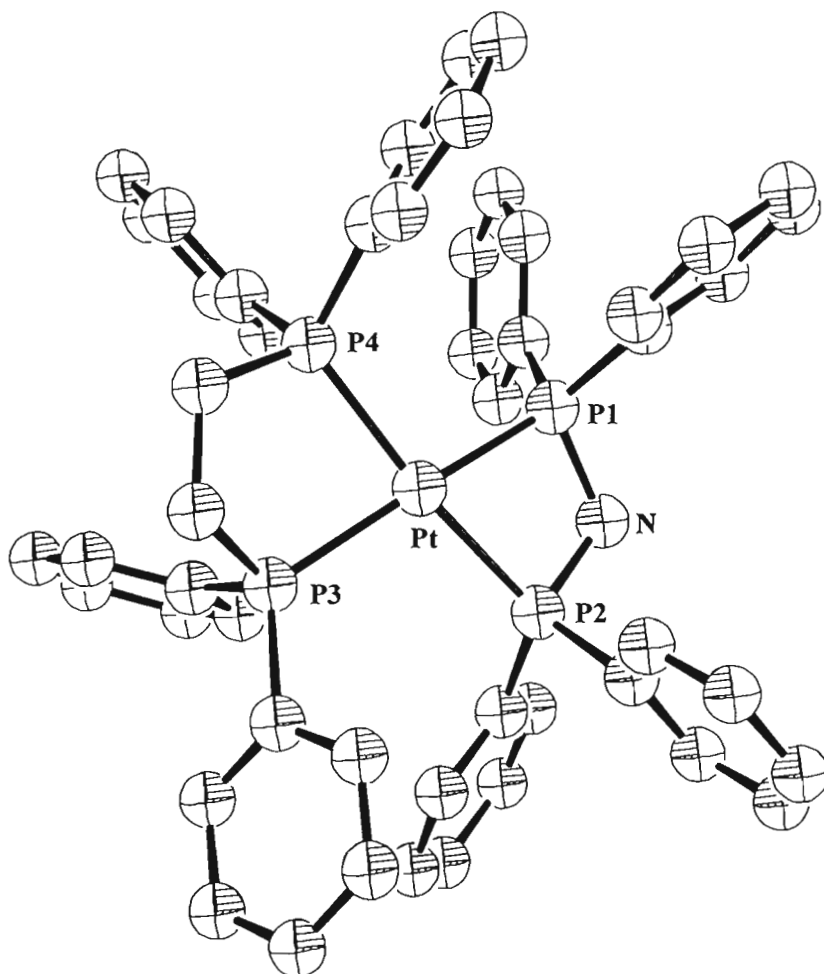


Fig. 1.19 : Structure of $[\text{PtCl}_2\{\eta^2\text{-Ph}_2\text{PN(H)PPh}_2\}(\text{dppe})]$ (Redrawn from ref. 21.)

Another structurally characterised complex $[\text{Pt}\{\eta^2\text{-Ph}_2\text{PNPPh}_2\}\{(\text{Ph}_2\text{PN})_2\text{PPh}_2\}]^{(22)}$ contains the anionic bis(diphenylphosphino)amido (dppa) ligand bonded to a platinum atom illustrated in **Fig. 1.20**. The compound was obtained by treatment of anhydrous "PtCl₂" with four equivalents of LiN(PPh₂)₂, and refluxed in toluene

for 6 hours. The X-ray crystal structure reveals that the phosphorus and platinum atoms are coplanar, but that the small P(1)-Pt-P(2) angle of $64.7(1)^\circ$ shows a marked deviation from the ideal value of 90° for a square-planar geometry.

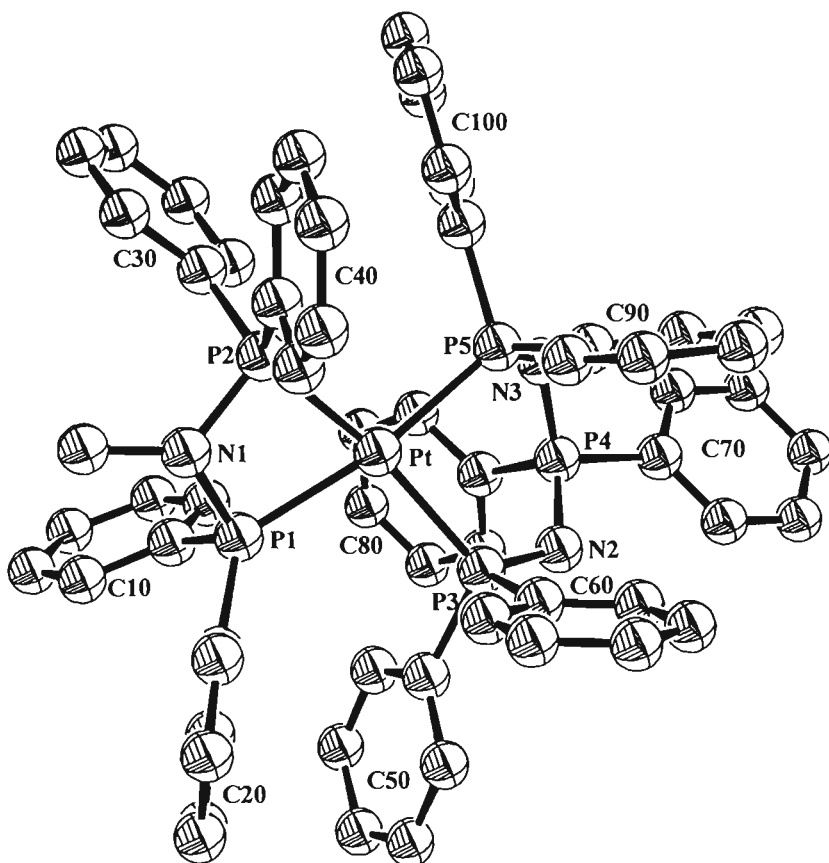


Fig. 1.20 : Structure of $[\text{Pt}\{\eta^2\text{-Ph}_2\text{PNPPh}_2\}\{(\text{Ph}_2\text{PN})_2\text{PPh}_2\}]$ (Redrawn from ref. 22.)

Addition of trace quantities of water to a solution of the iodide salt of $[\text{Pt}\{\eta^2\text{-Ph}_2\text{PN}(\text{CH}_3)\text{PPh}_2\}_2]^{2+}$ effected cleavage of both P-N bonds of one of its dppma ligands giving the complex $[\text{Pt}\{\eta^2\text{-Ph}_2\text{PN}(\text{CH}_3)\text{PPh}_2\}(\text{Ph}_2\text{PO})_2\text{H}]^{+(23)}$ as illustrated in **Fig. 1.21**. This complex contains two ligands: dppma and Ph₂POHOPPh₂. The average of the Pt-P-N bond angles of $91.8(5)^\circ$ [P(1)] and $90.8(5)^\circ$ [P(2)] is identical to that measured for the homoleptic species $[\text{Pt}\{\eta^2\text{-dppma}\}_2]^{2+}$. Ring strain in the four-membered PtP(1)NP(2) ring is evident in the $0.37(2)\text{\AA}$ displacement of

the methyl carbon atom from the NP_2 plane⁽²⁰⁾. An asymmetry in the lengths of the Pt-P bonds is observed with both ligands, the longer Pt-P bond of each ligand being situated *trans* to the shorter Pt-P bond of the other ligand.

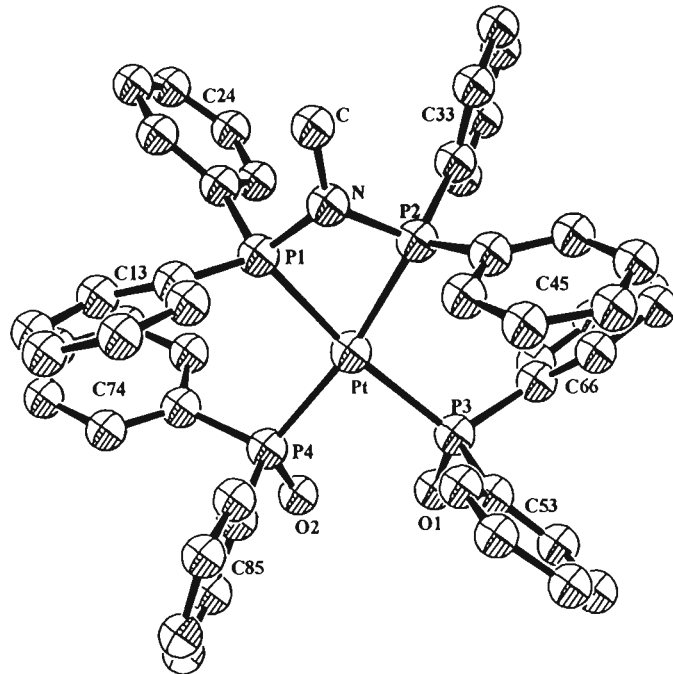


Fig. 1.21 : Structure of $[\text{Pt}\{\eta^2\text{-Ph}_2\text{PN}(\text{CH}_3)\text{PPh}_2\}(\text{Ph}_2\text{PO})_2\text{H}]^+$ (Redrawn from ref. 23.)

Two additional crystal structures of complexes containing the dppma ligand bonded to platinum have been reported. The complexes are $[\text{Pt}\{\eta^2\text{-Ph}_2\text{PN}(\text{CH}_3)\text{PPh}_2\}\text{Cl}_2]$ ⁽⁸⁾ (Fig. 1.22) and $[\text{Pt}\{\eta^2\text{-Ph}_2\text{PN}(\text{CH}_3)\text{PPh}_2\}(\text{CN})_2]$ ⁽⁸⁾ (Fig. 1.23). One of the complexes has two chloride ligands *trans* to the dppma ligand and the second complex has two cyanide groups *trans* to the dppma ligand. Both complexes have highly distorted, square-planar coordination geometries. The ring strain associated with the four-membered chelate rings is evident in the distorted tetrahedral angles at phosphorus, which range from 93.3(2) to 122.2(5) $^\circ$, and the trigonal-planar angles at N which are in the range 100.0(6) to 128.7(3) $^\circ$. The Pt-P bond lengths in each of these two complexes are almost identical, the averages being 2.206(4) and 2.268(2) \AA for the chloro and cyano derivatives respectively. The longer Pt-P bond

lengths observed in the $[\text{Pt}\{\eta^2\text{-Ph}_2\text{PN}(\text{CH}_3)\text{PPh}_2\}(\text{CN})_2]$ complex are consistent with the higher *trans*-influence of the cyanide group.

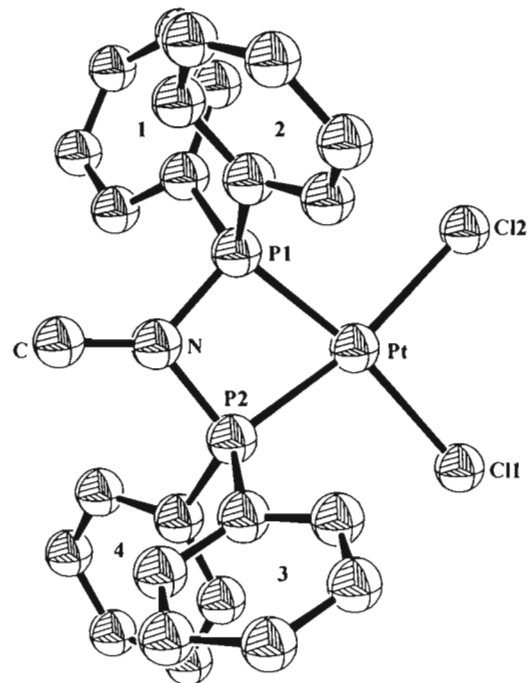


Fig. 1.22 : Structure of $[\text{Pt}\{\eta^2\text{-Ph}_2\text{PN}(\text{CH}_3)\text{PPh}_2\}(\text{Cl})_2]$ (Redrawn from ref. 8.)

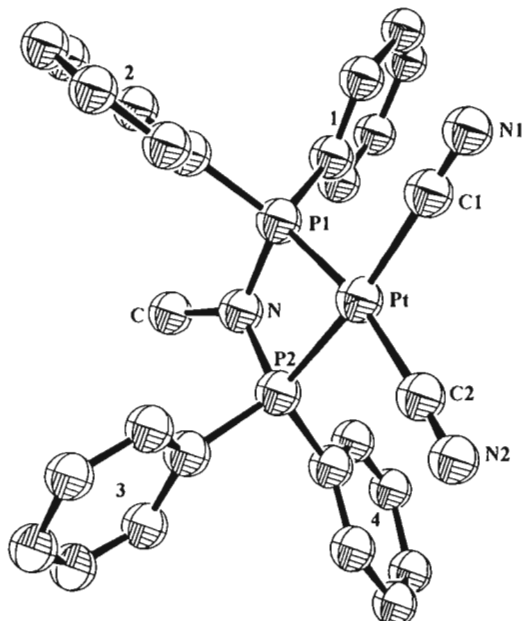


Fig. 1.23 : Structure of $[\text{Pt}\{\eta^2\text{-Ph}_2\text{PN}(\text{CH}_3)\text{PPh}_2\}(\text{CN})_2]$ (Redrawn from ref. 8.)

When hexafluorobut-2-yne, $\text{F}_3\text{CC}\equiv\text{CCF}_3$ was bubbled slowly into a mixture of $\text{Pt}(\text{C}_8\text{H}_{12})_2$ and $(-)(\text{MePhHC})\text{N}(\text{PPh}_2)_2$ in toluene the complex $[\text{Pt}\{(-)\text{Ph}_2\text{PN}(\text{MePhHC})\text{PPh}_2\}(\text{F}_3\text{CC}\equiv\text{CCF}_3)]^{(24)}$ was obtained. As illustrated in **Fig. 1.24**, the complex contains the enantiomeric $\text{Ph}_2\text{PN}(\text{MePhHC})\text{PPh}_2$ ligand bonded to platinum in the chelating mode. The angle subtended at the platinum atom by the two phosphorus atoms is $71.0(1)^\circ$, while that subtended by the two carbon atoms of the hexafluorobut-2-yne ligand is $36.3(6)^\circ$; average values are given since there are two molecules per asymmetric unit. Thus, although the atoms in the inner coordination sphere are essentially coplanar, the geometry is very different from square-planar. As noted by the authors, the bond angles around the P atoms indicate that they adopt a greatly distorted tetrahedral geometry

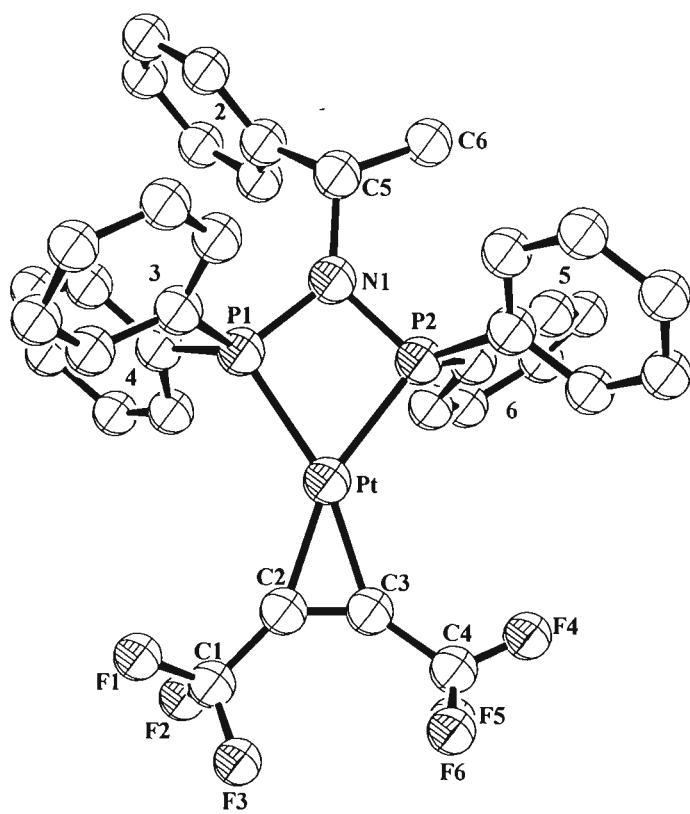


Fig. 1.24 : Structure of $[\text{Pt}\{(-)\text{-(MePhHC)}\text{N}(\text{PPh}_2)_2\}(\text{F}_3\text{CC}\equiv\text{CCF}_3)]$ (Redrawn from ref. 24.)

1.3.3 Bridging Mode(III)

There is only one example of a diplatinum complex, in which the two platinum atoms are bridged by a bis(phosphino)amine ligand, and for which a crystal structure has been reported. This is the Pt(0) species $[\text{Pt}_2\{\mu\text{-F}_2\text{PN}(\text{Me})\text{PF}_2\}_3(\text{PPh}_3)]^{(25)}$. As shown in Fig. 1.25, the platinum atoms are bridged by three $\text{F}_2\text{PN}(\text{Me})\text{PF}_2$ ligands. The geometry at the Pt(1) is trigonal planar while that at the four-coordinate platinum atom, Pt(2), is essentially tetrahedral. The $^{31}\text{P}\{^1\text{H}\}$ NMR spectrum consists of two broad, overlapping triplet patterns for the diphosphazane ligands and a narrower multiplet for PPh_3 having ^{195}Pt satellites.

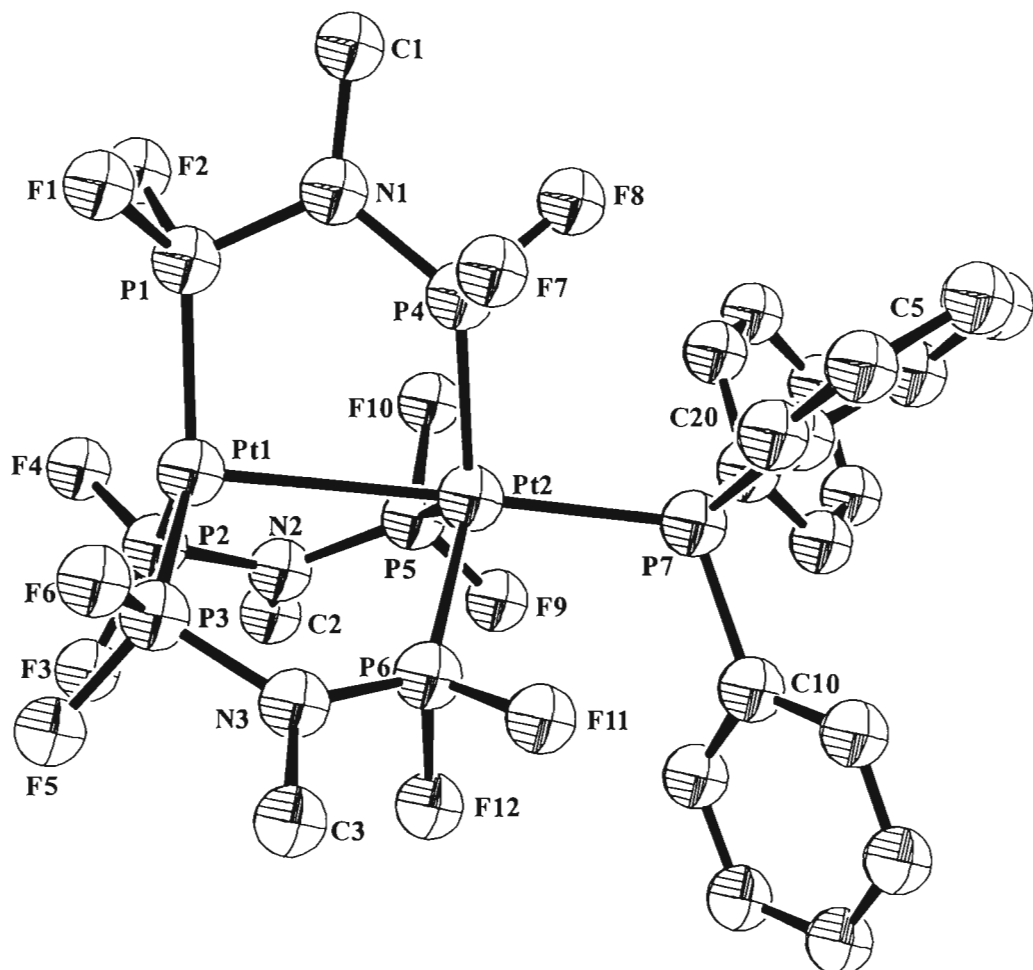


Fig. 1.25 : Structure of $[\text{Pt}_2\{\mu\text{-PF}_2\text{PN}(\text{Me})\text{PF}_2\}_3(\text{PPh}_3)]$ (Redrawn from ref. 25.)

An example of a complex containing the dppaH ligand coordinating in a bridging fashion is the Pt(I) dimer $[\text{Pt}_2\{\mu\text{-Ph}_2\text{PN}(\text{H})\text{Ph}_2\text{P}\}_2(\text{CN})_2]^{(20)}$, obtained by addition of one equivalent of $[\text{Pt}(\text{cod})_2]$ to a solution of $[\text{Pt}\{\eta^1\text{-Ph}_2\text{PN}(\text{H})\text{PPh}_2\}(\text{CN})_2]$. The identity of the product was established by IR spectroscopy [$\nu(\text{C}\equiv\text{N})$ 2110 cm^{-1} in CH_2Cl_2], mass spectroscopy, elemental analysis and by $^{31}\text{P}\{^1\text{H}\}$ NMR spectroscopy. The $^{31}\text{P}\{^1\text{H}\}$ NMR spectrum shows a singlet in this case at δ 53.9.

1.4 Conclusion

The aim of this section is to summarise some useful trends which can be distilled from the above survey of the spectroscopic and structural properties of homonuclear bis(phosphino)amine complexes of Ni, Pd and Pt. These trends will be described in relation to the coordination mode of the ligand *i.e.*, monodentate (η^1 -), bidentate chelating (η^2 -), or bridging (μ -).

1.4.1 ^{31}P NMR chemical shifts

The ^{31}P NMR chemical shifts for selected bis(phosphino)amine ligand complexes of Ni, Pd and Pt are listed in **Table 1.1**. Examination of the data in **Table 1.1** shows that there is an upfield shift of these values for the coordinated ligand relative to that of the free ligand for **η^2 -bonded** bis(phosphino)amine ligands. This trend is independent of ligand, metal and metal oxidation state. A similar trend is **not** observed for the η^1 -and μ -coordinated ligands. A general observation is that for the latter two modes of coordination, the ^{31}P chemical shifts are close to the free ligand value, or slightly downfield of the free ligand chemical shift value. On the basis of these trends it should be simple to establish from the ^{31}P chemical shift values whether the ligand is η^2 -bonded, as opposed to η^1 - or μ -coordinated.

Table 1.1 ^{31}P NMR chemical shifts (ppm relative to 85% H_3PO_4) for selected bis(phosphino)amine ligand complexes of Ni, Pd and Pt.

Note: Only the chemical shifts for the P-atoms of the bis(phosphino)amine ligand are given.

Table 1.1.1 Complexes of the $\text{Ph}_2\text{PN}(\text{H})\text{PPh}_2$ ligand. (Free ligand value: 41.6 ppm).

Metal	Complex	η^1	η^2	μ	Ref.
Pt(II)	$trans$ -[Pt{ η^1 - $\text{Ph}_2\text{PN}(\text{H})\text{PPh}_2\}$ ₂ (CN) ₂]	43.6(Pt-P); 27.3(P/term.)			20
Ni(II)	[NiBr{ η^2 - $\text{Ph}_2\text{PN}(\text{H})\text{PPh}_2\}$ (PEt ₃)] ⁺		-34.2(P1); 11.6(P2, <i>trans</i> to Br)		4
Pd(II)	[Pd{ η^2 - $\text{Ph}_2\text{PNPPPh}_2\}$ Cl(PEt ₃)]		-42.8(P1); -18.9 (P2, <i>trans</i> to Cl)		4
Pt(II)	[PtCl{ η^2 - $\text{Ph}_2\text{PN}(\text{H})\text{PPh}_2\}$ (PBu ⁿ ₃)] ⁺		9.45(P1, <i>trans</i> to Cl); 2.50 (P2)		21
Pt(II)	[PtCl{ η^2 - $\text{Ph}_2\text{PN}(\text{H})\text{PPh}_2\}$ (PMe ₂ Ph)] ⁺		7.8(P1, <i>trans</i> to Cl); 1.7 (P2)		21

Cont. Table 1.1.1

Metal	Complex	η^1	η^2	μ	Ref.
Pt(II)	$[\text{Pt}\{\eta^2\text{-Ph}_2\text{PN(H)PPh}_2\}_2]^{2+}$		22.0		20
Ni(0)	$[\text{Ni}_2(\mu\text{-SO}_2)(\text{CO})_2\{\mu\text{-Ph}_2\text{PN(H)PPh}_2\}_2]$			68.3	5
Pd(0)	$[\text{Pd}_2\{\mu\text{-Ph}_2\text{PN(H)PPh}_2\}_2(\text{PPh}_3)_2]$			54.8	14
Pd(I)	$[\text{Pd}_2\text{Cl}_2\{\mu\text{-Ph}_2\text{PN(H)PPh}_2\}_2]$			58.9	14
Pt(I)	$[\text{Pt}_2\{\mu\text{-Ph}_2\text{PN(H)PPh}_2\}_2(\text{CN})_2]$			53.9	20

Table 1.1.2 Complexes of the $\text{Ph}_2\text{PN}(\text{CH}_3)\text{PPh}_2$ ligand. (Free ligand value: 71.4 ppm).

Metal	Complex	η^1	η^2	μ	Ref.
Ni(II)	$[\text{Ni}(\text{C}_5\text{H}_5)\{\eta^1\text{-Ph}_2\text{P}(\text{CH}_3)\text{PPh}_2\}(\text{CN})]$	69.0 (Pt-P); 82.7(P/term.)			1
Ni(II)	$[\text{Ni}\{\eta^2\text{-Ph}_2\text{PN}(\text{CH}_3)\text{PPh}_2\}\text{Cl}_2]$		57.0		3
Ni(II)	$[\text{Ni}(\text{C}_5\text{H}_5)\{\eta^2\text{-Ph}_2\text{PN}(\text{CH}_3)\text{PPh}_2\}]^+$		65.9		1
Pd(II)	$[\text{Pd}\{\eta^2\text{-Ph}_2\text{PN}(\text{CH}_3)\text{PPh}_2\}_2]^{2+}$		44.5		3
Pt(II)	$[\text{Pt}\{\eta^2\text{-Ph}_2\text{PN}(\text{CH}_3)\text{PPh}_2\}_2]^{2+}$		39.6		20
Pt(II)	$[\text{Pt}\{\eta^2\text{-Ph}_2\text{PN}(\text{CH}_3)\text{PPh}_2\}(\text{Ph}_2\text{PO})_2\text{H}]^+$		41.4		23

Table 1.1.3 Complexes of the $(\text{PhO})_2\text{PN}(\text{CH}_3)\text{P}(\text{OPh})_2$ ligand. (Free ligand value: 135.7 ppm).

Metal	Complex	η^1	η^2	μ	Ref.
Pd(II)	$[\text{PdCl}_2\{\eta^2-(\text{PhO})_2\text{PN}(\text{Me})\text{P}(\text{OPh})_2\}]$		65.5		18
Pt(II)	$[\text{PtCl}_2\{\eta^2-(\text{PhO})_2\text{PN}(\text{Me})\text{P}(\text{OPh})_2\}]$		46.5		18
Pd(0)	$[\text{Pd}_2\{\mu-(\text{PhO})_2\text{PN}(\text{Me})\text{P}(\text{OPh})_2\}_3]$			124.5	18

Table 1.1.4 Complexes of the $(\text{PhO})_2\text{PN}(\text{Ph})\text{P}(\text{OPh})_2$ ligand. (Free ligand value: 127.7 ppm).

Metal	Complex	η^1	η^2	μ	Ref.
Pd(II)	$[\text{PdCl}_2\{\eta^2-(\text{PhO})_2\text{PN}(\text{Ph})\text{P}(\text{OPh})_2\}]$		82.2		18
Pt(II)	$[\text{PtCl}_2\{\eta^2-(\text{PhO})_2\text{PN}(\text{Ph})\text{P}(\text{OPh})_2\}]$		78.3		18
Pd(I)	$[\text{Pd}_2\text{Cl}_2\{\mu-(\text{PhO})_2\text{PN}(\text{Ph})\text{P}(\text{OPh})_2\}_2]$			111.5	18

The following explanation is offered for the upfield shift in the η^2 -bonded case. As will be documented in the next section (**Section 1.4.2**) the valence angle at the P-atom *i.e.*, the N-P-M (M = metal) angle in the η^2 -case is typically $90\text{--}95^\circ$. This is considerably less than the idealised tetrahedral value of 109.5° and implies that there is substantial atomic character in the orbitals employed by the P-atom for bonding. In particular, a higher s-electron density is expected at the P-atom nucleus as compared to the free ligand, where the hybridisation at the P-atom closely approximates sp^3 . A higher s-electron density implies that the P-atom nucleus is shielded relative to that in the free ligand, and an upfield shift in the ^{31}P NMR resonance is therefore expected. An advantage of this explanation is that it is

directly linked to the angle strain, only experienced by bis(phosphino)-amine ligands when bonded in the chelating mode. A dependence on metal, metal oxidation state and choice of ligand is not expected and, as noted above, none is observed. Also consistent with this explanation is the absence of any clear pattern in the ^{31}P chemical shifts for bis(phosphino)amine ligands bonded in the η^1 - or μ -modes. In these cases the angle subtended at the P-atom more-or-less approximates the idealised tetrahedral value, though there is some variation (see Section 1.4.2). Other workers have also noted a dependence of the ^{31}P chemical shift on the bond angles at a P-atom of a phosphine or phosphite ligand bonded to a metal^(26,27).

1.4.2 Structural parameters

The structural parameters surveyed are those common to all coordinated bis(phosphino)amine ligands *viz.* the P-N distances, the P-N-P and N-P-M angles and the deviation of the nitrogen atom from the plane defined by the two P-atoms and the third (non-P) atom bonded to nitrogen. These parameters, taken together, provide a guide to the angle strain experienced by the PNP ligand in a particular bonding mode. They are tabulated according to the coordination mode in **Table 1.2**.

Table. 1.2 Structural parameters for selected bis(phosphino)amine ligand complexes of Ni, Pd and Pt. Averaged values are given where there is more than one parameter for the complex.

Complex	P-N (Å)	P-N-P (°)	Deviation ^a (Å)	N-P-M (°)	Ref.
<i>trans</i> -[Pt{ η^1 -Ph ₂ PN(H)PPh ₂ } ₂ (CN) ₂]	1.69	125.2	<i>b</i>	111.12	20
[Pd{ η^2 -Ph ₂ PN(CH ₃)PPh ₂ }Cl ₂]	1.68	100.4	0.17	93.83	8

Cont. Table 1.2

Complex	P-N (Å)	P-N-P (°)	Deviation ^a (Å)	N-P-M (°)	Ref.
[PdI ₂ {η ² -Ph ₂ PN(Pr ⁱ)PPhMe}] ²⁺	1.68	100.0	0.048	94.38	10
[Pd{η ² -Ph ₂ PN(CH ₃)PPh ₂ }] ²⁺	1.69	102.6	0.099	93.48	3
[PdCl ₂ {η ² -(Ph ₂ P) ₂ N(S-CHMePh)}]	1.70	98.15	0.028	95.19	11
[Pt{η ² -Ph ₂ PN(H)PPh ₂ } ₂] ²⁺	1.68	102.7	b	92.29	20
[Pt{η ² -Ph ₂ PN(CH ₃)PPh ₂ } ₂] ²⁺	1.69	101.5	0.197	92.01	20
[PtCl{η ² -Ph ₂ PN(H)PPh ₂ }(PMe ₂ Ph)] ⁺	1.67	102.1	b	93.84	21
[PtCl{η ² -Ph ₂ PN(H)PPh ₂ }(PBu ⁿ ₃)] ⁺	1.66	102.2	b	93.57	21
[PtCl ₂ {η ² -Ph ₂ PN(H)PPh ₂ }(dppe)]	1.67	103.9	b	92.72	21
[Pt{η ² -Ph ₂ PN(CH ₃)PPh ₂ }(Ph ₂ PO) ₂ H] ⁺	1.68	104.1	0.154	91.33	23
[PtCl ₂ {η ² -Ph ₂ PN(CH ₃)PPh ₂ }]	1.68	99.94	0.156	93.98	8
[Pt{η ² -Ph ₂ PN(CH ₃)PPh ₂ }](CN) ₂]	1.68	102.4	0.166	93.27	8
[Pt{(-)η ² -(MePhHC)N(PPh ₂) ₂ }(FCC≡CCF ₃)] ²⁺	1.71	99.6	0.047	94.55	24
[Pd ₂ Cl ₂ {μ-Ph ₂ PN(H)PPh ₂ } ₂]	1.68	116.0	b	111.69	13
[Pd ₂ {μ-Ph ₂ PN(H)PPh ₂ } ₂ (THF)(PPh ₃)] ²⁺	1.67	118.9	b	111.33	14
[Pd ₂ {μ-Ph ₂ PN(H)PPh ₂ } ₂ Cl ₂]	1.67	116.3	b	110.43	14
[Pd ₂ Cl ₂ {μ-(OPh) ₂ PN(Ph)P(OPh) ₂ } ₂]	1.67	113.3	0.0029	114.57	18
[Pd ₂ {μ-(OPh) ₂ PN(Me)P(OPh) ₂ } ₃]	1.70	116.9	0.0089	118.81	18
[Pt ₂ {μ-PF ₂ PN(Me)PF ₂ } ₃ (PPh ₃)] ²⁺	1.66	116.1	0.087	118.91	25

^a This is the deviation of N from the plane defined by the two P-atoms and the

third (non-P) atom bonded to nitrogen.

^b Reliable value not available because of uncertainty in the position of the H-atom.

From **Table 1.2** it is clear that there are only small variations in the P-N distances. Thus this parameter is not sensitive to changes in coordination mode. The P-N-P angle on the other hand is very sensitive to coordination mode: $\pm 100^\circ$ for η^2 *i.e.*, considerably smaller than the ideal tetrahedral value of 109.5° ; typically a few degrees less than 120° for μ -bonded; while for the η^1 -mode, of which there is only one example, the P-N-P angle approximates well the ideal sp^2 -value of 120° . Marked deviations from the P_2R plane exist for η^2 -bonded ligands providing further evidence of angle strain. The N-P-M angle approximates the tetrahedral value for the η^1 -and μ -bonding modes but is typically $91\text{--}95^\circ$ for η^2 -bonded ligands; again evidence of angle strain in this coordination mode.

From the earlier surveys in **Section 1.1.2, 1.2.1** and **1.3.2** it is clear that the chelating (η^2 -) mode is the most common mode of coordination for bis(phosphino)amine ligands. These ligands form stable chelate complexes with Ni, Pt and Pd despite the strain caused by the formation of the four-membered chelate ring. The small bite angle of the ligand compresses the P-N-P bond angle to approximately 100° which is a severe distortion from the ideal trigonal-planar angle expected at a sp^2 -hybridised nitrogen centre. Ring strain is further evident in the pyramidal character assumed at the nitrogen centres upon chelation. Clearly, angle strain is at its most severe when the bis(phosphino)amine ligand coordinates in the chelating mode. Yet, as already noted, this is the most common mode of coordination for ligands of this type. Browning and Farrar have noted that a bent M-P (M = Pd or Pt) bond is an effective model of the interaction between the metal

and the phosphorus centres in chelate complexes of bis(phosphino)amine ligands⁽²⁰⁾. This model allows for a strong metal-ligand interaction in the η^2 -mode, despite the small bond angles subtended at the P-and N-atoms. They tentatively suggest that it is for this reason that the chelating mode is favoured for bis(phosphino)amine ligands⁽²⁰⁾.

Also clear from the previous discussion is that bis(phosphino)amine ligands have received some considerable attention in Group 10 metal coordination chemistry. In addition to a number of examples of mononuclear palladium(II) complexes containing the ligand bonded in the monodentate or chelating modes, dipalladium(I) complexes in which the P-donor ligand acts as a bridge between two metal centres have been synthesised. The coordination mode adopted depends on the metal and the conditions of the synthesis but can, to some extent, be controlled by the choice of substituents on the N- and P-atoms. Clearly bis(phosphino)amines are versatile ligands, in that they can often be rotated to adopt a particular coordination mode and so confer the desired stereochemistry on the metal complex.

1.5 Aims of this work

The overall aim of this work is to further develop the coordination chemistry of the bis(diphenylphosphino)ethylamine (dppea) ligand; a natural extension of this aim has been to briefly study the coordination behaviour of the closely-related bis(2-pyridyl)phenylphosphine [PhP(py)₂] and 2,5-bis(diphenylphosphino)thienyl (PSP) ligands. The metal chosen for the study is palladium, for several reasons. Firstly, the range of stable oxidation states accessible to palladium *viz.* +II, +I and 0, means that a range of compounds with different structural types and chemistries can be prepared. Linked to this is the intrinsic reactivity of palladium compounds,

in particular phosphine-ligand complexes of palladium, many of which are catalysts for industrially important chemical transformations. Finally, palladium is a platinum group metal mined in South Africa and important to the South African economy. Hence, any study that develops new compounds of palladium (possibly with future applications) is relevant in the South African context.

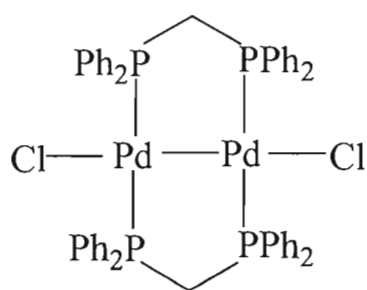
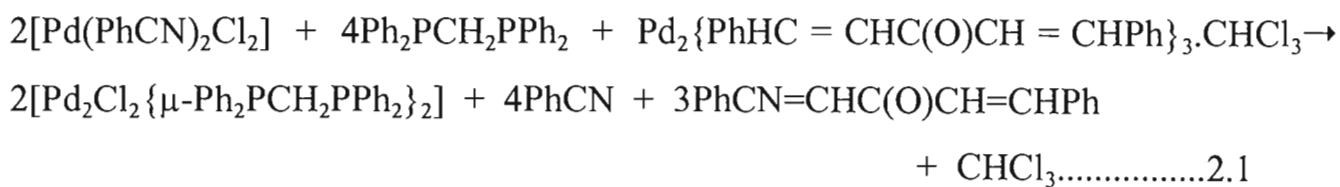
The emphasis of the work will be on the structural characterisation of various new compounds. Thus where possible, single crystals will be grown, and the crystal structure determined by means of X-ray diffraction methods. Of particular interest will be the mode of coordination of the bidentate ligand *i.e.*, terminal (η^1 -), chelating (η^2 -) or bridging (μ -). As shown by the earlier reviews, all three structural types are possible for a bis(phosphino)amine ligand.

CHAPTER 2

BIS(DIPHENYLPHOSPHINO)ETHYLAMINE (DPPEA) LIGAND DERIVATIVES OF PALLADIUM(II) AND PALLADIUM(0)

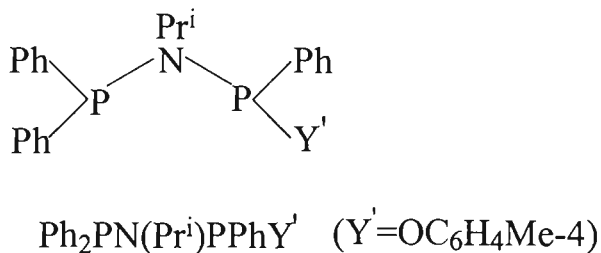
2.1 INTRODUCTION

Many studies of the coordination behavior of nitrogen and phosphorus donor ligands with the palladium(I) precursor $[PdCl_2(PhCN)_2]$ have been made. As discussed in Chapter 1, diphosphazane ligands based on the P-N-P framework offer considerable scope and versatility as ligands since the substituents on both the nitrogen and phosphorus atoms can be altered readily with attendant changes in the P-N-P angle and the conformations around the phosphorus centres. In particular it was found that dppm, bis(diphenylphosphino)methane, reacted with $[Pd(PhCN)_2Cl_2]$ and $Pd_2(dba)_3 \cdot CHCl_3$ ($dba =$ dibenzylideneacetone) to afford the bridged dinuclear complex $[Pd_2Cl_2(\mu\text{-dppm})_2]^{(28)}$ as shown in equation 2.1 and illustrated below.



The ligand bis(diphenylphosphino)methane (dppm) has been extensively used as a bridging ligand to stabilize bimetallic and polymetallic complexes of the platinum group metals⁽²⁹⁾. The formation of dppm-bridged, rather than chelated complexes, is due to ring strain associated with the formation of a four-membered ring when the ligand chelates to one metal center. Substituting the methylene group in dppm with the smaller amino group, NH, may increase the ligand's propensity to bridge two metal centres, but as outlined, in Chapter 1, there is also a strong tendency for bis(phosphino)amine ligands to form chelate complexes.

Krishmurthy and co-workers⁽¹⁰⁾ have recently synthesised the diphosphazane ligand, Ph₂PN(Prⁱ)PPhY' [Y' = OC₆H₄Me-4] illustrated below. This ligand was reacted with Pd₂(dba)₃.CHCl₃ in the presence of MeI to afford the chelating complex [PdI₂{η²-Ph₂PN(Prⁱ)PPhMe}]. Clearly substitution of the *p*-methylphenoxy on the P-atom by a methyl group has occurred⁽¹⁰⁾.

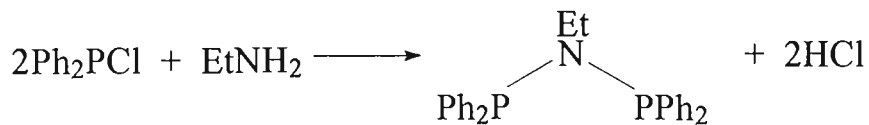


More recently the Ph₂PN(H)PPh₂ (dppaH) ligand has been reacted with [Pd(CH₃CN)₄][BF₄] in CH₃CN to afford the dinuclear palladium complex [Pd₂(μ-dppa)₂(CH₃CN)₂]₂[BF₄]₂⁽¹⁴⁾. Thus, diphosphazane ligands have attracted much attention because of the ease of their synthesis, their high stability, and their ability to bond to metal atoms in three different modes of coordination *viz* bridging (μ-), chelating (η²-) and monodentate (η¹-)⁽³⁰⁾.

2.2 RESULTS AND DISCUSSION

2.2.1 Synthesis of the bis(diphenylphosphino)ethylamine (dppea) ligand

The procedure used is that described by G. Ewart and co-workers⁽³¹⁾ and is summarised below in **Scheme 2.1**.



Scheme 2.1: Synthesis of the $\text{Ph}_2\text{PN}(\text{Et})\text{PPh}_2$ ligand

The synthesis of the ligand was performed under an atmosphere of nitrogen, and a white air-stable solid was isolated.

Characterisation data (**Tables 2.2 and 2.3**) obtained for the ligand were in good agreement with those reported in the literature⁽³¹⁾. The ^1H NMR spectrum consisted of a broad series of multiplets ranging from δ 7.2 - 7.5 and also at δ 3.3 and δ 0.7, the latter assigned to the ethyl group protons. The $^{31}\text{P}\{^1\text{H}\}$ NMR spectrum of the $\text{Ph}_2\text{PN}(\text{Et})\text{PPh}_2$ ligand shows a sharp singlet at δ 62.3, which is characteristic of these types of ligands⁽²⁰⁾. Elemental analysis is in good agreement with ligand's formulation.

2.2.2 Reaction of the dppea ligand with $[\text{PdCl}_2(\text{PhCN})_2]$

Reaction of $[\text{PdCl}_2(\text{PhCN})_2]$ with an equimolar amount of $\text{Ph}_2\text{PN}(\text{Et})\text{PPh}_2$ in CH_2Cl_2

at room temperature for 24 hours afforded in good yield a light yellow product characterised as $[\text{PdCl}_2(\eta^2\text{-Ph}_2\text{PN(Et)PPh}_2)]$ **1**.

This product was isolated by addition of hexane and recrystallised from CH_2Cl_2 and hexane. The complex $[\text{PdCl}_2(\eta^2\text{-Ph}_2\text{PN(Et)PPh}_2)]$ was soluble in most organic solvents, but insoluble in diethylether, toluene and hexane. It was stable to air both in the solid state and in solution. **Tables 2.2** and **2.3** list microanalytical and spectroscopic data for compound **1**.

The $^{31}\text{P}\{\text{H}\}$ NMR spectrum obtained for this complex in CDCl_3 contains a sharp singlet peak centred at δ 31.8, which is shifted upfield of the signal recorded for the free dppea ligand at δ 62.3. As discussed in Section 1.4.1 such an upfield shift is indicative of the ligand bonded in the chelating (η^2 -) mode. This was confirmed by an X-ray structure analysis, see below.

The ^1H NMR spectrum of $[\text{PdCl}_2(\eta^2\text{-Ph}_2\text{PN(Et)PPh}_2)]$ in CDCl_3 at room temperature exhibits resonances between δ 7.1 and δ 7.9 associated with the phenyl rings of the ligands, and also at δ 3.0 and δ 0.8 assigned to the ligand ethyl group hydrogen atoms.

Single crystals of the complex were grown for the purpose of a structural determination by X-ray diffraction methods. An ORTEP generated representation of the structure is illustrated in **Fig. 2.1** along with the atom numbering scheme. A full list of interatomic distances and angles is given in **Tables 2.6** and **2.7** at the end of this Chapter. There were no unusual intermolecular non-bonded distances in crystals of **1** and thus each molecule can be treated as a discrete entity.

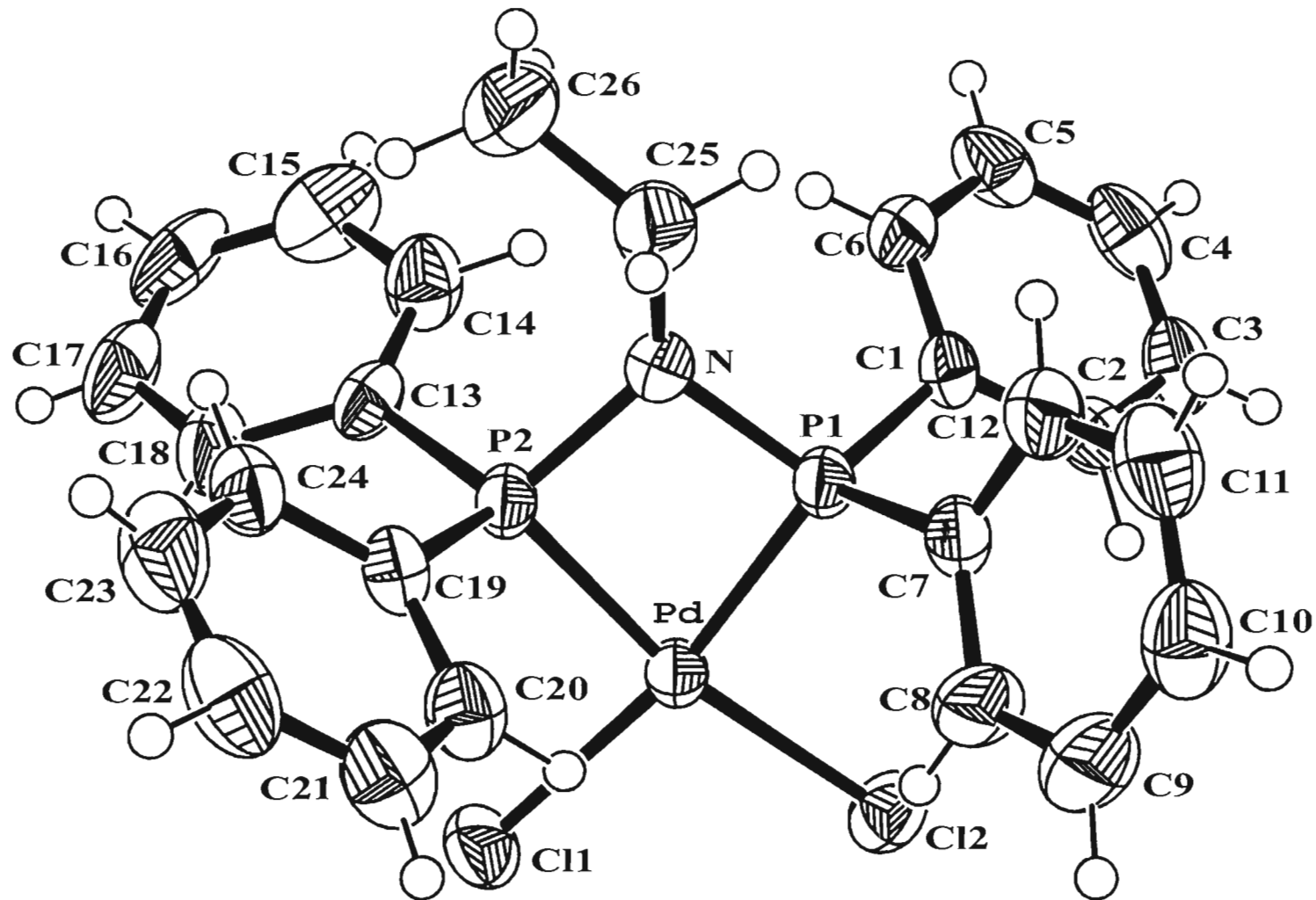


Fig. 2.1: Molecular Structure of $[\text{PdCl}_2\{\eta^2\text{-Ph}_2\text{PN}(\text{Et})\text{PPh}_2\}]$ 1

The ligand bonds through the two phosphorus atoms to the palladium *i.e.*, the chelating mode is clearly demonstrated⁽³²⁾. Complex **1** is structurally similar to other complexes of palladium(II) of general formula $[PdX_2(\eta^2\text{-PNP})_2]$ ($X = \text{halogen}$; PNP = diphosphazane ligand)^(20,21). The P(1)-N-P(2) bond angle [98.90(3)]° is considerably less than the idealised tetrahedral or trigonal angle and indicates considerable strain in the four-membered PdP_2N ring. This P-N-P bond angle is comparable to the corresponding values observed for other structurally characterised palladium complexes containing a chelating diphosphazane ligand⁽⁸⁾. The angle subtended by the ligand at the metal, P-Pd-P, is 71.33(6)°, which represents a considerable distortion from the 90° expected for a square-planar configuration. The Pd-Cl(1) and Pd-Cl(2) distances of 2.363(17) and 2.360(16) Å respectively, show no significant differences, as expected given the symmetrical nature of the complex. Similarly, the Pd-P(1) and Pd-P(2) interatomic distances of 2.214(16) and 2.219(17) Å, agree within experimental error. Again the range of distances and angles are similar to those reported for other chelated diphosphazane complexes of palladium(II)^(10,11).

The synthesis, characterisation and X-ray structure determination of complex **1** was an independent study by the author of this work, forming part of an investigation of the coordination behavior of the dppea ligand to palladium(II). However, it should be noted this compound had been previously synthesised and structurally characterised by Speakman and co-workers⁽³³⁾. In **Table 2.1** a comparison of key bond lengths and angles from the two structure determinations is given.

Table 2.1 Selected bond lengths and angles for complex
 $[\text{PdCl}_2\{\eta^2\text{-Ph}_2\text{PN(Et)PPh}_2\}] \mathbf{1}$

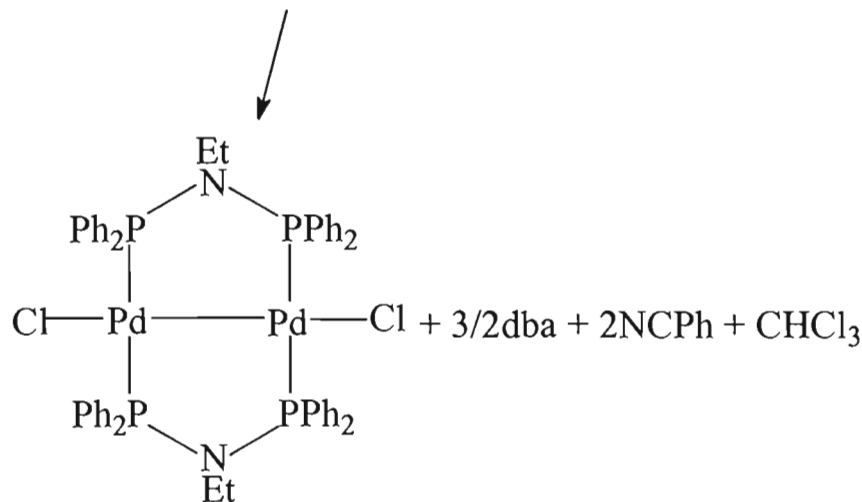
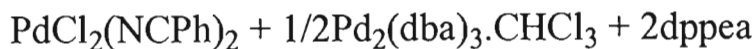
Bond angles (°)	This work	Literature ⁽³³⁾
Cl(1)-Pd-Cl(2)	94.83(7)	94.8
P(1)-Pd-P(2)	71.33(6)	71.4
P(1)-N-P(2)	98.90(3)	97.7
Pd-P(1)-N	94.73(18)	95.2
Pd-P(2)-N	94.38(17)	95.0
Bond lengths (Å)		
Pd-Cl(1)	2.36(17)	2.37
Pd-Cl(2)	2.36(16)	2.37
Pd-P(1)	2.21(16)	2.22
Pd-P(2)	2.21(17)	2.23

As can be seen from the data in **Table 2.1** the agreement between the two independent structure determinations of compound **1** is excellent.

2.2.3 Reactions of the dppea with $[\text{PdCl}_2(\text{PhCN})_2]$ and $[\text{Pd}_2(\text{dba})_3]$

Treatment of a dichloromethane solution of $[\text{PdCl}_2(\text{PhCN})_2]$ with a twice molar amount of $\text{Ph}_2\text{PN(Et)PPh}_2$ in CH_2Cl_2 and a half molar amount of $[\text{Pd}_2(\text{dba})_3 \cdot \text{CHCl}_3]$ in CH_2Cl_2 , afforded a red-orange product characterised as $[\text{Pd}_2\text{Cl}_2\{\mu\text{-Ph}_2\text{PN(Et)PPh}_2\}_2] \mathbf{2}$. Optimum yields were obtained when the reaction was carried-out at room temperature and allowed to proceed for 30 minutes. The reaction is summarised in **Scheme 2.2**, below. This product was isolated by addition of hexane

and recrystallised from CH_2Cl_2 and hexane. Compound **2** is an air-stable solid, soluble in most organic solvents, but insoluble in diethyl ether, toluene and alkanes. It is not stable when in solution and in contact with air.



Scheme 2.2 : Synthesis of $[\text{Pd}_2\text{Cl}_2\{\mu\text{-Ph}_2\text{PN}(\text{Et})\text{PPh}_2\}_2]$ **2**

The microanalytical and spectroscopic data obtained for this complex are listed in **Tables 2.2** and **2.3** at the end of this Chapter.

The ^1H NMR spectrum of complex **2** in CDCl_3 exhibits resonances between δ 7.0 and δ 7.9 that are readily assigned to the phenyl rings of the coordinated $\text{Ph}_2\text{PN}(\text{Et})\text{PPh}_2$ ligand. A triplet and a quartet centred at δ 2.5 and δ 0.3 respectively, confirm the presence of the ethyl group of the ligand.

The $^{31}\text{P}\{^1\text{H}\}$ NMR spectrum exhibits a sharp singlet at δ 78.1, downfield of the free ligand value of δ 62.3. As noted in section **1.4.1** this is typical of the ^{31}P

chemical shift for the phosphorus atoms when the ligand is coordinated in the bridging mode.

Single crystals of complex **2** were obtained, and an X-ray crystal structure analysis confirmed that the complex is indeed $[\text{Pd}_2\text{Cl}_2\{\mu\text{-Ph}_2\text{PN(Et)PPh}_2\}_2]$. An ORTEP generated representation of the structure is illustrated in **Fig. 2.2**. A full list of interatomic distances and angles is given in **Tables 2.12** and **2.13** at the end of this Chapter.

The molecules of $[\text{Pd}_2\text{Cl}_2\{\mu\text{-Ph}_2\text{PN(Et)PPh}_2\}_2]$ **2** are situated on a centre of inversion in the triclinic space group, $P\bar{1}$. Thus the molecule possesses an exact centre of inversion. The crystal structure is complicated by the fact that the molecules are disordered between two equally occupied position. These two positions (labelled A and B) share common sites for the palladium, chlorine and ligand NEt group atoms. Thus, the disorder is a consequence of a rotation about the Cl-Pd-Pd-Cl vector and with the NEt-atoms common to both positions. The rotation angle is *ca.* 40° *i.e.*, the average P(A)-Pd-P(B) angle approximates to 40° . Fortunately, it was possible to discern in the difference electron density maps these two positions and to refine molecules A and B with equal site occupation factors. The phenyl groups on the ligand were refined as rigid groups but, in view of the disorder, the phenyl carbon atom positions must be treated with caution, at least for those carbons not bonded directly to phosphorus. (It is for this reason that the full phenyl groups are not illustrated in **Fig. 2.2**). Despite the disorder, the core structure of compound **2** has been established unequivocally and the interatomic distances and angles associated with the core are reliable within the standard errors quoted.

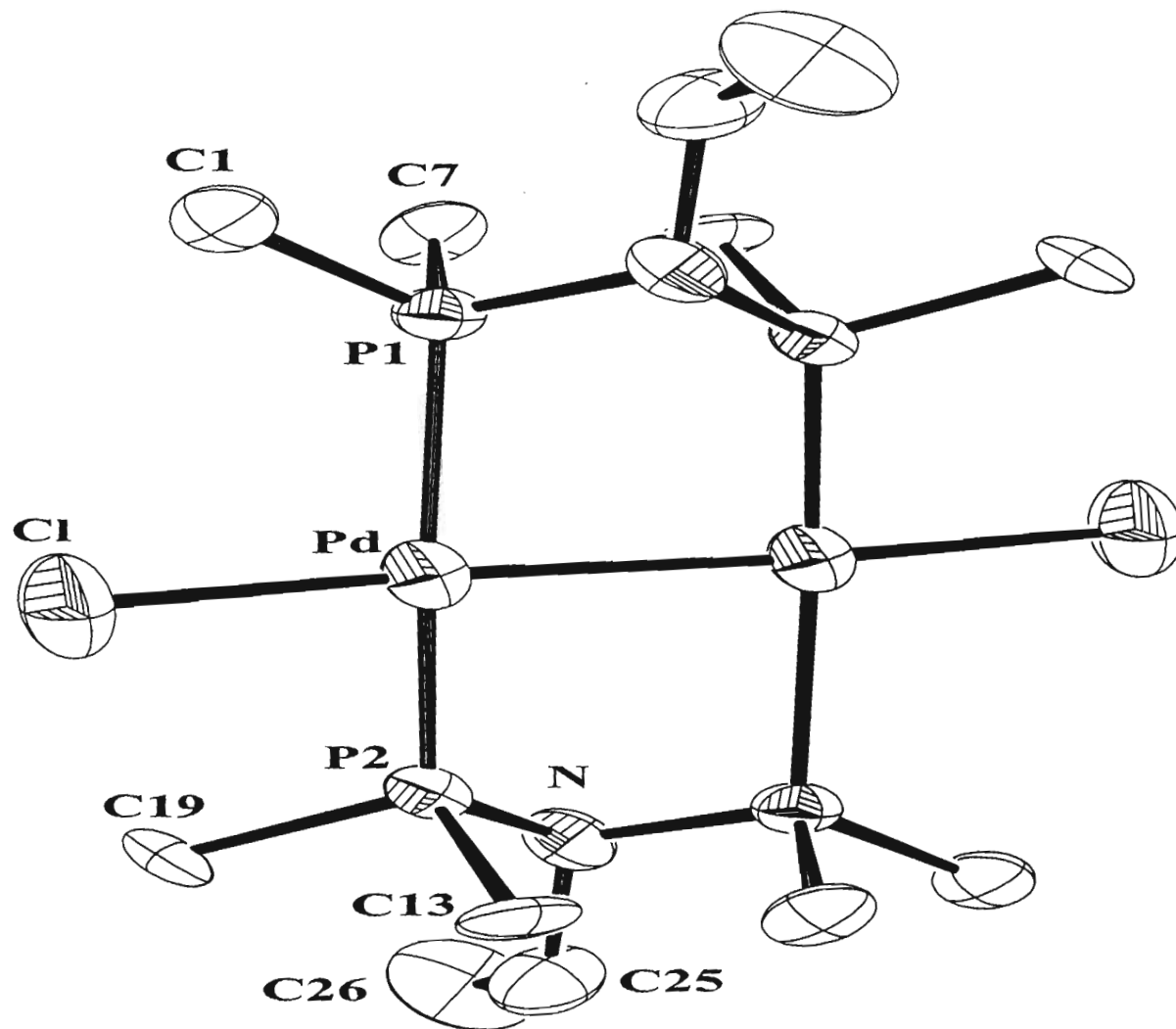
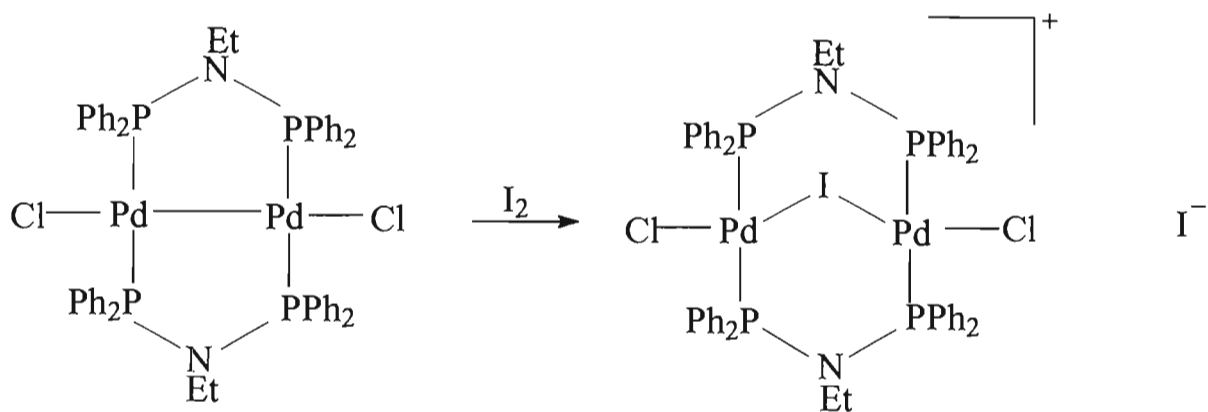


Fig. 2.2: Molecular Structure of $[\text{Pd}_2\text{Cl}_2\{\mu\text{-Ph}_2\text{PN}(\text{Et})\text{PPh}_2\}_2]$ 2. There is a crystallographically imposed centre of inversion midway between the two palladium atoms. (See text)
Ph groups not shown for clarity.

The crystal structure of complex **2** shows that the two metal atoms are connected by a direct single bond. The Pd-Pd bond distance is 2.600(1)Å, a value which can be compared with Pd-Pd distances in other ligand-bridged dipalladium(I) complexes e.g., in $[\text{Pd}_2\text{Cl}_2(\mu\text{-dppaH})_2]$ ⁽¹³⁾ it is 2.637(6)Å. The P-Pd-P groups are approximately linear with a P(1)-Pd-P(2) angle of 171.48(13)° and 172.43(13)° for each rotamer. The remaining angles at each Pd atom fall in the range 86-90° so that a near idealised square-planar environment is completed for each palladium atom. The Pd-Cl distance of 2.397(2)Å is comparable to those reported for other Pd(I) complexes^(13,14). Similarly the Pd-P distances that range from 2.136(4) to 2.17(3)Å are close to the literature values^(13,14).

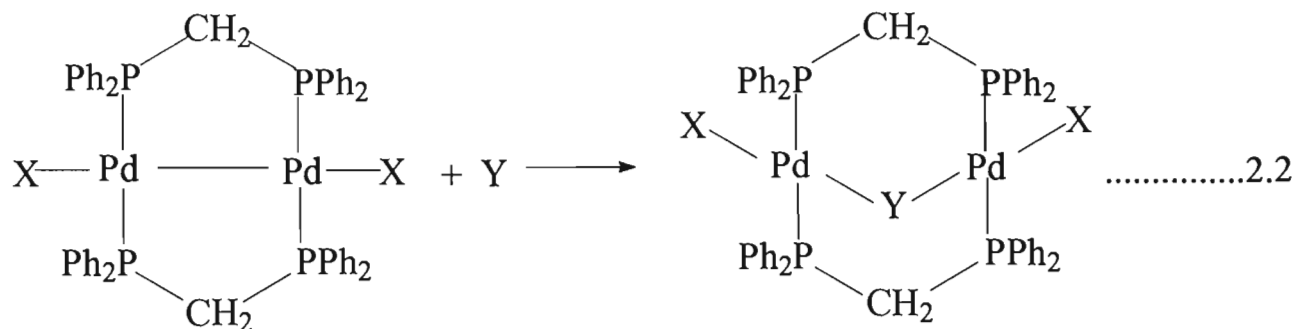
2.2.4 Addition of I₂ to $[\text{Pd}_2\text{Cl}_2(\mu\text{-Ph}_2\text{PN(Et)}\text{PPh}_2)_2]$ **2**

It was hoped to extend the chemistry $[\text{Pd}_2\text{Cl}_2\{\mu\text{-Ph}_2\text{PN(Et)}\text{PPh}_2\}_2]$ **2** by addition of I₂, with the prospect of breaking the metal-metal bond and forming the A-frame species $[\text{Pd}_2\text{Cl}_2(\mu\text{-I})\{\mu\text{-Ph}_2\text{PN(Et)}\text{PPh}_2\}_2]^+\text{I}^-$ according to **Scheme 2.3**.



Scheme 2.3: Proposed synthesis of $[\text{Pd}_2\text{Cl}_2(\mu\text{-I})\{\mu\text{-Ph}_2\text{PN(Et)}\text{PPh}_2\}_2]\text{I}$

Balch and co-workers⁽²⁸⁾ have made A-frame complexes of this type with the dppm ligand as shown in equation 2.2.



[X = Cl, Br, I and NO₂] [Y = CO, SO₂ and CNCH₃]

Unfortunately attempts to synthesise a similar A-frame complex were not successful. Addition of I₂ to [Pd₂Cl₂{μ-Ph₂PN(Et)PPh₂}₂] in a 1:1 molar ratio in a CH₂Cl₂ solution followed by stirring for one hour at room temperature afforded a dark-yellow coloured solution. This solution contained more than one product as evidenced by the ³¹P{¹H} NMR spectrum (**Fig. 2.3**). However, addition of hexane allowed the selective isolation of a yellow solid which was subsequently recrystallised from dichloromethane/hexane as an air-stable crystalline compound soluble in most organic solvents, but insoluble in diethylether, toluene and hexane. This compound was characterised as [PdI₂{η²-Ph₂PN(Et)PPh₂}] **3** by elemental analysis and spectroscopy. The microanalytical and spectroscopic data for complex **3** are listed in **Tables 2.2** and **2.3**. The composition and structure of compound **3** were confirmed by X-ray analysis, (see below).

The ³¹P{¹H} NMR spectrum recorded in CDCl₃ for the dark-yellow solution is

shown in **Fig. 2.3**. It is clear from the number of peaks present that more than one species has formed in this reaction. The sharp singlet peak at δ 24.9 is readily assigned to $[\text{PdI}_2\{\eta^2\text{-Ph}_2\text{PN(Et)PPh}_2\}]$ **3** since an authentic sample of this

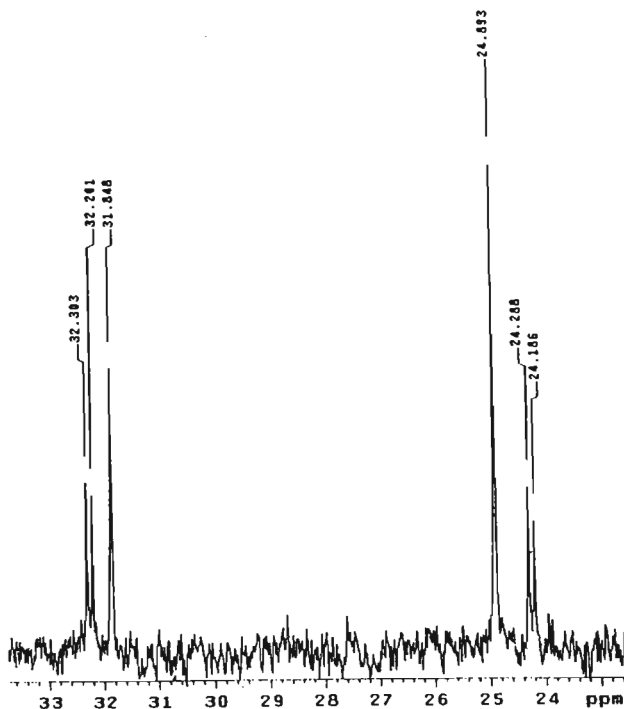
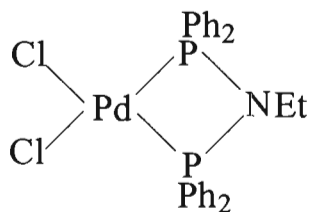


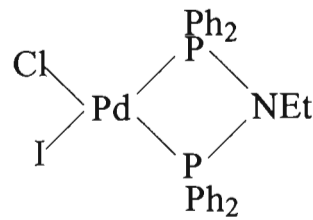
Figure : 2.3 The $^{31}\text{P}\{^1\text{H}\}$ NMR spectrum of product mixture obtained after reaction of I_2 with $[\text{Pd}_2\text{Cl}_2\{\mu\text{-Ph}_2\text{PN(Et)PPh}_2\}]$ **2**

compound gives rise to a $^{31}\text{P}\{^1\text{H}\}$ NMR spectrum in CDCl_3 with a singlet peak also at δ 24.9. Examination of the spectrum illustrated in **Fig. 2.3** shows, in addition to the peak at δ 24.9, the following features: A doublet centred at δ 24.20; a doublet centred at δ 32.25; and a further singlet at δ 31.8. Before suggesting assignments for these peaks it is important to note that all the peaks are at positions considerably upfield of the free ligand value of δ 62.3. On the basis of the survey carried-out in Chapter 1 of the dependence of the ^{31}P chemical

shifts for bis(phosphino)amine ligands on the mode of coordination of the ligand, it is concluded that all the species present in the dark-yellow product solution contain the dppea ligand bonded in the chelating mode (**see Section 1.4.1**). Given this conclusion it is reasonable to suggest that the following two species are also present in the dark-yellow solution; certainly their formation is feasible given the reaction conditions and the fact the di-iodo species $[\text{PdI}_2\{\eta^2\text{-Ph}_2\text{PN(Et)}\text{PPh}_2\}]$ **3** is the major product.



1



4

Compound **1** would be expected to give rise to a singlet in its $^{31}\text{P}\{^1\text{H}\}$ spectrum. As discussed in section 2.2.2, the resonance recorded using an authentic sample of the compound does, indeed, occur at δ 31.8 *i.e.*, an exact match to the peak at δ 31.8 observed in **Fig. 2.3**. Compound **4** is a mixed chloro- iodo-species and, as such, the two P-atoms are in chemically distinct environments. Each P-atom will exhibit its own resonance and, moreover, will couple with the other P-atom. Thus, two well-separated doublets are expected, exactly as is observed in **Fig. 2.3**.

The ^1H NMR spectrum of $[\text{PdI}_2\{\eta^2\text{-Ph}_2\text{PN(Et)}\text{PPh}_2\}]$ **3** in CDCl_3 at room temperature exhibits resonances between δ 7.2 and δ 7.9 associated with the aromatic rings of the ligand, together with a triplet and a quartet centred at δ 3.0

and δ 0.7 respectively, that confirm the presence of the ethyl group of the ligand.

Single crystals of complex **3** were grown by the slow solvent diffusion of hexane into a dichloromethane solution of the compound. An X-ray crystal structure analysis confirmed that the complex is indeed, correctly formulated as $[\text{PdI}_2\{\eta^2\text{-Ph}_2\text{PN(Et)PPh}_2\}]$ **3**. A perspective view of the molecule is shown in **Fig. 2.4** and a full list of interatomic distances and angles are given in **Tables 2.17** and **2.18** respectively, at the end of this Chapter. There are no unusual intermolecular non-bonded contacts between the molecules in the crystal.

As shown in **Fig. 2.4** the diphosphazane ligand is coordinated in a chelating fashion. The overall molecular structure of this complex is very similar to that of complex **2**. The chelate bite angle [P1-Pd-P2=71.22(4) $^\circ$] shows much distortion from the value expected (90°) for a square-planar configuration. The bond angle at the nitrogen [P1-N-P2=100.24(19) $^\circ$] is considerably less than the idealised tetrahedral or trigonal angle. This indicates substantial strain in the 4-membered chelate ring. The Pd-I(1) and Pd-I(2) distances of 2.648(1) and 2.618(1) \AA respectively are typical of Pd-I bond lengths⁽²⁵⁾. The Pd-P(1) and Pd-P(2) interatomic distances of 2.22(12) and 2.23(12) \AA respectively are also similar to those reported in the literature^(10,11).

Complex **2** was also reacted with CO, $\text{CH}_3\text{O}_2\text{CC}\equiv\text{CCO}_2\text{CH}_3$ and AgPF_6 in an attempt to form A-frame type complexes.

The reaction with CO was effected by bubbling the gas through a solution of $[\text{Pd}_2\text{Cl}_2\{\mu\text{-Ph}_2\text{PN(Et)PPh}_2\}_2]$ **2** in CH_2Cl_2 at room temperature. The colour of the

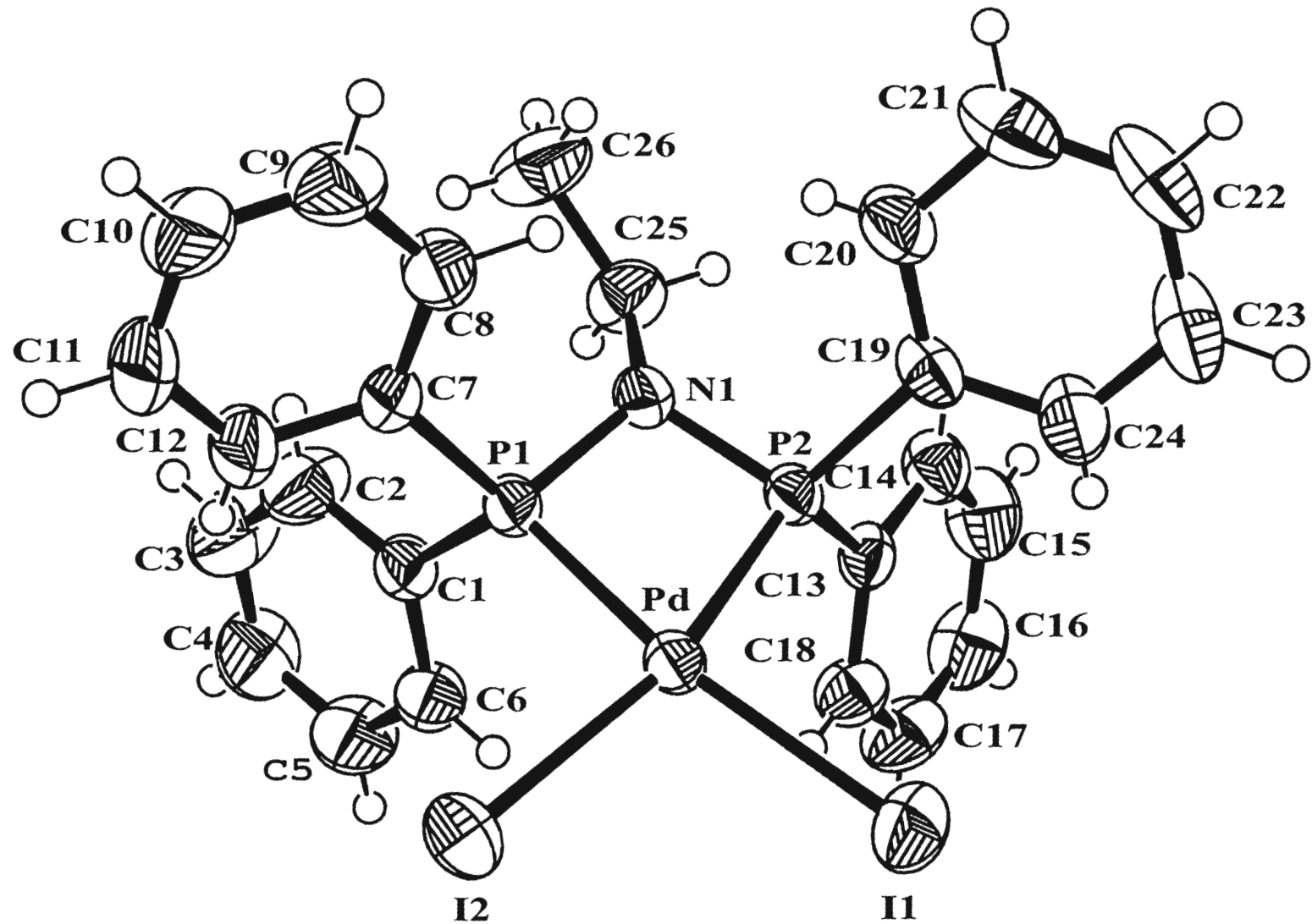


Fig. 2.4: Molecular Structure of $[\text{PdI}_2\{\eta^2\text{-Ph}_2\text{PN}(\text{Et})\text{PPh}_2\}]$ 3

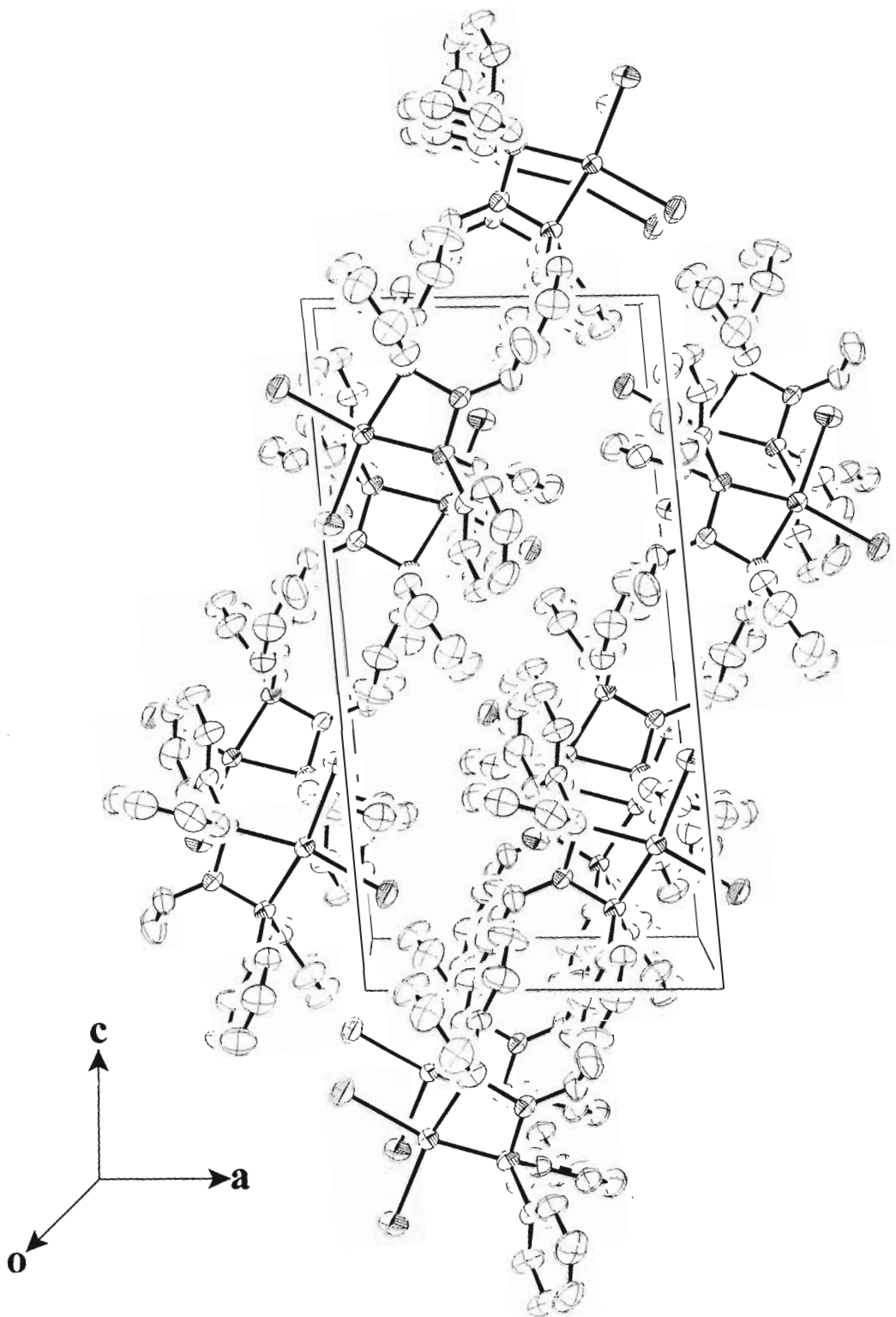


Fig. 2.5: Packing diagram of $[PdI_2\{\eta^2-Ph_2PN(Et)PPh_2\}]$ 3

solution turned from red-orange to a yellow colour, indicating that a reaction had, indeed, taken place. However, it was not possible to isolate any product despite repeated attempts using a variety of reaction conditions.

A solution in CH_2Cl_2 of $\text{CH}_3\text{O}_2\text{CC}\equiv\text{CCO}_2\text{CH}_3$ was added to an equimolar amount of $[\text{Pd}_2\text{Cl}_2\{\mu\text{-Ph}_2\text{PN}(\text{Et})\text{PPh}_2\}_2]$ **2** in CH_2Cl_2 at room temperature and the reaction allowed to proceed for 30 minutes. Again the colour of the solution turned from red-orange to yellow, indicating that a reaction had taken place. No product could be isolated however.

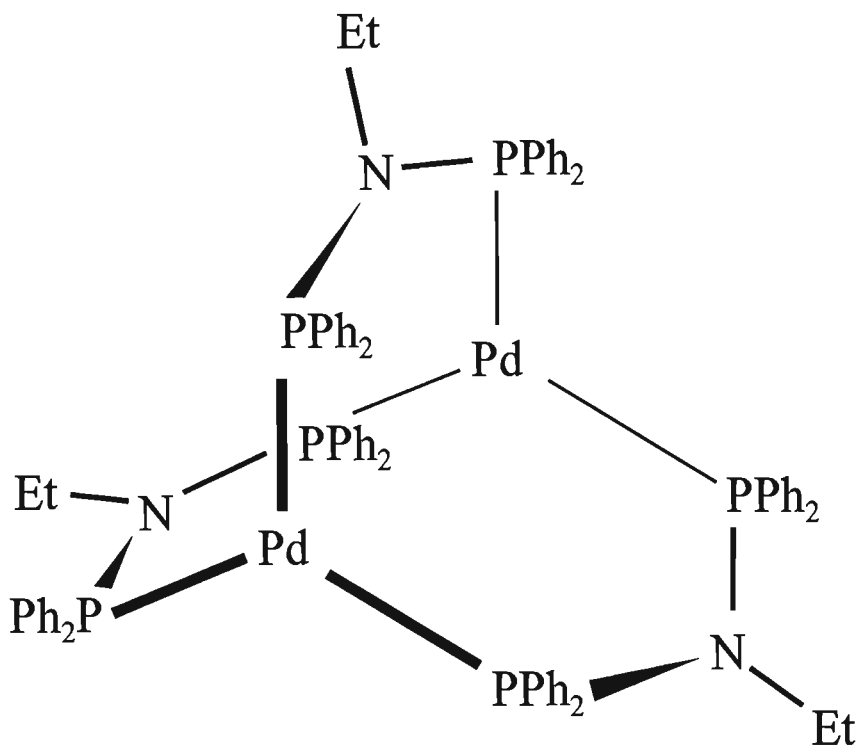
Finally, an equimolar amount of AgPF_6 dissolved in acetonitrile was added to **2** in acetonitrile solution at room temperature and the reaction allowed to proceed for 24 hours. Acetonitrile was used as it is a coordinating solvent. It is noted that Balch and co-workers successfully synthesised $[\text{Pd}_2(\mu\text{-CH}_3\text{CN})\text{Cl}_2(\mu\text{-dppm})_2]^+$ ⁽²⁸⁾ by using acetonitrile as a solvent. However, it was not possible to isolate a defined product.

Clearly, the above addition reactions are reversible. The lower stability of the addition products for the diphosphazane-ligand-bridged complex **2**, as compared to those for the dppm-bridged analogue, may be associated with the reduced electron-donating power of $\text{Ph}_2\text{PN}(\text{Et})\text{PPh}_2$ compared to $\text{Ph}_2\text{PCH}_2\text{PPh}_2$. This implies that complex **2** is less susceptible to electrophilic addition by CO , $\text{CH}_3\text{O}_2\text{CC}\equiv\text{CCO}_2\text{CH}_3$ and Ag^+ , and thus these reactions are less likely to proceed to completion.

2.2.5 Reactions of the dppea ligand with $[\text{Pd}_2(\text{dba})_3]$

The purpose of the reaction of the dppea ligand with $[\text{Pd}_2(\text{dba})_3]$ was to attempt

to synthesise the dipalladium(0) species, $[\text{Pd}_2\{\mu\text{-Ph}_2\text{PN(Et)}\text{PPh}_2\}_3]$ **5** (shown below) in which the palladium atoms are bridged by three dppea ligands. Complexes of this type have been synthesised before *e.g.*, $[\text{Pt}_2\{\mu\text{-F}_2\text{PN(Me)}\text{PF}_2\}_3(\text{PPh}_3)]^{(25)}$ and $[\text{Pd}_2\{\mu\text{-(PhO)}_2\text{PN(Me)}\text{P(OPh)}_2\}_3]^{(18)}$.



5

Thus, a toluene solution of $[\text{Pd}_2(\text{dba})_3]$ was reacted with 3 equivalents of $\text{Ph}_2\text{PN(Et)}\text{PPh}_2$. An excess of ligand was used in the hope of obtaining the desired product in good yield. However the $^{31}\text{P}\{^1\text{H}\}$ NMR spectrum of the orange-red product mixture showed that more than one product was formed in this reaction. This spectrum is illustrated in **Fig. 2.6** below.

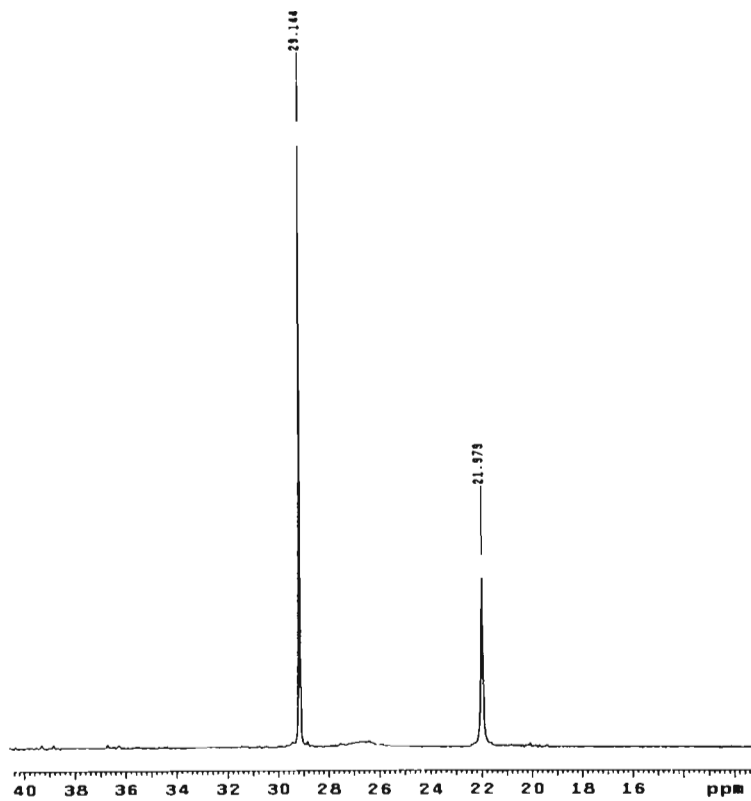


Fig. 2.6: The $^{31}\text{P}\{\text{H}\}$ NMR spectrum of the orange-red product mixture. This spectrum was obtained by taking the product solution to dryness and dissolving the residue in C_6D_6

Assignment of these peaks was difficult and thus an attempt was made to isolate pure compounds using fractional crystallisation methods. Careful addition of hexane to the toluene solution led to the co-precipitation of red and yellow crystals. Examination of these crystals under a microscope showed that they had different morphologies. Whereas the red crystals are blocklike, the yellow crystals are needle-shaped. The microscope view suggested that both sets of crystal were single, and thus they were hand-separated with a view to determining their crystal structures.

The red crystals were assigned to the monoclinic crystal system on the basis of the setting angles of 25 accurately centred reflections with $\theta \leq 12^\circ$. Three space groups are possible on the basis of the systematic absences $hkl; h+k = 2n+1$ viz. C2, Cm and C2/m. Solution of the Patterson function showed clearly the positions of the Pd atoms. An electron-density map phased on the Pd atoms revealed the positions of three dppea ligands all bridging the two Pd atoms. This solution is consistent with the formulation of the compound as $[Pd_2\{\mu\text{-Ph}_2PN(Et)PPh_2\}_3]$. Unfortunately, there is considerable disorder associated with the phenyl groups and all attempts to refine the structure in a meaningful way proved fruitless. Since only a few hand-selected red crystals of this dipalladium(0) species could be isolated (of which most were used in preliminary X-ray photography) it was not possible to employ other methods of characterisation to confirm the formulation of the compound as the triply-bridged species. However, the colour red is consistent with a dipalladium(0) compound; $[Pd_2\{\mu\text{-(PhO)}_2PN(Me)P(OPh)_2\}_3]^{(18)}$ for example, is red. Thus there was a measure of confidence in concluding that the formula of the red crystals is $[Pd_2\{\mu\text{-Ph}_2PN(Et)PPh_2\}_3]$. Several attempts were made to improve the yield of this compound since it is the desired product. To this end a wide range of ligand to $[Pd_2(dbu)_3]$ mole ratios, temperatures, and reaction times were employed; the order of addition was varied as well. Other solvents (such as CH_2Cl_2 and CH_3CN) were also used. No success was achieved, the relative proportions of the various species formed staying much the same, as indicated by the $^{31}P\{^1H\}$ NMR spectrum of the product mixture. Attempts to separate the products using chromatographic methods led to decomposition of the compounds as evidenced by the formation of a black residue of palladium metal.

The yellow crystals were assigned to the triclinic crystal system on the basis of the setting angles of 25 accurately centred reflections with $\theta \leq 12^\circ$. Of the two

triclinic space groups, $P\bar{1}$, and $P\bar{1}\bar{1}$, the former gave the best solution refinement of the structure. The X-ray analysis showed this product to be a totally unexpected one: the yellow crystals contained the oxidised form of the dppea ligand *i.e.*, $\text{Ph}_2\text{P}(\text{O})\text{N}(\text{Et})\text{P}(\text{O})\text{Ph}_2$, as well as free dibenzylideneacetone (dba) molecules and water molecules. As such it can be described as a clathrate. **Fig. 2.7** gives a view of the packing of these molecules in relation to the unit cell outline. A useful description of the crystal structure is that the $\text{Ph}_2\text{P}(\text{O})\text{N}(\text{Et})\text{P}(\text{O})\text{Ph}_2$ molecules form a column along a direction closely parallel to the [c]-axis; the dba molecules do the same in an adjacent column.

Thus, the structure is one of alternating columns of $\text{Ph}_2\text{P}(\text{O})\text{N}(\text{Et})\text{P}(\text{O})\text{Ph}_2$ and dba molecules roughly lined-up parallel to the [c]-axis. (Note: The [c]-axis is about double the lengths of the other two axes consistent with this structural motif.) Interestingly, there are no unusually short non-bonded contacts between columns or within columns. The crystals are, therefore, accurately described as molecular clathrates.

Fig. 2.8 gives a view of the two independent $\text{Ph}_2\text{P}(\text{O})\text{N}(\text{Et})\text{P}(\text{O})\text{Ph}_2$, dba and water molecules in the triclinic unit cell ($Z = 2$). This indicates the atom labelling and gives a perspective view of each molecule. The two independent molecules are labelled A and B in the list of atom coordinates, interatomic distances and angles, and anisotropic displacement parameters, see **Tables 2.22 to 2.26**. There is no significant difference between the structural parameters for independent molecules of the same type and thus the following discussion will be based on averaged values for the important bonding parameters.

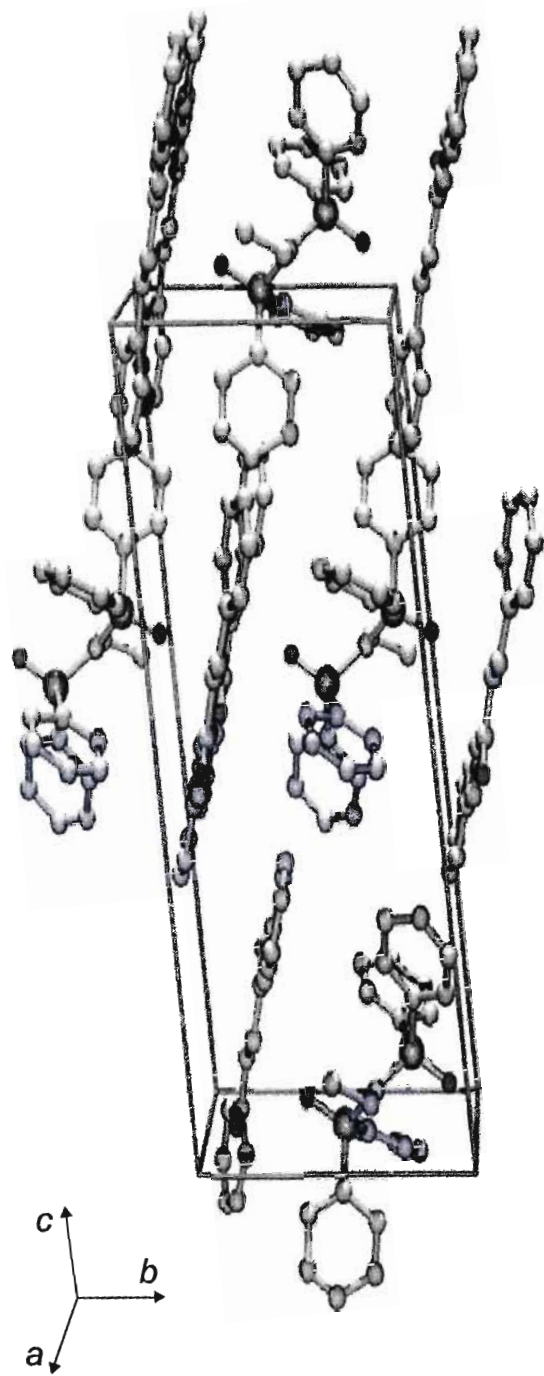


Fig. 2.7: Packing diagram of $\text{Ph}_2\text{P}(\text{O})\text{N}(\text{Et})\text{P}(\text{O})\text{Ph}_2 \cdot \text{dba} \cdot \text{H}_2\text{O}$. The water molecules are omitted for clarity.

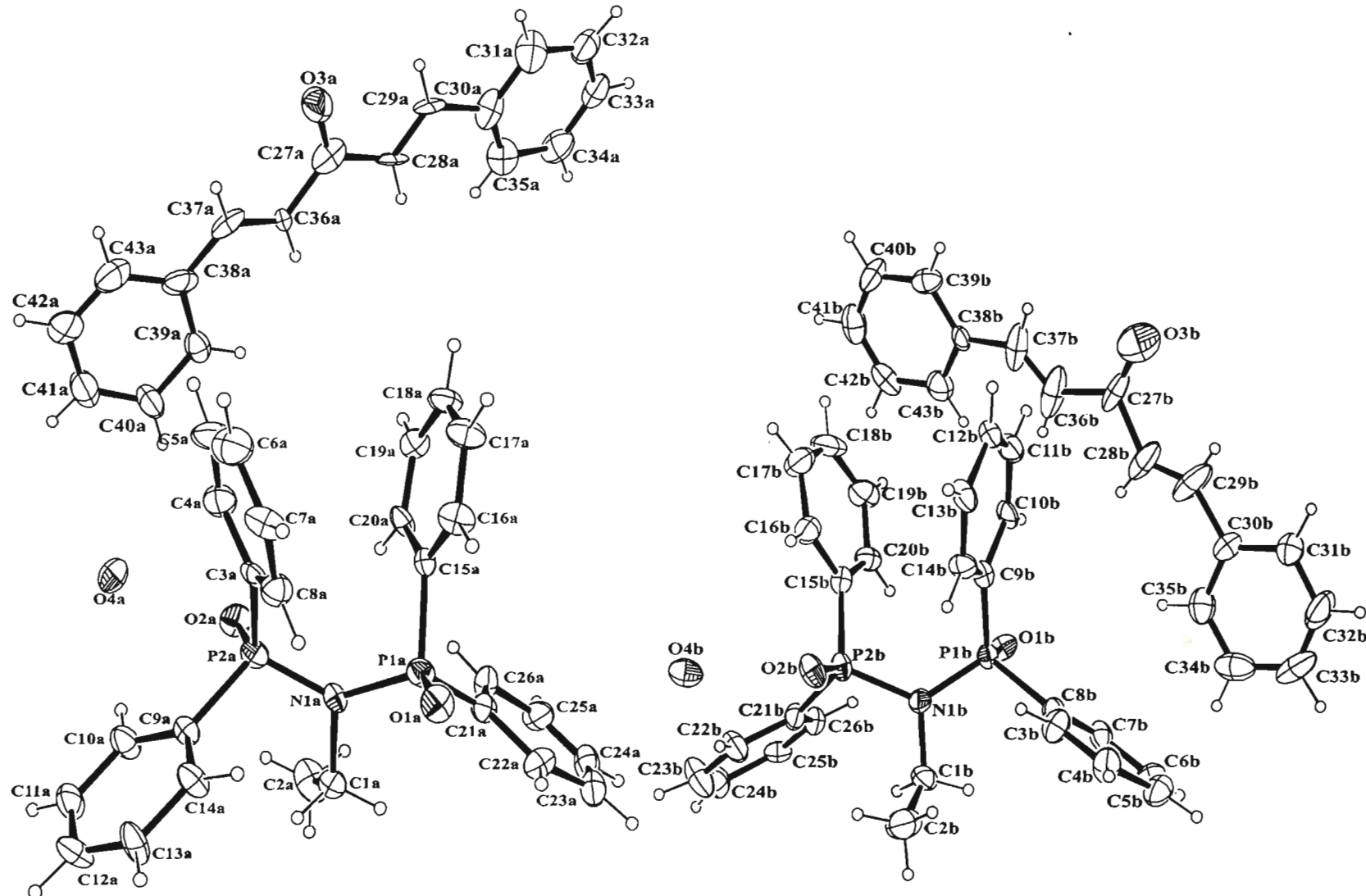


Fig. 2.8: Perspective view of the contents of the asymmetric unit in $\text{Ph}_2\text{P}(\text{O})\text{N}(\text{Et})\text{P}(\text{O})\text{Ph}_2$, dba, H_2O showing the atom labelling scheme.
Note: There are 2 formula units per asymmetric unit. The H-atoms of the water molecules were not located

The P=O groups adopt an *anti*- conformation. As illustrated in Fig. 2.7 one pair of phenyl rings is approximately parallel, the averaged dihedral angles between their planes being 28.5°. The distances between equivalent carbon atoms in these two rings range from 3.1 to 4.7 Å, values which may be compared with the upper distance limit of 3.8 Å for π -interactions in organic species⁽³⁴⁾. It is concluded that, though there may be a weak π -interaction between the phenyl rings, it is fundamentally packing forces *i.e.*, non-bonded interactions that are responsible for the observed conformation of the Ph₂P(O)N(Et)P(O)Ph₂ molecule.

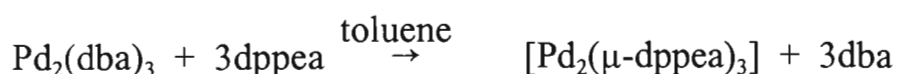
The average P-N-P angle is 128.8° a value close to that reported for the ligand in the complex [Th(NO₃)₂{Ph₂P(O)N(Prⁱ)P(O)Ph₂}₃]²⁺ (120.8°)⁽³⁵⁾. This indicates approximate sp²-hybridization at the N-atom. The angles subtended at the P-atoms fall in the range 104.6(5) to 115.5(5)° and, as such, span the idealised tetrahedral value of 109.5°. The P-N distances range from 1.725(10) to 1.633(10) Å and are close to literature values⁽³⁶⁾.

A small sample of the yellow crystals was dissolved in CDCl₃ and the ³¹P{¹H} NMR spectrum of the solution recorded. This spectrum exhibited a peak at δ 30.6 a value which corresponds closely to the peak at δ 29.1 in the spectrum of the orange-red product mixture (see Fig. 2.5). The small difference is probably due to the different solvents used to record the spectra. The conclusion must be that this peak is assigned to the oxidised form of the dppea ligand *i.e.*, Ph₂P(O)N(Et)P(O)Ph₂. It is noted that the upfield shift of the ³¹P resonance from δ 62.3 for the parent (unoxidised) ligand to δ 29.1 for the oxidised form. There appears to be no obvious explanation for this shift. However, it is well-established that there is no simple relationship between the ³¹P chemical shift and the electron density at the P-atom, as predicted on the basis of the electron-withdrawing/donating

effects of the substituents attached to the P-atom⁽²⁶⁾.

Unfortunately, very few of the red crystals were available to record their $^{31}\text{P}\{^1\text{H}\}$ NMR spectrum. A further problem is that the red compound appeared to decompose in the NMR solvent (CDCl_3 and C_6D_6), as evidenced by a black precipitate on the bottom of the NMR tube. The black solid is probably Pd metal. As a result it was not possible to record a reliable $^{31}\text{P}\{^1\text{H}\}$ NMR spectrum of the red solid. Nevertheless it is concluded that the second peak in **Fig. 2.5** is correctly assigned to $[\text{Pd}_2\{\mu\text{-Ph}_2\text{PN}(\text{Et})\text{PPh}_2\}]_3$. However, the red crystals were isolated in such low yield that this must be regarded as a tentative conclusion.

The reaction of the dppea ligand with $[\text{Pd}_2(\text{dba})_3]$ as carried-out in this work may be summarised as follows:



The likely source of oxygen is dissolved oxygen in the solvent. Certainly, the reaction mixture was kept under an atmosphere of nitrogen at all times. It is well-established that compounds of Pd(0) are extremely air-sensitive *e.g.*, $[\text{Pd}_2(\mu\text{-dppm})_3]$ ⁽³⁷⁾ and $[\text{Pd}_2\{\mu\text{-(PhO)}_2\text{PN}(\text{Me})\text{P}(\text{OPh})_2\}]_3$ ⁽¹⁸⁾. Possible evidence for the above reaction scheme is that black palladium metal was observed to deposit on the sides of the flask during the course of the reaction. Also as already noted, attempts to record the $^{31}\text{P}\{^1\text{H}\}$ NMR spectrum of the red crystals of $[\text{Pd}_2\{\mu\text{-Ph}_2\text{PN}(\text{Et})\text{PPh}_2\}]_3$ led to the appearance of a black solid on the sides of the NMR tube, presumably due to Pd metal.

The seems to be no doubt that the desired product $[\text{Pd}_2\{\mu\text{-Ph}_2\text{PN}(\text{Et})\text{PPh}_2\}_3]$ is formed under the conditions of the reaction, possibly in a good initial yield. However, mere traces of dissolved oxygen lead to its decomposition to palladium metal with the concomitant oxidation of the dppea ligand. Since the dppea ligand is known to be stable in toluene solution under the conditions of the reaction, it appears that either (i) the ligand is oxidised while coordinated to the metal or (ii) the palladium metal heterogeneously catalyses the oxidation of free dppea ligand.

Clearly, future work should involve repetition of this reaction under rigorous exclusion of oxygen, in particular, from the solvent.

2.4 EXPERIMENTAL

2.4.1 Synthesis

General experimental methods are outlined in Appendix A1 and A2. Sources of commercially available chemicals are given in Appendix B.

2.4.1.1: Synthesis of $\text{Ph}_2\text{PN}(\text{Et})\text{PPh}_2$, dppea⁽³¹⁾

Chlorodiphenylphosphine (9ml, 50 mmol) was added dropwise to ethylamine (12.5ml, 25 mmol) at -10° under dry nitrogen. [Distilled triethylamine (7ml, 50 mmol) was also added to the mixture to remove excess HCl that forms in the reaction.] The reactants were stirred for 2 hours, sodium-dried ether added to effect precipitation. The solid was filtered off and dried by removing the ether under vacuum. This solid was washed with ethanol and filtered off and dried under vacuum. Yield: 3.5g (37%).

2.4.1.2: Synthesis of $[\text{PdCl}_2\{\eta^2\text{-Ph}_2\text{PN(Et)PPh}_2\}]$ 1

A dichloromethane solution (20 ml) of $[\text{PdCl}_2(\text{PhCN})_2]$ ⁽³⁸⁾ (25mg, 0.065 mmol) was added dropwise to a suspension in dichloromethane (10 ml) of $\text{Ph}_2\text{PN(Et)PPh}_2$ ⁽³¹⁾ (26mg, 0.0629mmol). The resultant light yellow coloured solution was stirred at room temperature for 24 hours. The volume of the solution was then decreased to ca. 5 ml under reduced pressure. A light yellow coloured precipitate was obtained after filtration. This was recrystallised from dichloromethane/hexane to afford a yellow crystalline material. Yield: 30mg (77%).

2.4.1.3: Synthesis of $[\text{Pd}_2\text{Cl}_2\{\mu\text{-Ph}_2\text{PN(Et)PPh}_2\}_2]$ 2

A dichloromethane solution (15 ml) of $[\text{PdCl}_2(\text{PhCN})_2]$ (25 mg, 0.065 mmol) was added dropwise to a dichloromethane suspension (15 ml) of $\text{Ph}_2\text{PN(Et)PPh}_2$ (54 mg, 0.130 mmol). Solid $\text{Pd}_2(\text{dba})_3\cdot\text{CHCl}_3$ ⁽³⁹⁾ (30 mg, 0.032 mmol) was then added to the mixture of $[\text{PdCl}_2(\text{PhCN})_2]$ and $\text{Ph}_2\text{PN(Et)PPh}_2$. The resultant solution was stirred at room temperature for 30 minutes. After 30 minutes, the red solution was filtered and the filtrate condensed to a volume of 5 ml under reduced pressure. Hexane (20 ml) was added to the dichloromethane solution to precipitate the product. The red-orange solid was collected by filtration. The product was purified by dissolution in dichloromethane, filtration of the solution, and reprecipitation of the product by the addition of hexane. The red-orange, crystalline product was dried under vacuum. Yield: 40mg (55%).

2.4.1.4: Synthesis of $[\text{PdI}_2\{\eta^2\text{-Ph}_2\text{PN(Et)PPh}_2\}]$ 3

A dichloromethane solution (5 ml) of I_2 , (11.4 mg, 0.045 mmol) was added dropwise

to a dichloromethane solution (10 ml) of $[\text{Pd}_2\text{Cl}_2\{\mu\text{-Ph}_2\text{PN(Et)PPh}_2\}_2]$ (50 mg, 0.045 mmol) and the resultant solution stirred at room temperature for an hour. The colour of the solution turned from red-orange to dark-yellow. The solution was evaporated to *ca.* 5 ml under reduced pressure. Hexane (10 ml) was added slowly and the mixture allowed to stand overnight at 0°C. The orange-yellow crystals that formed were isolated and then washed with hexane and dried *in vacuo*. Yield: 20mg (57%).

2.4.1.5: Synthesis of $[\text{Pd}_2\{\mu\text{-Ph}_2\text{PN(Et)PPh}_2\}_3]$ 5 and $\text{Ph}_2\text{P(O)N(Et)P(O)Ph}_2$. dba. H_2O

The complex $[\text{Pd}_2(\text{dba})_3]\text{CHCl}_3$ (30mg, 0.0328mmol) was dissolved in toluene (10 ml) and $\text{Ph}_2\text{PN(Et)PPh}_2$ (40mg, 0.0968mmol) also in toluene (10 ml) was added dropwise with stirring. Stirring was continued for 2 hours and the solvent was evaporated to *ca.* 5 ml under reduced pressure and the black precipitate (of palladium metal) was removed by filtration. Hexane (15 ml) was added to the filtrate and the flask placed in a refrigerator at -10°C for a period of *ca.* 48h. Red and yellow crystals appeared at the bottom of the flask. The solvent was removed by decantation and the crystals transferred to a microscope slide. The red crystals of $[\text{Pd}_2\{\mu\text{-Ph}_2\text{PN(Et)PPh}_2\}_3]$ 5 and the yellow crystals of $\text{Ph}_2\text{P(O)N(Et)P(O)Ph}_2$. dba. H_2O were separated by hand. Owing to the very small amount of product that formed (see text) it was not possible to estimate yields.

Table 2.2 Physical and microanalytical data for Ph₂PN(Et)PPh₂ and its complexes

Complex	Colour	Molar Mass g.mol ⁻¹	Analysis: Found(Calculated)		
			%C	%H	%N
Ph ₂ PN(Et)PPh ₂	White	411.00	63.20 (63.26)	5.97 (6.08)	3.39 (3.40)
[PdCl ₂ {η ² -Ph ₂ PN(Et)PPh ₂ }] 1	Light Yellow	590.72	52.95 (52.88)	4.70 (4.23)	2.02 (2.37)
[Pd ₂ Cl ₂ {μ-Ph ₂ PN(Et)PPh ₂ } ₂] 2	Red-Orange	1110.60	55.29 (56.18)	4.81 (4.50)	2.26 (2.52)
[PdI ₂ {η ² -Ph ₂ PN(Et)PPh ₂ }] 3	Orange-Yellow	773.00	40.36 (40.36)	3.71 (3.23)	1.32 (1.81)
[Pd ₂ {μ-Ph ₂ PN(Et)PPh ₂ } ₃] 5	Red	1445.00	Yield too low to obtain satisfactory microanalytical data		
Ph ₂ P(O)N(Et)P(O)Ph ₂ .dba.H ₂ O	Yellow	673.80			

Table 2.3 NMR spectroscopic data for Ph₂PN(Et)PPh₂ and its complexes

Complex	¹ H NMR ^a δ	³¹ P{ ¹ H} NMR ^b δ
Ph ₂ PN(Et)PPh ₂	7.2-7.5(m, 10H) 3.3(t, 2H) 0.7(q, 3H)	62.3(Ss)
[PdCl ₂ {η ² -Ph ₂ PN(Et)PPh ₂ }] 1	7.1-7.9(m, 10H) 3.0(t, 2H) 0.8(q, 3H)	31.8(Ss)
[Pd ₂ Cl ₂ {μ-Ph ₂ PN(Et)PPh ₂ } ₂] 2	7.0-7.9(m, 20H) 2.5(t, 2H) 0.3(q, 3H)	78.1(Ss)
[PdI ₂ {η ² -Ph ₂ PN(Et)PPh ₂ }] 3	7.2-7.9(m, 10H) 3.0(t, 2H) 0.7(q, 3H)	24.9(Ss)
[Pd ₂ {μ-Ph ₂ PN(Et)PPh ₂ } ₃] 5	7.0-7.8(m, 60H) 3.2(t, 2H) 0.9(q, 3H)	21.9(s)
PPh ₂ (O)N(Et)P(O)Ph ₂ .dba	7.0-7.8(m, 30H) 3.3(t, 2H) 0.8(q, 3H)	29.1(Ss)

a. Ph₂PN(Et)PPh₂, 1, 2 and 3 run in CDCl₃, 5 run in C₆D₆. m = multiplet, t = triplet, q = quartet.

b. Ph₂PN(Et)PPh₂, 1, 2 and 3 run in CDCl₃, 5 run in C₆D₆. s = singlet, Ss = sharpsinglet

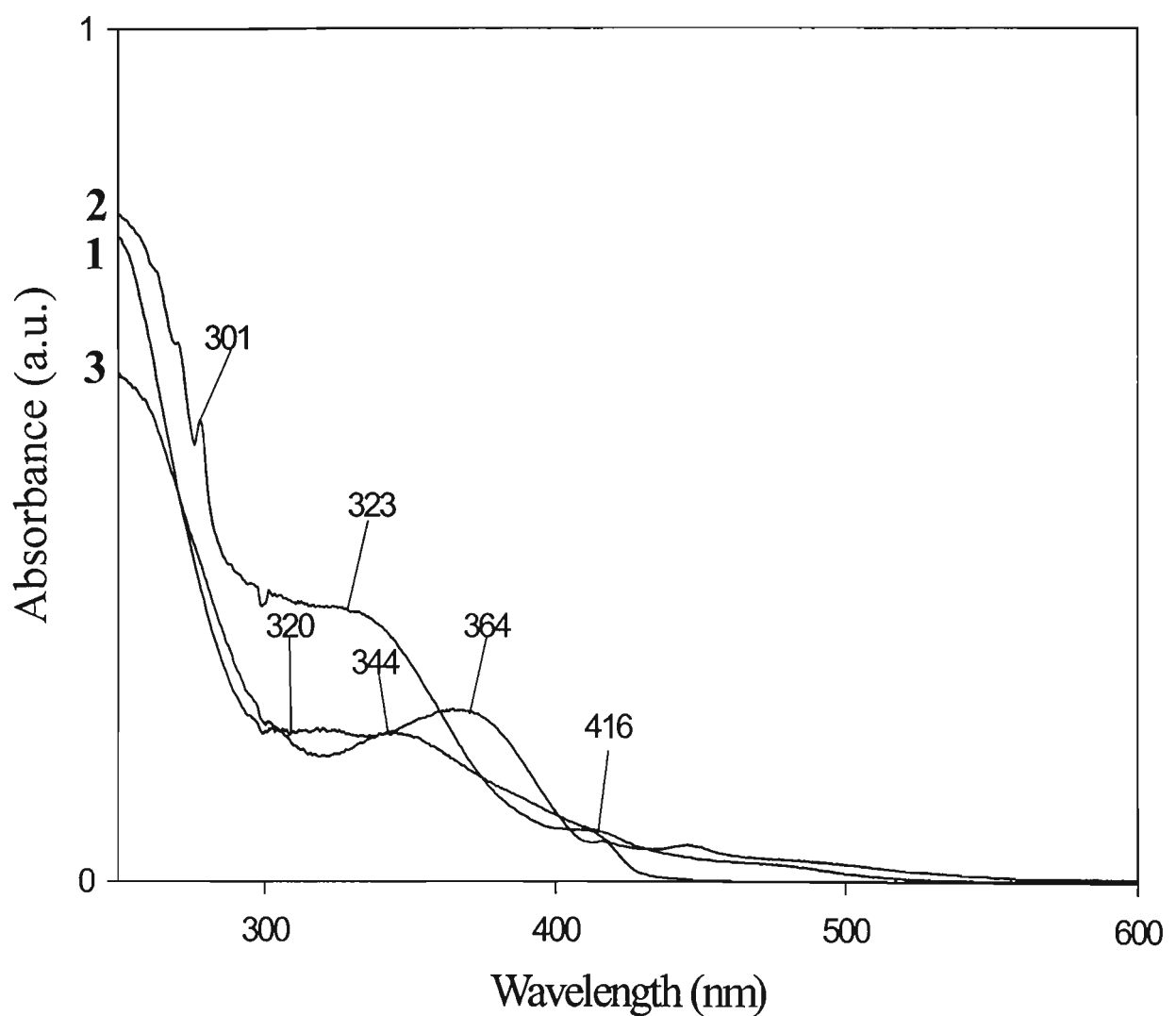


Fig. 2.9: UV/Vis spectra for complexes **1**, **2** and **3**

2.4.2 Crystal Structure Determination

2.4.2.1 X-ray diffraction study of $[\text{PdCl}_2\{\eta^2\text{-Ph}_2\text{PN(Et)PPh}_2\}]$ 1

Yellow single crystals of **1** were grown by slow vapour diffusion of hexane into a concentrated solution of **1** in dichloromethane. The general approach used for the intensity data collection and structure solution is described in Appendix A. The crystallographic data are given in **Table 2.4**, the fractional coordinates are given in **Table 2.5**, the anisotropic thermal parameters in **Table 2.8**, the interatomic distances in **Table 2.6** and the interatomic angles in **Table 2.7**. The hydrogen atom coordinates and isotropic displacement parameters are given in **Table 2.9**. A list of observed and calculated structure factors is available on request⁽⁴⁰⁾.

2.4.2.2 X-ray diffraction study of $[\text{Pd}_2\text{Cl}_2\{\mu\text{-Ph}_2\text{PN(Et)PPh}_2\}]_2$ 2

Red-orange single crystals **2** were grown by slow vapour diffusion of hexane into a concentrated solution of **2** in dichloromethane. The general approach used for the intensity data collection and structure solution is described in Appendix A. The crystallographic data are given in **Table 2.10**, the fractional coordinates are given in **Table 2.11**, the anisotropic thermal parameters in **Table 2.14**, the interatomic distances in **Table 2.12** and the interatomic angles in **Table 2.13**. A list of observed and calculated structure factors is available on request⁽⁴⁰⁾.

2.4.2.3 X-ray diffraction study of $[\text{PdI}_2\{\eta^2\text{-Ph}_2\text{PN(Et)PPh}_2\}]$ 3

Orange-yellow single crystals of **3** were grown by slow vapor diffusion of hexane into a concentrated solution of **3** in dichloromethane. The general approach used for

the intensity data collection and structure solution is described in Appendix A. The crystallographic data are given in **Table 2.15**, the fractional coordinates are given in **Table 2.16**, the anisotropic thermal parameters in **Table 2.19**, the interatomic distances in **Table 2.17** and the interatomic angles in **Table 2.18**. The hydrogen atom coordinates and isotropic displacement parameters are given in **Table 2.20**. A list of observed and calculated structure factors is available on request⁽⁴⁰⁾.

2.4.2.4 X-ray diffraction study of Ph₂P(O)N(Et)PPh₂O. dba. H₂O

Yellow single crystals of Ph₂P(O)N(Et)PPh₂. dba. H₂O were grown by slow cooling of the toluene/hexane solution obtained in the reaction of dppea with Pd₂(dba)₃ (see **Section 2.4.1.5**) The general approach used for the intensity data collection and structure solution is described in Appendix A. The crystallographic data are given in **Table 2.21**, the fractional coordinates are given in **Table 2.22**, the anisotropic thermal parameters in **Table 2.25**, the interatomic distances in **Table 2.23** and the interatomic angles in **Table 2.24**. The hydrogen atom coordinates and isotropic displacement parameters are given in **Table 2.26**. A list of observed and calculated structure factors is available on request⁽⁴⁰⁾.

Table 2.4
Crystal Data and Details of the Crystallographic Analysis for [PdCl₂{η²-Ph₂PN(Et)PPh₂}] 1

Empirical formula	C26 H25 Cl2 N P2 P
Formula weight	590.71
Temperature	293(2) K
Wavelength	0.71069 Å
Crystal system, space group	Orthorhombic <i>Pbca</i>
a(Å)	13.811(3)
b(Å)	20.799(6)
c(Å)	17.544(6)
α(°) A	90.00
β(°)	90.00
γ(°)	90.00
V(Å ³)	5040(3)
Z,	8
Calculated density	1.557 Mg/m ³
Absorption coefficient	1.091 mm ⁻¹
F(000)	2384
Crystal size	0.55 x 0.35 x 0.20 mm
Theta range for data collection	2.12 to 22.97 deg.
Index ranges	-1<=h<=15, -1<=k<=22, -1<=l<=19
Reflections collected / unique	4374 / 3501 [R(int) = 0.0480]
Completeness to 2theta = 22.97	99.9%
Max. and min. transmission	0.8114 and 0.5853
Refinement method	Full-matrix least-squares on F ²
Data / restraints / parameters	3501 / 0 / 389
Goodness-of-fit on F ²	1.218
Final R indices [I>2sigma(I)]	R1 = 0.0390, wR2 = 0.1016
R indices (all data)	R1 = 0.0585, wR2 = 0.1284
Largest diff. peak and hole	0.886 and -0.991 e.Å ⁻³

Table 2.5 Atomic coordinates ($\times 10^4$) and equivalent isotropic displacement parameters ($\text{\AA}^2 \times 10^3$) for $[\text{PdCl}_2\{\eta^2\text{-Ph}_2\text{PN(Et)PPh}_2\}]$ 1.
U(eq) is defined as one third of the trace of the orthogonalized U_{ij} tensor.

	x	y	z	U(eq)
Pd	2112(1)	1649(1)	120(1)	33(1)
Cl(1)	2088(1)	726(1)	905(1)	55(1)
Cl(2)	1588(1)	2358(1)	1087(1)	50(1)
P(1)	2173(1)	2375(1)	-803(1)	34(1)
P(2)	2599(1)	1170(1)	-943(1)	36(1)
N	2665(3)	1867(2)	-1453(3)	39(1)
C(1)	2942(4)	3063(3)	-693(3)	38(1)
C(2)	2582(5)	3571(3)	-262(4)	50(2)
C(3)	3169(6)	4087(4)	-93(5)	59(2)
C(4)	4086(6)	4120(4)	-389(5)	61(2)
C(5)	4447(5)	3623(4)	-829(4)	54(2)
C(6)	3876(5)	3098(3)	-972(4)	48(2)
C(7)	1029(4)	2687(3)	-1132(3)	37(1)
C(8)	205(4)	2547(4)	-733(4)	50(2)
C(9)	-684(5)	2774(4)	-969(5)	63(2)
C(10)	-757(6)	3147(3)	-1612(5)	58(2)
C(11)	66(6)	3275(4)	-2016(5)	61(2)
C(12)	962(5)	3051(3)	-1780(4)	53(2)
C(13)	3768(4)	789(3)	-972(3)	41(1)
C(14)	4594(5)	1169(4)	-1035(4)	58(2)
C(15)	5502(6)	885(5)	-1045(5)	72(2)
C(16)	5580(6)	229(5)	-975(4)	73(3)
C(17)	4776(7)	-140(5)	-898(5)	67(2)
C(18)	3866(6)	131(4)	-891(4)	55(2)
C(19)	1724(4)	650(3)	-1388(3)	41(1)
C(20)	760(5)	733(3)	-1181(4)	48(2)
C(21)	55(6)	386(4)	-1536(5)	56(2)
C(22)	270(6)	-60(3)	-2082(4)	60(2)
C(23)	1216(7)	-151(4)	-2278(5)	67(2)
C(24)	1957(5)	201(3)	-1944(4)	46(2)
C(25)	2649(6)	1946(4)	-2287(4)	56(2)
C(26)	3392(9)	1568(5)	-2693(6)	79(3)

Table 2.6 Interatomic Distances (Å) for [PdCl₂{η²-Ph₂PN(Et)PPh₂}] 1

Pd-P(1)	2.2147(16)
Pd-P(2)	2.2192(17)
Pd-Cl(2)	2.3601(16)
Pd-Cl(1)	2.3634(17)
P(1)-N	1.698(5)
P(1)-C(1)	1.792(6)
P(1)-C(7)	1.803(6)
P(1)-P(2)	2.585(2)
P(2)-N	1.705(5)
P(2)-C(13)	1.800(6)
P(2)-C(19)	1.800(6)
N-C(25)	1.471(9)
C(1)-C(6)	1.381(9)
C(1)-C(2)	1.393(9)
C(2)-C(3)	1.377(10)
C(3)-C(4)	1.370(11)
C(4)-C(5)	1.383(11)
C(5)-C(6)	1.369(10)
C(7)-C(12)	1.369(9)
C(7)-C(8)	1.367(9)
C(8)-C(9)	1.379(10)
C(9)-C(10)	1.373(11)
C(10)-C(11)	1.366(11)
C(11)-C(12)	1.385(10)
C(13)-C(18)	1.382(9)
C(13)-C(14)	1.393(9)
C(14)-C(15)	1.386(10)
C(15)-C(16)	1.373(13)
C(16)-C(17)	1.357(13)
C(17)-C(18)	1.377(11)
C(19)-C(20)	1.391(9)
C(19)-C(24)	1.388(9)
C(20)-C(21)	1.362(9)
C(21)-C(22)	1.367(11)
C(22)-C(23)	1.363(12)
C(23)-C(24)	1.387(10)
C(25)-C(26)	1.477(11)

Table 2.7 Interatomic Angles ($^{\circ}$) for $[\text{PdCl}_2\{\eta^2\text{-Ph}_2\text{PN(Et)PPh}_2\}]$ 1

P(1)-Pd-P(2)	71.33(6)	P(1)-Pd-Cl(2)	96.41(6)
P(2)-Pd-Cl(2)	167.75(6)	P(1)-Pd-Cl(1)	168.54(6)
P(2)-Pd-Cl(1)	97.42(6)	Cl(2)-Pd-Cl(1)	94.83(7)
N-P(1)-C(1)	109.4(3)	N-P(1)-C(7)	111.0(3)
C(1)-P(1)-C(7)	105.5(3)	N-P(1)-Pd	94.73(18)
C(1)-P(1)-Pd	119.2(2)	C(7)-P(1)-Pd	116.49(19)
N-P(1)-P(2)	40.65(17)	C(1)-P(1)-P(2)	130.47(19)
C(7)-P(1)-P(2)	121.15(19)	Pd-P(1)-P(2)	54.41(5)
N-P(2)-C(13)	108.2(3)	N-P(2)-C(19)	108.6(3)
C(13)-P(2)-C(19)	108.9(3)	N-P(2)-Pd	94.38(17)
C(13)-P(2)-Pd	119.5(2)	C(19)-P(2)-Pd	115.5(2)
N-P(2)-P(1)	40.47(16)	C(13)-P(2)-P(1)	129.3(2)
C(19)-P(2)-P(1)	118.2(2)	Pd-P(2)-P(1)	54.25(5)
C(25)-N-P(1)	126.3(4)	C(25)-N-P(2)	128.0(5)
P(1)-N-P(2)	98.9(3)	C(6)-C(1)-C(2)	119.0(6)
C(6)-C(1)-P(1)	123.9(5)	C(2)-C(1)-P(1)	116.9(5)
C(3)-C(2)-C(1)	119.9(7)	C(4)-C(3)-C(2)	120.1(8)
C(3)-C(4)-C(5)	120.5(7)	C(6)-C(5)-C(4)	119.3(7)
C(5)-C(6)-C(1)	121.1(7)	C(12)-C(7)-C(8)	119.1(6)
C(12)-C(7)-P(1)	121.6(5)	C(8)-C(7)-P(1)	119.3(5)
C(7)-C(8)-C(9)	121.0(7)	C(8)-C(9)-C(10)	120.4(7)
C(11)-C(10)-C(9)	118.4(7)	C(10)-C(11)-C(12)	121.5(8)
C(7)-C(12)-C(11)	119.7(7)	C(18)-C(13)-C(14)	119.3(6)
C(18)-C(13)-P(2)	121.4(6)	C(14)-C(13)-P(2)	119.2(5)
C(15)-C(14)-C(13)	120.0(8)	C(16)-C(15)-C(14)	119.6(9)
C(17)-C(16)-C(15)	120.4(8)	C(16)-C(17)-C(18)	121.1(9)
C(17)-C(18)-C(13)	119.6(9)	C(20)-C(19)-C(24)	119.3(6)
C(20)-C(19)-P(2)	117.0(5)	C(24)-C(19)-P(2)	123.6(5)
C(21)-C(20)-C(19)	119.9(7)	C(20)-C(21)-C(22)	121.7(8)
C(23)-C(22)-C(21)	118.6(7)	C(22)-C(23)-C(24)	121.8(8)
C(23)-C(24)-C(19)	118.7(7)	N-C(25)-C(26)	114.2(7)

**Table 2.8 Anisotropic displacement parameters ($\text{\AA}^2 \times 10^3$) for
[PdCl₂{ η^2 -Ph₂PN(Et)PPh₂}] 1.**
The anisotropic displacement factor exponent takes the form:
-2 $\Pi^2 [h^2 a^{*2} U_{11} + \dots + 2 h k a^* b^* U_{12}]$

	U11	U22	U33	U23	U13	U12
Pd	30(1)	28(1)	42(1)	-1(1)	-1(1)-	1(1)
Cl(1)	55(1)	40(1)	68(1)	14(1)	2(1)	6(1)
Cl(2)	50(1)	49(1)	52(1)	-15(1)	4(1)	0(1)
P(1)	30(1)	27(1)	45(1)	-1(1)	2(1)	2(1)
P(2)	35(1)	27(1)	46(1)	-3(1)	2(1)	3(1)
N	39(3)	34(3)	43(3)	2(2)	7(2)	5(2)
C(1)	41(3)	29(3)	43(3)	4(3)	-2(3)	8(3)
C(2)	48(4)	36(4)	65(4)	1(3)	8(3)	-5(3)
C(3)	73(5)	29(4)	75(5)	-7(4)	-6(4)	-5(4)
C(4)	63(5)	42(4)	77(5)	14(4)	-26(4)	-17(4)
C(5)	34(4)	50(4)	80(5)	20(4)	-5(3)	-8(3)
C(6)	40(4)	41(4)	63(4)	2(3)	11(3)	7(3)
C(7)	35(3)	27(3)	50(4)	-1(3)	-2(3)	2(2)
C(8)	34(3)	59(4)	58(4)	9(4)	3(3)	9(3)
C(9)	41(4)	71(5)	76(5)	3(4)	5(4)	13(4)
C(10)	48(4)	47(4)	80(5)	-6(4)	-15(4)	5(3)
C(11)	70(6)	50(4)	62(5)	11(4)	-16(4)	12(4)
C(12)	47(4)	44(4)	69(5)	10(3)	6(4)	11(3)
C(13)	37(3)	45(4)	41(3)	-5(3)	0(3)	14(3)
C(14)	46(4)	50(5)	78(5)	-4(4)	-6(3)	7(3)
C(15)	37(4)	105(8)	73(5)	-11(5)	-11(4)	9(5)
C(16)	52(5)	103(8)	64(5)	-11(5)	2(4)	48(5)
C(17)	78(6)	63(6)	61(5)	-2(4)	0(4)	43(5)
C(18)	65(5)	43(4)	58(4)	-1(3)	-3(4)	18(4)
C(19)	46(3)	27(3)	51(4)	-2(3)	-5(3)	1(3)
C(20)	48(4)	39(4)	57(4)	-4(3)	-8(3)	2(3)
C(21)	45(4)	48(4)	75(5)	6(4)	-13(4)	0(4)
C(22)	72(5)	44(4)	65(5)	-1(4)	-23(4)	-15(4)
C(23)	105(7)	47(4)	48(5)	-14(4)	-11(5)	-7(4)
C(24)	54(4)	32(3)	51(4)	-4(3)	-2(3)	3(3)
C(25)	70(5)	45(4)	53(4)	2(3)	5(4)	8(4)
C(26)	109(9)	69(6)	59(6)	4(4)	28(6)	25(6)

Table 2.9 Hydrogen atom coordinates ($\times 10^4$) and isotropic displacement parameters ($\text{\AA}^2 \times 10^3$) for $[\text{PdCl}_2\{\eta^2\text{-Ph}_2\text{PN(Et)PPPh}_2\}]$ 1

	x	y	z	U(iso)
H(1)	1950(5)	3530(4)	0(4)	60(2)
H(2)	2930(4)	4390(3)	-160(3)	41(19)
H(3)	4480(6)	4460(4)	-240(4)	70(2)
H(4)	5110(5)	3670(3)	-1000(3)	41(16)
H(5)	4140(4)	2800(3)	-1220(3)	18(13)
H(6)	230(4)	2290(3)	-290(3)	32(15)
H(7)	-1220(7)	2660(4)	-730(5)	100(3)
H(8)	-1390(7)	3290(4)	-1860(5)	100(3)
H(9)	70(5)	3470(3)	-2430(4)	41(18)
H(10)	1470(5)	3160(3)	-2060(4)	45(18)
H(11)	4510(5)	1620(3)	-1120(4)	60(2)
H(12)	6000(6)	1110(4)	-1070(5)	80(3)
H(13)	6130(6)	10(4)	-1020(4)	80(2)
H(14)	4820(7)	-530(4)	-820(5)	90(3)
H(15)	3390(6)	-110(4)	-860(4)	60(3)
H(16)	590(4)	1030(3)	-770(3)	41(16)
H(17)	-470(5)	390(3)	-1310(4)	50(2)
H(18)	-180(5)	-350(3)	-2360(4)	56(18)
H(19)	1330(5)	-340(3)	-2620(4)	40(2)
H(20)	2650(5)	170(3)	-2090(4)	56(19)
H(21)	2030(6)	1810(4)	-2470(5)	70(3)
H(22)	2740(6)	2380(4)	-2370(5)	100(3)
H(23)	4020(5)	1740(3)	-2490(4)	50(2)
H(24)	3250(8)	1090(6)	-2690(6)	140(4)
H(25)	3230(8)	1630(5)	-3210(7)	130(4)

Table 2.10
Crystal data and Details of the Crystallographic Analysis for [Pd₂Cl₂{μ-Ph₂PN(Et)PPh₂}₂] 2

Empirical formula,	C52 H50 Cl2 N2 P4 Pd2
Formula weight	1110.52
Temperature	293(2) K
Wavelength	0.71069 Å
Crystal system	Triclinic
Space group	<i>P</i> ī
a(Å)	10.3594(14)
b(Å)	11.1754(15)
c(Å)	12.0007(16)
α(°)	108.619(11)
β(°)	111.601(12)
γ(°)	95.153(11)
V(Å ³)	1189.8(3)
Z	1
Calculated density	1.550 Mg/m ³
Absorption coefficient	1.041 mm ⁻¹
F(000)	562
Crystal size	0.39 x 0.18 x 0.15 mm
Theta range for data collection	2.18 to 22.97 deg.
Index ranges	-11<=h<=11; -12<=k<=12; -3<=l<=13
Reflections collected/unique	4592/3305 [R(int) = 0.0191]
Reflections observed (>2sigma)	2708
Refinement method	Full-matrix least-squares on F ²
Data / restraints / parameters	3305 / 0 / 415
Goodness-of-fit on F ²	1.115
Final R indices [I>2sigma(I)]	R1 = 0.0441 wR2 = 0.1349
R indices (all data)	R1 = 0.0596 wR2 = 0.1591
Largest diff. peak and hole	0.633 and -0.687 e.Å ⁻³

Table 2.11 Atomic coordinates ($\times 10^4$) and equivalent isotropic displacement parameters ($\text{\AA}^2 \times 10^3$) for $[\text{Pd}_2\text{Cl}_2\{\mu\text{-Ph}_2\text{PN(Et)PPh}_2\}_2]$ 2. U(eq) is defined as one third of the trace of the orthogonalized U_{ij} tensor.

	x	y	z	U(eq)
Pd	468(1)	3980(1)	4594(1)	36(1)
Cl	1552(2)	2257(2)	3881(3)	66(1)
N	-1124(6)	5121(6)	2285(6)	37(1)
C(25)	-1363(10)	5274(8)	1031(8)	55(2)
C(26)	-2804(11)	4526(12)	-88(9)	82(3)
P(1A)	338(4)	3478(3)	6381(3)	32(1)
C(1A)	1313(16)	2305(14)	6839(19)	41(5)
C(2A)	675(11)	1122(14)	6775(13)	48(4)
C(3A)	1520(20)	333(12)	7231(18)	59(5)
C(4A)	3000(20)	730(20)	7750(20)	72(10)
C(5A)	3635(11)	1910(20)	7820(20)	59(9)
C(6A)	2793(17)	2700(12)	7360(20)	39(6)
C(7A)	-1520(8)	2877(12)	6109(11)	39(4)
C(8A)	-2557(11)	2628(13)	4876(10)	63(5)
C(9A)	-3979(10)	2113(14)	4549(10)	76(7)
C(10A)	-4363(9)	1846(14)	5455(12)	62(5)
C(11A)	-3326(13)	2096(17)	6687(11)	58(6)
C(12A)	-1905(12)	2611(16)	7014(9)	71(7)
P(2A)	254(4)	4424(3)	2940(3)	31(1)
C(13A)	1870(8)	5493(9)	3194(10)	43(4)
C(14A)	3141(10)	5088(9)	3520(10)	43(4)
C(15A)	4411(8)	5925(12)	3839(10)	55(5)
C(16A)	4410(10)	7166(11)	3832(11)	56(5)
C(17A)	3139(14)	7571(9)	3506(14)	60(7)
C(18A)	1869(10)	6734(10)	3188(13)	46(5)
C(19A)	-118(12)	2975(10)	1482(9)	32(4)
C(20A)	497(12)	2962(13)	627(13)	46(5)
C(21A)	52(18)	1894(16)	-527(13)	56(7)
C(22A)	-1008(18)	839(13)	-827(11)	73(13)
C(23A)	-1623(14)	851(10)	28(12)	61(5)
C(24A)	-1178(14)	1920(12)	1182(11)	56(6)
P(1B)	-1234(4)	3805(3)	2536(3)	30(1)

Table 2.11 / Cont.

C(1B)	-3028(11)	3304(11)	2406(11)	36(3)
C(2B)	-3136(10)	2665(11)	3201(10)	52(4)
C(3B)	-4469(13)	2189(12)	3118(12)	58(5)
C(4B)	-5693(9)	2352(14)	2240(14)	66(6)
C(5B)	-5585(12)	2992(17)	1446(14)	55(7)
C(6B)	-4252(16)	3468(14)	1529(12)	64(9)
C(7B)	-1218(9)	2558(7)	1111(3)	35(4)
C(8B)	-2370(9)	1506(10)	263(4)	45(4)
C(9B)	-2293(13)	586(8)	-796(3)	61(5)
C(10B)	-1065(14)	719(12)	-1007(3)	67(12)
C(11B)	87(11)	1771(15)	-159(4)	47(6)
C(12B)	10(10)	2691(11)	900(3)	45(5)
P(2B)	1868(4)	4307(3)	6583(3)	30(1)
C(13B)	3642(9)	5329(10)	7184(10)	33(3)
C(14B)	4479(11)	4891(9)	6533(9)	45(4)
C(15B)	5783(10)	5682(12)	6861(12)	60(5)
C(16B)	6249(10)	6911(12)	7840(13)	58(5)
C(17B)	5411(15)	7349(10)	8490(14)	66(8)
C(18B)	4108(14)	6558(12)	8162(13)	40(6)
C(19B)	2180(20)	2819(11)	6845(13)	42(5)
C(20B)	3531(16)	2788(16)	7657(16)	62(8)
C(21B)	3744(15)	1680(20)	7930(20)	75(11)
C(22B)	2610(20)	608(16)	7380(20)	66(9)
C(23B)	1259(18)	640(13)	6572(16)	67(7)
C(24B)	1046(13)	1746(17)	6303(13)	47(6)

Table 2.12 Interatomic distances [Å] for $[\text{Pd}_2\text{Cl}_2\{\mu\text{-Ph}_2\text{PN(Et)}\text{PPh}_2\}_2]^a$ 2

Pd-Pd'	2.600(1)	Pd-Cl	2.397(2)
N-C(25)	1.500(10)	C(25)-C(26)	1.521(13)
Molecule A		Molecule B	
Pd-P(1A)	2.429(3)	Pd-P(1B)	2.381(4)
Pd-P(2A)	2.136(4)	Pd-P(2B)	2.176(3)
P(1A)-C(1A)	1.825(10)	P(1B)-C(1B)	1.827(10)
P(1A)-C(7A)	1.851(9)	P(1B)-C(7B)	1.836(7)
P(2A)-C(13A)	1.831(7)	P(2B)-C(13B)	1.823(8)
P(2A)-C(19A)	1.848(9)	P(2B)-C(19B)	1.823(11)
P(1A)-N	1.700(7)	P(1B)-N	1.595(7)
P(2A)-N	1.740(7)	P(2B)-N	1.776(19)

^a All C-C distances within the phenyl rings were set at 1.390 Å as part of a rigid group refinement.

Table 2.13 Interatomic Angles ($^{\circ}$) for $[\text{Pd}_2\text{Cl}_2\{\mu\text{-Ph}_2\text{PN(Et)PPh}_2\}]^a$ 2

Pd-Pd'-Cl1	173.82(7)	N-C(25)-C(26)	115.3(8)
Molecule A			
Pd'-Pd-P(1A)	86.88(9)	Pd'-Pd-P(1B)	82.49(9)
Pd'-Pd-P(2A)	88.30(10)	Pd'-Pd-P(1B)	90.33(10)
Cl1-Pd-P(1A)	96.28(11)	Cl-Pd-P(1B)	98.87(11)
Cl1-Pd-P(2A)	89.19(12)	Cl-Pd-P(2B)	88.53(12)
P(1A)-Pd-P(2A)	171.48(13)	P(1B)-Pd-P(2B)	172.43(13)
Pd-P(1A)-N	106.3(3)	Pd-P(1B)-N	113.9(3)
Pd-P(1A)-C(1A)	117.4(5)	Pd-P(1B)-C(1B)	108.9(4)
Pd-P(1A)-C(7A)	112.7(4)	Pd-P(B)-C(7B)	116.5(2)
N-P(1A)-C(1A)	104.2(7)	N-P(1B)-C(1B)	108.3(5)
N-P(1A)-C(7A)	110.1(5)	N-P(1B)-C(7B)	105.4(4)
C(1A)-P(1A)-C(7A)	105.8(6)	C(1B)-P(1B)-C(7B)	103.1(5)
Pd-P(2A)-N	119.9(3)	Pd-P(2B)-N	114.6(3)
Pd-P(2A)-C(13A)	112.9(4)	Pd-P(2B)-C(13B)	114.4(4)
Pd-P(2A)-C(19A)	113.4(4)	Pd-P(2B)-C(19B)	113.7(5)
N-P(2A)-C(13A)	104.4(4)	N-P(2B)-C(13B)	109.7(4)
N-P(2A)-C(19A)	99.3(4)	N-P(2B)-C(19B)	97.8(6)
C(13A)-P(2A)-C(19A)	105.1(5)	C(13B)-P(2B)-C(19B)	105.1(7)
P(1A)-N-P(2A)	90.3(3)	P(1B)-N-P(2B)	86.4(7)
P(1A)-N-C(25A)	114.5(5)	P(1B)-N-C(25B)	127.8(5)
P(2A)-N-C(25A)	119.0(5)	P(2B)-N-C(25B)	132.1(6)
Molecule B			

^a The angles within the phenyl rings were constrained at 120° as part of the rigid group refinement.

**Table 2.14 Anisotropic displacement parameters ($\text{\AA}^2 \times 10^3$) for
[Pd₂Cl₂{μ-Ph₂PN(Et)PPh₂}₂] 2.**

The anisotropic displacement factor exponent takes the form:
 $-2\Pi^2 [h^2 a^{*2} U_{11} + \dots + 2 h k a^* b^* U_{12}]$

	U11	U22	U33	U23	U13	U12
Pd	30(1)	36(1)	36(1)	7(1)	13(1)	6(1)
Cl	57(1)	50(1)	83(2)	7(1)	37(1)	20(1)
N	33(3)	45(4)	27(3)	8(3)	11(3)	8(3)
C(25)	61(6)	55(5)	41(5)	26(4)	7(4)	6(4)
C(26)	52(6)	120(9)	41(5)	16(6)	-1(5)	8(6)
P(1A)	35(2)	35(2)	27(2)	14(2)	13(2)	6(2)
C(1A)	37(12)	49(13)	56(15)	27(12)	31(10)	16(10)
C(2A)	65(12)	50(11)	52(11)	38(10)	36(9)	6(9)
C(3A)	83(16)	37(10)	73(15)	39(10)	36(13)	13(10)
C(4A)	81(17)	100(30)	56(15)	44(15)	31(14)	48(17)
C(5A)	29(12)	100(30)	57(16)	38(17)	20(11)	31(14)
C(6A)	37(17)	26(9)	37(13)	-6(9)	14(13)	-5(9)
C(7A)	26(8)	44(9)	60(11)	29(8)	23(8)	5(7)
C(8A)	58(12)	72(12)	55(11)	33(10)	17(10)	-7(9)
C(9A)	33(10)	108(17)	98(16)	72(14)	15(10)	2(10)
C(10A)	43(10)	56(11)	69(13)	8(10)	22(10)	-9(9)
C(11A)	48(12)	108(17)	28(9)	27(11)	29(9)	-3(11)
C(12A)	39(11)	130(20)	43(11)	35(12)	18(9)	-14(12)
P(2A)	31(2)	35(2)	26(2)	10(2)	15(2)	7(2)
C(13A)	44(9)	49(9)	44(9)	28(7)	23(7)	-5(7)
C(14A)	13(7)	86(12)	27(8)	14(8)	11(6)	12(7)
C(15A)	45(10)	96(15)	29(8)	19(9)	24(8)	16(9)
C(16A)	63(12)	68(12)	28(9)	8(9)	26(8)	-14(9)
C(17A)	66(15)	80(14)	66(14)	44(11)	55(12)	-9(11)
C(18A)	45(10)	73(14)	47(11)	36(10)	38(9)	1(9)
C(19A)	30(9)	51(10)	17(9)	10(8)	12(7)	21(7)
C(20A)	70(14)	55(13)	31(9)	19(9)	32(9)	38(11)
C(21A)	92(17)	55(13)	40(11)	31(11)	36(12)	19(11)
C(22A)	80(30)	100(30)	57(16)	17(18)	55(18)	60(20)
C(23A)	89(15)	26(9)	37(10)	-7(8)	13(10)	4(9)
C(24A)	56(13)	52(13)	52(12)	23(10)	16(10)	-7(10)
P(1B)	28(2)	37(2)	24(2)	10(2)	10(2)	8(2)

Table 2.14 / Cont.

C(1B)	37(9)	41(8)	23(7)	3(6)	15(7)	-2(7)
C(2B)	42(9)	48(9)	57(11)	11(8)	21(8)	3(8)
C(3B)	64(12)	58(11)	44(10)	3(8)	32(10)	-10(9)
C(4B)	41(11)	69(13)	66(14)	-1(11)	22(11)	4(10)
C(5B)	34(12)	60(12)	67(17)	13(11)	28(12)	2(10)
C(6B)	46(16)	80(20)	80(17)	47(15)	24(13)	5(14)
C(7B)	42(11)	34(10)	29(9)	7(7)	17(8)	18(9)
C(8B)	57(11)	30(8)	44(10)	15(7)	17(9)	4(8)
C(9B)	96(17)	39(10)	36(11)	10(9)	20(11)	11(10)
C(10B)	100(30)	44(15)	50(14)	31(12)	19(17)	8(16)
C(11B)	61(13)	70(15)	44(13)	45(13)	34(10)	34(11)
C(12B)	63(14)	49(12)	20(12)	5(10)	22(10)	19(10)
P(2B)	25(2)	34(2)	24(2)	8(2)	8(2)	3(2)
C(13B)	23(7)	45(8)	31(7)	20(7)	7(6)	6(6)
C(14B)	37(8)	65(10)	50(9)	39(8)	23(8)	3(7)
C(15B)	50(10)	81(14)	74(13)	54(12)	31(10)	9(9)
C(16B)	25(9)	80(14)	61(12)	25(11)	11(9)	11(9)
C(17B)	63(18)	79(17)	47(15)	28(14)	10(13)	10(14)
C(18B)	40(15)	48(14)	23(8)	6(8)	14(9)	3(11)
C(19B)	27(12)	62(12)	20(9)	8(8)	-3(8)	13(9)
C(20B)	60(18)	84(17)	54(15)	43(13)	18(14)	30(15)
C(21B)	100(20)	35(13)	90(20)	47(15)	14(17)	18(14)
C(22B)	100(20)	42(14)	90(20)	43(13)	55(17)	38(15)
C(23B)	100(20)	37(12)	55(13)	-2(10)	48(14)	5(12)
C(24B)	53(12)	39(12)	46(13)	15(11)	18(10)	6(9)

Table 2.15
Crystal Data and Details of the Crystallographic Analysis for [PdI₂{η²-Ph₂PN(Et)PPh₂}] 3

Empirical formula	C ₂₆ H ₂₅ I ₂ N P ₂ Pd
Formula weight	773.61
Temperature	296(2) K
Wavelength	0.71069 Å
Crystal system,	Monoclinic
Space group	<i>P2₁/c</i>
a(Å)	9.8294(18)
b(Å)	14.828(3)
c(Å)	18.950(2)
α(°)	90
β(°)	94.740(13)
γ(°)	90
V(Å ³)	2752.5(8) Å ³
Z,	4
Calculated density	1.867 Mg/m ³
Absorption coefficient	3.048 mm ⁻¹
F(000)	1480
Crystal size	0.50 x 0.40 x 0.30 mm
Theta range for data collection	2.16 to 22.99 deg.
Index ranges	-2<=h<=10, -8<=k<=16, -20<=l<=20
Reflections collected / unique	6203 / 3824 [R(int) = 0.0337]
Completeness to 2theta = 22.99	99.9%
Max. and min. transmission	0.4616 and 0.3110
Refinement method	Full-matrix least-squares on F ²
Data / restraints / parameters	3824 / 0 / 311
Goodness-of-fit on F ²	1.043
Final R indices [I>2sigma(I)]	R1 = 0.0327, wR2 = 0.0877
R indices (all data)	R1 = 0.0370, wR2 = 0.0905
Largest diff. peak and hole	0.752 and -1.178 e.Å ⁻³

Table 2.16 Atomic coordinates ($\times 10^4$) and equivalent isotropic displacement parameters ($\text{\AA}^2 \times 10^3$) for $[\text{PdI}_2\{\eta^2\text{-Ph}_2\text{PN(Et)PPh}_2\}] \cdot 3$. U(eq) is defined as one third of the trace of the orthogonalized U_{ij} tensor.

	x	y	z	U(eq)
Pd	1415(1)	8084(1)	8036(1)	34(1)
I(1)	249(1)	8566(1)	6783(1)	63(1)
I(2)	-800(1)	8164(1)	8713(1)	58(1)
P(1)	2749(1)	7685(1)	8994(1)	35(1)
P(2)	3561(1)	7957(1)	7741(1)	35(1)
N(1)	4157(3)	7560(2)	8545(2)	37(1)
C(1)	3099(5)	8508(3)	9684(2)	42(1)
C(2)	3808(7)	8282(4)	10307(3)	71(2)
C(3)	4117(8)	8917(5)	10829(3)	85(2)
C(4)	3683(8)	9782(4)	10728(3)	76(2)
C(5)	2992(7)	10017(4)	10108(3)	67(2)
C(6)	2681(5)	9394(3)	9583(3)	48(1)
C(7)	2411(5)	6647(3)	9437(2)	40(1)
C(8)	2788(5)	5822(3)	9175(3)	51(1)
C(9)	2464(7)	5037(4)	9525(4)	71(2)
C(10)	1773(7)	5073(4)	10109(4)	78(2)
C(11)	1377(7)	5881(4)	10367(4)	78(2)
C(12)	1679(7)	6661(4)	10036(3)	64(2)
C(13)	4409(5)	8994(3)	7542(2)	38(1)
C(14)	5757(5)	8994(3)	7354(3)	50(1)
C(15)	6398(7)	9798(4)	7220(3)	67(2)
C(16)	5704(7)	10598(4)	7255(3)	67(2)
C(17)	4379(7)	10606(4)	7434(3)	63(2)
C(18)	3731(6)	9804(3)	7584(3)	48(1)
C(19)	4070(5)	7170(3)	7090(2)	42(1)
C(20)	4637(6)	6338(3)	7271(3)	57(1)
C(21)	5058(7)	5773(4)	6757(4)	76(2)
C(22)	4871(7)	6023(5)	6056(4)	75(2)
C(23)	4262(7)	6824(5)	5865(3)	72(2)
C(24)	3881(6)	7399(4)	6386(3)	59(2)
C(25)	5597(5)	7556(4)	8840(3)	53(1)
C(26)	6008(6)	6744(4)	9273(4)	77(2)

Table 2.17 Interatomic Distances (Å) for [PdI₂{η²-Ph₂PN(Et)PPh₂}] 3

Pd-P(1)	2.2294(12)
Pd-P(2)	2.2343(12)
Pd-I(2)	2.6189(6)
Pd-I(1)	2.6484(6)
P(1)-N(1)	1.695(4)
P(1)-C(7)	1.797(4)
P(1)-C(1)	1.801(5)
P(1)-P(2)	2.5992(15)
P(2)-N(1)	1.692(4)
P(2)-C(19)	1.800(4)
P(2)-C(13)	1.804(4)
N(1)-C(25)	1.478(6)
C(1)-C(2)	1.362(8)
C(1)-C(6)	1.385(7)
C(2)-C(3)	1.381(8)
C(3)-C(4)	1.360(9)
C(4)-C(5)	1.353(9)
C(5)-C(6)	1.373(8)
C(7)-C(8)	1.381(7)
C(7)-C(12)	1.395(7)
C(8)-C(9)	1.390(8)
C(9)-C(10)	1.347(9)
C(10)-C(11)	1.362(9)
C(11)-C(12)	1.360(8)
C(13)-C(18)	1.380(7)
C(13)-C(14)	1.400(7)
C(14)-C(15)	1.381(8)
C(15)-C(16)	1.373(9)
C(16)-C(17)	1.373(9)
C(17)-C(18)	1.389(8)
C(19)-C(24)	1.373(7)
C(19)-C(20)	1.384(7)
C(20)-C(21)	1.374(8)
C(21)-C(22)	1.378(10)
C(22)-C(23)	1.366(10)
C(23)-C(24)	1.380(8)
C(25)-C(26)	1.495(8)

Table 2.18 Interatomic Angles ($^{\circ}$) for $[\text{PdI}_2\{\eta^2\text{-Ph}_2\text{PN(Et)PPh}_2\}] \cdot 3$

P(1)-Pd-P(2)	71.22(4)	P(1)-Pd-I(2)	94.01(3)
P(2)-Pd-I(2)	165.14(3)	P(1)-Pd-I(1)	169.59(3)
P(2)-Pd-I(1)	98.38(4)	I(2)-Pd-I(1)	96.37(2)
N(1)-P(1)-C(7)	109.3(2)	N(1)-P(1)-C(1)	108.9(2)
C(7)-P(1)-C(1)	105.9(2)	N(1)-P(1)-Pd	93.97(13)
C(7)-P(1)-Pd	119.24(16)	C(1)-P(1)-Pd	118.40(16)
N(1)-P(1)-P(2)	39.84(13)	C(7)-P(1)-P(2)	129.93(15)
C(1)-P(1)-P(2)	120.20(16)	Pd-P(1)-P(2)	54.48(4)
N(1)-P(2)-C(19)	107.2(2)	N(1)-P(2)-C(13)	110.7(2)
C(19)-P(2)-C(13)	104.5(2)	N(1)-P(2)-Pd	93.88(12)
C(19)-P(2)-Pd	123.22(16)	C(13)-P(2)-Pd	116.29(15)
N(1)-P(2)-P(1)	39.92(12)	C(19)-P(2)-P(1)	130.53(16)
C(13)-P(2)-P(1)	120.38(15)	Pd-P(2)-P(1)	54.30(4)
C(25)-N(1)-P(2)	126.2(3)	C(25)-N(1)-P(1)	127.3(3)
P(2)-N(1)-P(1)	100.24(19)	C(2)-C(1)-C(6)	118.6(5)
C(2)-C(1)-P(1)	121.0(4)	C(6)-C(1)-P(1)	120.4(4)
C(1)-C(2)-C(3)	121.3(6)	C(4)-C(3)-C(2)	119.7(6)
C(5)-C(4)-C(3)	119.5(6)	C(4)-C(5)-C(6)	121.5(6)
C(5)-C(6)-C(1)	119.4(5)	C(8)-C(7)-C(12)	118.6(4)
C(8)-C(7)-P(1)	121.7(4)	C(12)-C(7)-P(1)	119.6(4)
C(7)-C(8)-C(9)	119.5(5)	C(10)-C(9)-C(8)	120.6(6)
C(9)-C(10)-C(11)	120.5(6)	C(12)-C(11)-C(10)	120.3(6)
C(11)-C(12)-C(7)	120.6(6)	C(18)-C(13)-C(14)	119.1(4)
C(18)-C(13)-P(2)	119.8(4)	C(14)-C(13)-P(2)	121.1(4)
C(15)-C(14)-C(13)	120.1(5)	C(16)-C(15)-C(14)	120.0(6)
C(17)-C(16)-C(15)	120.4(5)	C(16)-C(17)-C(18)	120.2(5)
C(13)-C(18)-C(17)	120.1(5)	C(24)-C(19)-C(20)	118.8(5)
C(24)-C(19)-P(2)	118.8(4)	C(20)-C(19)-P(2)	122.4(4)
C(21)-C(20)-C(19)	120.3(6)	C(20)-C(21)-C(22)	119.8(6)
C(23)-C(22)-C(21)	120.7(6)	C(22)-C(23)-C(24)	119.1(6)
C(19)-C(24)-C(23)	121.3(6)	N(1)-C(25)-C(26)	114.7(4)

**Table 2.19 Anisotropic displacement parameters ($\text{\AA}^2 \times 10^3$) for
[PdI₂{η²-Ph₂PN(Et)PPh₂}] 3**

The anisotropic displacement factor exponent takes the form:
 $-2\pi^2 [h^2 a^{*2} U_{11} + \dots + 2 h k a^* b^* U_{12}]$

	U11	U22	U33	U23	U13	U12
Pd	36(1)	33(1)	33(1)	-1(1)	6(1)	0(1)
I(1)	66(1)	81(1)	42(1)	4(1)	-4(1)	5(1)
I(2)	44(1)	71(1)	61(1)	3(1)	20(1)	0(1)
P(1)	41(1)	31(1)	32(1)	0(1)	8(1)	2(1)
P(2)	41(1)	29(1)	34(1)	0(1)	10(1)	1(1)
N(1)	37(2)	39(2)	37(2)	3(2)	11(2)	2(2)
C(1)	50(3)	39(2)	38(3)	-3(2)	8(2)	3(2)
C(2)	104(5)	49(3)	55(4)	-9(3)	-14(3)	17(3)
C(3)	129(6)	71(4)	51(4)	-18(3)	-28(4)	8(4)
C(4)	106(5)	63(4)	59(4)	-23(3)	2(3)	-2(4)
C(5)	92(4)	39(3)	71(4)	-11(3)	5(3)	5(3)
C(6)	59(3)	39(3)	47(3)	-3(2)	4(2)	3(2)
C(7)	49(3)	37(2)	35(2)	6(2)	8(2)	4(2)
C(8)	64(3)	40(3)	52(3)	0(2)	16(3)	-2(2)
C(9)	87(4)	36(3)	92(5)	7(3)	21(4)	6(3)
C(10)	87(4)	52(3)	99(5)	34(3)	34(4)	4(3)
C(11)	99(5)	74(4)	68(4)	25(3)	44(4)	9(4)
C(12)	88(4)	50(3)	57(3)	12(3)	33(3)	9(3)
C(13)	48(3)	34(2)	32(2)	2(2)	7(2)	-4(2)
C(14)	60(3)	43(3)	48(3)	0(2)	15(2)	-4(2)
C(15)	71(4)	69(4)	64(4)	2(3)	19(3)	-22(3)
C(16)	90(5)	46(3)	63(4)	8(3)	2(3)	-22(3)
C(17)	82(4)	36(3)	68(4)	5(2)	-9(3)	0(3)
C(18)	53(3)	38(3)	52(3)	2(2)	1(2)	0(2)
C(19)	45(3)	39(2)	45(3)	-7(2)	19(2)	-5(2)
C(20)	75(4)	44(3)	53(3)	-9(2)	18(3)	6(3)
C(21)	81(4)	54(3)	95(5)	-23(3)	23(4)	11(3)
C(22)	77(4)	73(4)	80(5)	-40(4)	38(3)	-13(3)
C(23)	98(5)	75(4)	47(3)	-16(3)	29(3)	-20(4)
C(24)	80(4)	52(3)	48(3)	-3(2)	20(3)	-4(3)
C(25)	40(3)	57(3)	60(3)	10(3)	2(2)	-1(2)
C(26)	52(3)	76(4)	101(5)	32(4)	-8(3)	9(3)

Table 2.20 Hydrogen atom coordinates ($\times 10^4$) and isotropic displacement parameters ($\text{\AA}^2 \times 10^3$) for $[\text{PdI}_2\{\eta^2\text{-Ph}_2\text{PN(Et)PPPh}_2\}] \cdot 3$

	x	y	z	U(iso)
H(2)	4050(2)	7780(5)	10371(7)	85
H(3)	4600(5)	8760(15)	11230(4)	103
H(4)	3849(16)	10180(3)	11060(3)	91
H(5)	2750(2)	10540(4)	10045(6)	81
H(6)	2230(3)	9553(11)	9200(3)	58
H(8)	3290(3)	5791(4)	8740(2)	62
H(9)	2700(2)	4530(4)	9368(14)	85
H(10)	1578(19)	4570(4)	10325(19)	94
H(11)	900(4)	5898(5)	10770(3)	94
H(12)	1440(2)	7120(4)	10182(13)	76
H(14)	6140(3)	8550(3)	7325(3)	60
H(15)	7260(7)	9797(4)	7112(9)	81
H(16)	6140(3)	11150(4)	7156(8)	80
H(17)	3920(4)	11140(4)	7455(4)	75
H(18)	2960(6)	9813(3)	7695(9)	58
H(20)	4715(9)	6195(12)	7650(3)	68
H(21)	5460(3)	5240(4)	6880(11)	91
H(22)	5120(2)	5700(3)	5760(3)	90
H(23)	4101(14)	6986(13)	5370(4)	87
H(24)	3590(3)	7810(4)	6291(10)	71
H(25A)	5746(9)	8050(2)	9110(12)	63
H(25B)	6140(2)	7595(4)	8480(16)	63
H(26A)	6890(4)	6789(5)	9431(8)	116
H(26B)	5885(8)	6250(2)	9007(13)	116
H(26C)	5500(2)	6708(5)	9641(17)	116

Table 2.21
Crystal Data and Details of the Crystallographic Analysis for
Ph₂P(O)N(Et)P(O)Ph₂. dba. H₂O

Empirical formula	C43 H39 N O4 P2
Formula weight	695.69
Temperature	293(2) K
Wavelength	0.71073 Å
Crystal system	Triclinic
Space group	<i>P</i> 1
a(Å)	9.4865(12)
b(Å)	9.583(4)
c(Å)	20.796(4)
α(°)	97.586(19)
β(°)	97.577(13)
γ(°)	93.01(2)
V(Å ³)	1852.9(9)
Z	2
Calculated density	1.247 Mg/m ³
Absorption coefficient	0.161 mm ⁻¹
F(000)	732
Crystal size	0.35 x 0.25 x 0.20 mm
Theta range for data collection	2.15 to 22.97 deg.
Index ranges	-10<=h<=10, -10<=k<=10, -4<=l<=22
Reflections collected / unique	5713 / 5654 [R(int) = 0.0049]
Completeness to 2theta = 22.97	99.9%
Max. and min. transmission	0.9686 and 0.9459
Refinement method	Full-matrix least-squares on F ²
Data / restraints / parameters	5654 / 305 / 901
Goodness-of-fit on F ²	0.944
Final R indices [I>2sigma(I)]	R1 = 0.0426, wR2 = 0.0990
R indices (all data)	R1 = 0.0815, wR2 = 0.1110
Absolute structure parameter	0.2(2)
Largest diff. peak and hole	0.289 and -0.196 e.Å ⁻³

Table 2.22 Atomic coordinates ($\times 10^4$) and equivalent isotropic displacement parameters ($\text{\AA}^2 \times 10^3$) for $\text{Ph}_2\text{P(O)N(Et)P(O)Ph}_2$, dba, H_2O . $U(\text{eq})$ is defined as one third of the trace of the orthogonalized U_{ij} tensor.

	x	y	z	$U(\text{eq})$
P(1A)	5956(3)	6177(3)	5473(2)	47(1)
P(2A)	6585(3)	8943(3)	6408(1)	45(1)
N(1A)	5564(10)	7741(10)	5902(4)	41(2)
O(1A)	5913(10)	4972(8)	5815(5)	60(2)
O(2A)	6766(10)	10268(9)	6134(5)	62(2)
C(1A)	3933(13)	7883(13)	5905(7)	56(3)
C(2A)	3487(17)	9176(17)	5660(8)	88(5)
C(3A)	8296(13)	8245(14)	6642(5)	43(2)
C(4A)	9517(16)	9109(17)	6683(7)	65(3)
C(5A)	10811(17)	8710(2)	6880(9)	86(5)
C(6A)	10920(17)	7440(2)	7120(8)	85(4)
C(7A)	9740(15)	6602(17)	7104(7)	68(4)
C(8A)	8405(15)	6957(15)	6874(7)	56(3)
C(9A)	5754(12)	9194(13)	7144(6)	41(2)
C(10A)	5500(17)	10514(15)	7400(7)	63(4)
C(11A)	4847(17)	10799(15)	7953(7)	67(3)
C(12A)	4526(16)	9616(17)	8287(7)	75(4)
C(13A)	4756(16)	8367(15)	8041(6)	68(4)
C(14A)	5381(15)	8118(14)	7463(6)	57(3)
C(15A)	7700(13)	6531(12)	5235(6)	42(2)
C(16A)	8646(14)	5514(14)	5299(6)	56(3)
C(17A)	9936(14)	5679(15)	5086(8)	62(4)
C(18A)	10220(13)	6850(15)	4796(7)	61(3)
C(19A)	9332(14)	7854(14)	4747(6)	51(3)
C(20A)	8080(14)	7773(13)	4968(5)	49(3)
C(21A)	4741(13)	5944(11)	4765(6)	45(2)
C(22A)	3845(13)	4705(13)	4631(7)	56(3)
C(23A)	2881(16)	4415(15)	4032(7)	67(3)
C(24A)	2770(15)	5395(15)	3599(7)	61(3)
C(25A)	3576(14)	6532(16)	3720(7)	66(4)
C(26A)	4623(15)	6904(14)	4277(6)	56(3)
O(3A)	11128(10)	11726(13)	4791(5)	94(3)
C(27A)	10255(11)	11916(14)	5169(6)	77(3)

Table 2.22 / Cont.

C(28A)	8672(10)	11575(12)	4935(3)	60(2)
C(29A)	8258(9)	11225(9)	4332(3)	54(2)
C(30A)	6729(10)	10880(12)	4097(6)	75(4)
C(31A)	6454(14)	10336(19)	3435(7)	105(5)
C(32A)	5113(12)	9971(14)	3141(6)	87(4)
C(33A)	4015(13)	10290(16)	3456(6)	85(4)
C(34A)	4215(12)	10823(19)	4111(7)	94(5)
C(35A)	5606(11)	11167(16)	4447(7)	83(4)
C(36A)	10672(7)	12430(10)	5896(4)	60(3)
C(37A)	11944(8)	12724(10)	6133(4)	58(2)
C(38A)	12369(17)	13330(14)	6826(5)	82(4)
C(39A)	11504(13)	13268(14)	7320(6)	62(3)
C(40A)	12062(14)	13747(17)	7979(7)	82(4)
C(41A)	13409(18)	14403(17)	8120(7)	90(4)
C(42A)	14263(15)	14444(15)	7650(7)	85(4)
C(43A)	13754(17)	13917(18)	7025(8)	96(5)
O(4A)	7524(10)	13248(9)	6578(5)	83(3)
P(1B)	6734(3)	7962(3)	1142(1)	41(1)
P(2B)	6107(3)	5222(3)	214(1)	45(1)
N(1B)	7222(10)	6527(11)	724(5)	47(2)
O(1B)	6824(8)	9234(9)	785(4)	55(2)
O(2B)	5884(10)	3884(8)	487(5)	60(2)
C(1B)	8774(15)	6399(16)	736(7)	74(4)
C(2B)	9332(17)	5095(18)	1024(10)	101(5)
C(3B)	8042(13)	8294(13)	1916(5)	46(3)
C(4B)	8157(16)	7383(15)	2351(7)	63(3)
C(5B)	9051(15)	7600(13)	2921(7)	69(4)
C(6B)	9941(15)	8928(17)	3033(8)	72(4)
C(7B)	9872(14)	9804(16)	2571(8)	67(4)
C(8B)	8909(14)	9510(14)	2044(6)	55(3)
C(9B)	5021(13)	7597(13)	1371(5)	41(2)
C(10B)	4646(13)	6438(13)	1643(6)	52(3)
C(11B)	3294(15)	6243(14)	1866(7)	60(3)
C(12B)	2305(14)	7326(13)	1820(6)	54(3)
C(13B)	2721(15)	8484(15)	1556(8)	64(4)
C(14B)	4034(14)	8645(12)	1333(6)	54(3)
C(15B)	4461(13)	5929(13)	-32(6)	47(3)
C(16B)	3250(14)	5043(17)	-5(7)	61(3)

Table 2.22 / Cont.

C(17B)	1896(17)	5490(2)	-267(8)	86(5)
C(18B)	1755(16)	6770(2)	-459(9)	89(5)
C(19B)	2954(16)	7690(18)	-461(7)	73(4)
C(20B)	4272(14)	7226(15)	-254(6)	52(3)
C(21B)	6966(13)	4957(13)	-511(6)	49(3)
C(22B)	7184(17)	3586(16)	-787(8)	69(4)
C(23B)	7720(2)	3402(19)	-1386(9)	98(6)
C(24B)	8103(16)	4415(16)	-1669(7)	67(4)
C(25B)	7873(12)	5867(15)	-1411(7)	57(3)
C(26B)	7335(14)	6106(14)	-843(6)	52(3)
O(3B)	1401(13)	12402(16)	1904(6)	131(4)
C(27B)	2270(11)	12304(15)	1532(5)	81(4)
C(28B)	3839(11)	12582(13)	1746(6)	111(5)
C(29B)	4517(11)	12942(14)	2268(7)	121(5)
C(30B)	6003(9)	13265(14)	2561(5)	62(3)
C(31B)	6339(11)	13862(14)	3211(5)	69(3)
C(32B)	7710(14)	14070(19)	3482(7)	116(6)
C(33B)	8805(14)	13900(2)	3150(8)	114(6)
C(34B)	8544(13)	13321(17)	2499(8)	98(5)
C(35B)	7131(12)	13052(17)	2205(6)	82(4)
C(36B)	1954(14)	11769(12)	811(5)	121(5)
C(37B)	819(15)	11346(14)	493(5)	109(5)
C(38B)	318(12)	10908(11)	-199(4)	53(3)
C(39B)	-1065(12)	10295(15)	-367(7)	70(3)
C(40B)	-1515(15)	9825(16)	-1031(8)	101(5)
C(41B)	-610(2)	9891(15)	-1481(7)	89(4)
C(42B)	746(16)	10416(16)	-1301(7)	84(4)
C(43B)	1196(16)	10991(17)	-675(8)	83(4)
O(4B)	5138(9)	1075(9)	68(5)	66(2)

Table 2.23 Intertatomic Distances (Å) for Ph₂P(O)N(Et)P(O)Ph₂. dba. H₂O

P(1A)-O(1A)	1.435(9)	P(1A)-C(21A)	1.728(13)
P(1A)-N(1A)	1.725(10)	P(1A)-C(15A)	1.816(12)
P(2A)-O(2A)	1.470(9)	P(2A)-N(1A)	1.633(10)
P(2A)-C(9A)	1.806(12)	P(2A)-C(3A)	1.820(13)
N(1A)-C(1A)	1.561(16)	C(1A)-C(2A)	1.463(19)
C(3A)-C(4A)	1.374(19)	C(3A)-C(8A)	1.387(18)
C(4A)-C(5A)	1.33(2)	C(5A)-C(6A)	1.38(3)
C(6A)-C(7A)	1.34(2)	C(7A)-C(8A)	1.37(2)
C(9A)-C(14A)	1.353(18)	C(9A)-C(10A)	1.353(18)
C(10A)-C(11A)	1.38(2)	C(11A)-C(12A)	1.45(2)
C(12A)-C(13A)	1.279(19)	C(13A)-C(14A)	1.408(17)
C(15A)-C(16A)	1.367(17)	C(15A)-C(20A)	1.427(17)
C(16A)-C(17A)	1.363(19)	C(17A)-C(18A)	1.372(19)
C(18A)-C(19A)	1.318(19)	C(19A)-C(20A)	1.332(17)
C(21A)-C(22A)	1.398(16)	C(21A)-C(26A)	1.454(17)
C(22A)-C(23A)	1.430(19)	C(23A)-C(24A)	1.38(2)
C(24A)-C(25A)	1.274(19)	C(25A)-C(26A)	1.417(19)
O(3A)-C(27A)	1.218(9)	C(27A)-C(36A)	1.520(11)
C(27A)-C(28A)	1.521(10)	C(28A)-C(29A)	1.258(9)
C(29A)-C(30A)	1.474(10)	C(30A)-C(35A)	1.387(11)
C(30A)-C(31A)	1.393(12)	C(31A)-C(32A)	1.344(11)
C(32A)-C(33A)	1.331(11)	C(33A)-C(34A)	1.374(11)
C(34A)-C(35A)	1.410(11)	C(36A)-C(37A)	1.244(9)
C(37A)-C(38A)	1.476(10)	C(38A)-C(43A)	1.39(2)
C(38A)-C(39A)	1.402(18)	C(39A)-C(40A)	1.411(16)
C(40A)-C(41A)	1.372(19)	C(41A)-C(42A)	1.35(2)
C(42A)-C(43A)	1.346(18)	P(1B)-O(1B)	1.513(9)
P(1B)-N(1B)	1.648(10)	P(1B)-C(9B)	1.783(12)
P(1B)-C(3B)	1.878(11)	P(2B)-O(2B)	1.486(9)
P(2B)-N(1B)	1.738(10)	P(2B)-C(15B)	1.775(13)
P(2B)-C(21B)	1.804(13)	N(1B)-C(1B)	1.481(17)
C(1B)-C(2B)	1.54(2)	C(3B)-C(4B)	1.335(18)
C(3B)-C(8B)	1.366(17)	C(4B)-C(5B)	1.350(19)
C(5B)-C(6B)	1.464(19)	C(6B)-C(7B)	1.35(2)
C(7B)-C(8B)	1.320(19)	C(9B)-C(10B)	1.362(16)
C(9B)-C(14B)	1.412(17)	C(10B)-C(11B)	1.431(17)
C(11B)-C(12B)	1.440(19)	C(12B)-C(13B)	1.365(18)
C(13B)-C(14B)	1.393(19)	C(15B)-C(20B)	1.395(18)

Table 2.23 / Cont.

C(15B)-C(16B)	1.404(18)	C(16B)-C(17B)	1.44(2)
C(17B)-C(18B)	1.34(3)	C(18B)-C(19B)	1.40(2)
C(19B)-C(20B)	1.384(19)	C(21B)-C(22B)	1.400(19)
C(21B)-C(26B)	1.425(18)	C(22B)-C(23B)	1.40(2)
C(23B)-C(24B)	1.26(2)	C(24B)-C(25B)	1.462(19)
C(25B)-C(26B)	1.346(18)	O(3B)-C(27B)	1.201(11)
C(27B)-C(28B)	1.496(11)	C(27B)-C(36B)	1.505(11)
C(28B)-C(29B)	1.184(11)	C(29B)-C(30B)	1.460(10)
C(30B)-C(31B)	1.385(10)	C(30B)-C(35B)	1.388(10)
C(31B)-C(32B)	1.341(11)	C(32B)-C(33B)	1.327(13)
C(33B)-C(34B)	1.376(12)	C(34B)-C(35B)	1.394(11)
C(36B)-C(37B)	1.207(11)	C(37B)-C(38B)	1.453(10)
C(38B)-C(39B)	1.390(16)	C(38B)-C(43B)	1.383(18)
C(39B)-C(40B)	1.398(18)	C(40B)-C(41B)	1.35(2)
C(41B)-C(42B)	1.35(2)	C(42B)-C(43B)	1.349(19)

Table 2.24 Interatomic Angles ($^{\circ}$) for $\text{Ph}_2\text{P}(\text{O})\text{N}(\text{Et})\text{P}(\text{O})\text{Ph}_2$, dba, H_2O

O(1A)-P(1A)-C(21A)	111.7(6)	O(1A)-P(1A)-N(1A)	115.5(5)
C(21A)-P(1A)-N(1A)	104.6(5)	O(1A)-P(1A)-C(15A)	112.0(6)
C(21A)-P(1A)-C(15A)	107.0(6)	N(1A)-P(1A)-C(15A)	105.4(5)
O(2A)-P(2A)-N(1A)	112.4(6)	O(2A)-P(2A)-C(9A)	111.8(6)
N(1A)-P(2A)-C(9A)	105.9(6)	O(2A)-P(2A)-C(3A)	111.3(6)
N(1A)-P(2A)-C(3A)	109.3(5)	C(9A)-P(2A)-C(3A)	105.9(5)
C(1A)-N(1A)-P(2A)	114.4(7)	C(1A)-N(1A)-P(1A)	113.5(7)
P(2A)-N(1A)-P(1A)	130.9(6)	C(2A)-C(1A)-N(1A)	111.3(11)
C(4A)-C(3A)-C(8A)	118.4(13)	C(4A)-C(3A)-P(2A)	118.7(11)
C(8A)-C(3A)-P(2A)	122.3(10)	C(5A)-C(4A)-C(3A)	122.9(15)
C(4A)-C(5A)-C(6A)	118.6(14)	C(7A)-C(6A)-C(5A)	119.1(16)
C(6A)-C(7A)-C(8A)	123.2(16)	C(7A)-C(8A)-C(3A)	117.5(14)
C(14A)-C(9A)-C(10A)	117.6(11)	C(14A)-C(9A)-P(2A)	123.1(9)
C(10A)-C(9A)-P(2A)	119.3(10)	C(9A)-C(10A)-C(11A)	123.1(14)
C(10A)-C(11A)-C(12A)	116.7(13)	C(13A)-C(12A)-C(11A)	119.8(13)
C(12A)-C(13A)-C(14A)	121.4(14)	C(9A)-C(14A)-C(13A)	121.1(12)
C(16A)-C(15A)-C(20A)	120.2(11)	C(16A)-C(15A)-P(1A)	116.7(10)
C(20A)-C(15A)-P(1A)	123.0(9)	C(17A)-C(16A)-C(15A)	119.3(12)
C(16A)-C(17A)-C(18A)	118.4(12)	C(19A)-C(18A)-C(17A)	122.8(12)
C(18A)-C(19A)-C(20A)	121.3(13)	C(19A)-C(20A)-C(15A)	117.8(12)
C(22A)-C(21A)-C(26A)	117.0(11)	C(22A)-C(21A)-P(1A)	117.8(10)
C(26A)-C(21A)-P(1A)	125.1(9)	C(21A)-C(22A)-C(23A)	120.2(13)
C(24A)-C(23A)-C(22A)	120.2(13)	C(25A)-C(24A)-C(23A)	119.9(13)
C(24A)-C(25A)-C(26A)	125.2(14)	C(25A)-C(26A)-C(21A)	117.4(12)
O(3A)-C(27A)-C(36A)	122.8(9)	O(3A)-C(27A)-C(28A)	120.8(9)
C(36A)-C(27A)-C(28A)	116.3(7)	C(29A)-C(28A)-C(27A)	119.0(7)
C(28A)-C(29A)-C(30A)	119.7(8)	C(35A)-C(30A)-C(31A)	119.9(10)
C(35A)-C(30A)-C(29A)	126.7(10)	C(31A)-C(30A)-C(29A)	113.1(10)
C(32A)-C(31A)-C(30A)	120.9(12)	C(33A)-C(32A)-C(31A)	120.2(12)
C(32A)-C(33A)-C(34A)	121.3(11)	C(33A)-C(34A)-C(35A)	120.1(11)
C(30A)-C(35A)-C(34A)	117.1(11)	C(37A)-C(36A)-C(27A)	120.8(7)
C(36A)-C(37A)-C(38A)	121.9(9)	C(43A)-C(38A)-C(39A)	116.3(10)
C(43A)-C(38A)-C(37A)	118.9(12)	C(39A)-C(38A)-C(37A)	124.6(12)
C(38A)-C(39A)-C(40A)	120.2(12)	C(41A)-C(40A)-C(39A)	118.8(13)
C(42A)-C(41A)-C(40A)	121.1(11)	C(43A)-C(42A)-C(41A)	119.6(14)
C(42A)-C(43A)-C(38A)	123.5(14)	O(1B)-P(1B)-N(1B)	112.5(5)
O(1B)-P(1B)-C(9B)	113.8(5)	N(1B)-P(1B)-C(9B)	109.1(5)
O(1B)-P(1B)-C(3B)	108.6(5)	N(1B)-P(1B)-C(3B)	105.1(6)

Table 2.24 / Cont.

C(9B)-P(1B)-C(3B)	107.2(5)	O(2B)-P(2B)-N(1B)	115.3(6)
O(2B)-P(2B)-C(15B)	111.4(6)	N(1B)-P(2B)-C(15B)	109.0(5)
O(2B)-P(2B)-C(21B)	111.7(5)	N(1B)-P(2B)-C(21B)	103.2(5)
C(15B)-P(2B)-C(21B)	105.6(6)	C(1B)-N(1B)-P(1B)	116.6(8)
C(1B)-N(1B)-P(2B)	116.4(8)	P(1B)-N(1B)-P(2B)	126.7(6)
N(1B)-C(1B)-C(2B)	114.4(13)	C(4B)-C(3B)-C(8B)	118.4(12)
C(4B)-C(3B)-P(1B)	122.4(10)	C(8B)-C(3B)-P(1B)	119.2(10)
C(3B)-C(4B)-C(5B)	124.3(13)	C(4B)-C(5B)-C(6B)	114.8(13)
C(7B)-C(6B)-C(5B)	120.3(14)	C(8B)-C(7B)-C(6B)	119.4(13)
C(7B)-C(8B)-C(3B)	122.7(14)	C(10B)-C(9B)-C(14B)	117.3(11)
C(10B)-C(9B)-P(1B)	124.4(9)	C(14B)-C(9B)-P(1B)	117.9(9)
C(9B)-C(10B)-C(11B)	122.5(12)	C(10B)-C(11B)-C(12B)	119.1(12)
C(13B)-C(12B)-C(11B)	117.1(12)	C(12B)-C(13B)-C(14B)	122.9(13)
C(13B)-C(14B)-C(9B)	121.1(12)	C(20B)-C(15B)-C(16B)	118.6(13)
C(20B)-C(15B)-P(2B)	126.9(10)	C(16B)-C(15B)-P(2B)	114.5(10)
C(15B)-C(16B)-C(17B)	116.9(15)	C(18B)-C(17B)-C(16B)	122.3(15)
C(17B)-C(18B)-C(19B)	121.0(15)	C(20B)-C(19B)-C(18B)	117.0(16)
C(19B)-C(20B)-C(15B)	123.8(14)	C(22B)-C(21B)-C(26B)	118.7(12)
C(22B)-C(21B)-P(2B)	119.6(11)	C(26B)-C(21B)-P(2B)	121.5(9)
C(21B)-C(22B)-C(23B)	118.4(15)	C(24B)-C(23B)-C(22B)	123.3(16)
C(23B)-C(24B)-C(25B)	120.5(14)	C(26B)-C(25B)-C(24B)	118.6(13)
C(25B)-C(26B)-C(21B)	120.3(12)	O(3B)-C(27B)-C(28B)	123.4(10)
O(3B)-C(27B)-C(36B)	125.2(11)	C(28B)-C(27B)-C(36B)	111.2(10)
C(29B)-C(28B)-C(27B)	132.1(13)	C(28B)-C(29B)-C(30B)	139.4(14)
C(31B)-C(30B)-C(35B)	117.0(8)	C(31B)-C(30B)-C(29B)	120.5(10)
C(35B)-C(30B)-C(29B)	122.5(10)	C(32B)-C(31B)-C(30B)	119.5(10)
C(33B)-C(32B)-C(31B)	124.2(12)	C(32B)-C(33B)-C(34B)	118.8(12)
C(33B)-C(34B)-C(35B)	118.3(11)	C(30B)-C(35B)-C(34B)	121.6(10)
C(37B)-C(36B)-C(27B)	128.2(13)	C(36B)-C(37B)-C(38B)	135.0(14)
C(39B)-C(38B)-C(43B)	120.3(9)	C(39B)-C(38B)-C(37B)	117.3(12)
C(43B)-C(38B)-C(37B)	122.2(12)	C(38B)-C(39B)-C(40B)	116.8(12)
C(41B)-C(40B)-C(39B)	121.3(12)	C(40B)-C(41B)-C(42B)	120.8(11)
C(43B)-C(42B)-C(41B)	120.1(13)	C(42B)-C(43B)-C(38B)	120.4(13)

**Table 2.25 Anisotropic Displacement parameters ($\text{\AA}^2 \times 10^3$) for
 $\text{Ph}_2\text{P(O)N(Et)P(O)Ph}_2$. dba. H_2O**
The anisotropic displacement factor exponent takes the form:
 $-2 \Pi^2 [h^2 a^{*2} U_{11} + \dots + 2 h k a^* b^* U_{12}]$

	U11	U22	U33	U23	U13	U12
P(1A)	52(2)	42(2)	51(2)	10(2)	17(2)	4(2)
P(2A)	50(2)	47(2)	43(2)	14(2)	12(2)	9(2)
N(1A)	49(4)	44(4)	32(4)	5(3)	7(4)	13(3)
O(1A)	82(6)	34(4)	71(6)	21(4)	18(5)	12(4)
O(2A)	76(6)	57(5)	58(6)	24(4)	15(5)	-8(4)
C(1A)	49(5)	57(6)	62(8)	1(6)	13(6)	6(4)
C(2A)	93(10)	104(10)	70(8)	12(7)	1(7)	55(8)
C(3A)	46(4)	61(7)	28(6)	6(5)	20(4)	8(4)
C(4A)	68(6)	63(8)	68(9)	10(7)	23(7)	-7(6)
C(5A)	53(6)	115(11)	95(12)	19(10)	34(8)	-14(7)
C(6A)	62(7)	133(12)	59(8)	21(9)	1(7)	11(7)
C(7A)	62(7)	83(8)	72(9)	32(8)	31(7)	28(6)
C(8A)	54(6)	55(7)	61(9)	9(7)	10(7)	6(5)
C(9A)	44(6)	48(6)	33(5)	10(4)	6(5)	14(5)
C(10A)	88(10)	47(6)	62(8)	9(6)	38(7)	2(7)
C(11A)	84(9)	50(6)	68(7)	-10(5)	28(6)	7(6)
C(12A)	71(9)	90(8)	72(9)	9(6)	44(8)	17(8)
C(13A)	115(10)	65(7)	30(6)	9(5)	28(6)	15(8)
C(14A)	76(9)	52(6)	51(7)	16(5)	29(7)	19(7)
C(15A)	47(5)	33(6)	45(7)	-6(5)	11(5)	3(4)
C(16A)	61(6)	65(7)	52(7)	32(6)	14(6)	12(5)
C(17A)	45(6)	70(8)	81(10)	27(7)	13(6)	31(6)
C(18A)	44(6)	77(8)	66(8)	13(6)	28(6)	0(5)
C(19A)	56(6)	50(7)	50(7)	18(6)	9(5)	-2(5)
C(20A)	69(7)	47(6)	35(6)	6(5)	27(6)	11(5)
C(21A)	54(6)	25(5)	59(6)	4(4)	16(4)	7(4)
C(22A)	48(7)	48(7)	71(7)	17(6)	0(5)	2(5)
C(23A)	81(9)	56(7)	62(8)	-10(5)	15(6)	1(6)
C(24A)	60(8)	68(7)	47(7)	-9(5)	-11(6)	17(5)
C(25A)	65(8)	93(9)	41(6)	14(6)	9(5)	-14(6)
C(26A)	76(8)	45(6)	43(6)	-1(5)	1(5)	-3(5)
O(3A)	77(5)	126(8)	74(5)	-5(6)	15(4)	-10(5)

Table 2.25 / Cont.

C(27A)	82(6)	51(7)	112(7)	19(6)	46(5)	20(6)
C(28A)	109(6)	58(6)	29(4)	17(4)	46(4)	22(5)
C(29A)	98(5)	37(6)	41(4)	5(4)	58(4)	17(5)
C(30A)	70(6)	26(6)	133(9)	12(7)	17(6)	17(6)
C(31A)	85(7)	92(13)	132(10)	-11(11)	26(7)	7(9)
C(32A)	92(8)	64(7)	109(9)	13(7)	31(6)	-14(7)
C(33A)	74(7)	71(10)	111(9)	28(9)	14(7)	-15(7)
C(34A)	63(6)	114(13)	116(10)	31(10)	35(8)	3(9)
C(35A)	77(6)	70(10)	103(9)	13(9)	5(6)	23(8)
C(36A)	30(4)	58(6)	107(5)	19(5)	57(4)	6(4)
C(37A)	41(4)	53(6)	100(6)	37(5)	49(4)	27(4)
C(38A)	129(10)	58(8)	70(6)	35(6)	27(6)	0(7)
C(39A)	60(7)	59(8)	64(6)	8(6)	-8(5)	8(6)
C(40A)	81(7)	97(11)	59(6)	2(7)	-18(6)	-3(7)
C(41A)	87(8)	94(11)	79(8)	5(9)	-18(6)	-3(8)
C(42A)	85(8)	79(9)	103(8)	58(7)	0(6)	18(6)
C(43A)	113(10)	78(12)	105(8)	28(10)	39(8)	-8(9)
O(4A)	88(6)	54(5)	98(7)	-10(4)	19(5)	-28(4)
P(1B)	49(2)	37(2)	37(2)	4(1)	3(1)	6(1)
P(2B)	60(2)	32(2)	44(2)	2(1)	12(2)	-1(1)
N(1B)	39(4)	53(4)	48(5)	-2(4)	11(4)	-5(3)
O(1B)	48(5)	62(5)	59(5)	27(4)	2(4)	-7(4)
O(2B)	87(6)	35(4)	64(6)	11(4)	27(5)	10(4)
C(1B)	58(5)	107(10)	50(8)	-17(7)	-1(6)	35(6)
C(2B)	62(8)	93(10)	142(14)	10(9)	-3(8)	8(6)
C(3B)	47(6)	62(7)	30(5)	2(4)	8(4)	4(5)
C(4B)	68(8)	59(7)	61(7)	14(6)	3(6)	-12(6)
C(5B)	93(10)	48(6)	61(7)	12(6)	-12(6)	16(6)
C(6B)	55(8)	101(9)	58(7)	4(6)	12(6)	-13(6)
C(7B)	35(6)	76(8)	86(9)	4(6)	13(5)	-16(6)
C(8B)	64(8)	54(7)	48(6)	-3(5)	23(5)	-5(5)
C(9B)	57(5)	40(6)	27(6)	10(5)	7(4)	7(4)
C(10B)	46(6)	41(6)	72(8)	17(6)	7(6)	12(5)
C(11B)	79(8)	47(7)	59(8)	0(6)	35(7)	1(5)
C(12B)	56(6)	55(6)	49(7)	-7(5)	11(5)	11(5)
C(13B)	67(7)	52(7)	76(9)	1(7)	24(7)	11(6)
C(14B)	64(6)	25(5)	72(8)	-8(5)	18(6)	7(5)
C(15B)	55(5)	43(6)	40(7)	3(5)	5(5)	-4(4)

Table 2.25 / Cont.

C(16B)	53(5)	78(8)	51(7)	2(6)	12(6)	-6(5)
C(17B)	54(6)	116(11)	79(11)	-4(10)	-1(7)	-9(7)
C(18B)	50(6)	133(13)	91(11)	13(10)	26(8)	36(7)
C(19B)	73(7)	94(9)	56(8)	20(8)	0(7)	32(6)
C(20B)	51(6)	66(7)	43(7)	12(6)	11(6)	13(5)
C(21B)	50(7)	45(6)	47(6)	-3(4)	8(5)	-8(5)
C(22B)	76(9)	46(6)	88(10)	-2(6)	36(8)	6(7)
C(23B)	134(14)	63(8)	110(12)	0(8)	69(11)	14(9)
C(24B)	71(8)	78(7)	46(7)	-19(6)	14(6)	-2(7)
C(25B)	36(5)	70(7)	69(7)	14(6)	14(5)	6(5)
C(26B)	60(8)	42(6)	51(7)	2(5)	6(6)	-4(6)
O(3B)	112(8)	138(10)	148(9)	53(7)	6(7)	8(7)
C(27B)	94(7)	59(8)	75(7)	23(7)	-51(6)	-26(8)
C(28B)	89(6)	49(7)	167(12)	7(8)	-68(7)	-9(6)
C(29B)	81(6)	85(10)	176(12)	43(9)	-75(7)	-7(7)
C(30B)	52(5)	72(9)	62(6)	21(6)	-6(4)	-7(6)
C(31B)	76(6)	65(9)	65(6)	11(6)	10(5)	-8(7)
C(32B)	101(9)	131(14)	94(10)	-2(10)	-48(7)	1(10)
C(33B)	61(7)	108(14)	162(14)	47(12)	-42(8)	-9(8)
C(34B)	70(7)	73(11)	165(13)	45(11)	29(9)	20(8)
C(35B)	106(7)	81(10)	57(7)	7(8)	11(6)	-4(9)
C(36B)	191(12)	51(8)	93(6)	18(6)	-84(7)	-2(7)
C(37B)	166(12)	66(9)	74(6)	-7(7)	-31(7)	-11(8)
C(38B)	57(5)	42(6)	53(5)	-12(5)	-2(4)	23(5)
C(39B)	53(6)	67(9)	95(7)	28(8)	9(5)	10(6)
C(40B)	75(9)	93(10)	114(9)	-16(9)	-17(7)	-31(8)
C(41B)	144(11)	49(7)	70(8)	7(7)	-7(7)	25(8)
C(42B)	110(9)	74(10)	78(7)	11(7)	43(8)	36(8)
C(43B)	82(9)	63(9)	104(8)	-1(8)	25(7)	3(7)
O(4B)	61(5)	66(5)	76(6)	33(4)	5(4)	27(4)

Table 2.26 Hydrogen atom coordinates ($\times 10^4$) and isotropic displacement parameters ($\text{\AA}^2 \times 10^3$) for $\text{Ph}_2\text{P}(\text{O})\text{N}(\text{Et})\text{P}(\text{O})\text{Ph}_2$, dba. H_2O

	x	y	z	U(iso)
H(1A)	3405	7073	5633	67
H(2A)	3714	7891	6348	67
H(3A)	2485	9243	5674 -	133
H(4A)	3675	9156	5217	133
H(5A)	4008	9978	5929	133
H(6A)	9437	10009	6567	79
H(7A)	11623	9281	6857	103
H(8A)	11804	7167	7291	102
H(9A)	9830	5736	7255	82
H(10A)	7602	6357	6874	68
H(11A)	5780	11266	7194	76
H(12A)	4624	11707	8102	81
H(13A)	4153	9762	8681	89
H(14A)	4505	7607	8249	82
H(15A)	5540	7199	7297	68
H(16A)	8413	4718	5485	68
H(17A)	10608	5015	5136	75
H(18A)	11076	6937	4628	73
H(19A)	9584	8634	4553	61
H(20A)	7473	8503	4950	58
H(21A)	3875	4067	4932	67
H(22A)	2327	3564	3934	81
H(23A)	2110	5225	3220	74
H(24A)	3468	7167	3418	80
H(25A)	5211	7730	4329	68
H(26A)	8019	11625	5232	72
H(27A)	8914	11183	4036	65
H(28A)	7208	10223	3193	125
H(29A)	4952	9494	2715	105
H(30A)	3095	10150	3230	101
H(31A)	3432	10957	4332	113
H(32A)	5763	11568	4885	100
H(33A)	9968	12526	6167	72
H(34A)	12647	12556	5865	69

Table 2.26 / Cont.

H(35A)	10560	12910	7212	75
H(36A)	11527	13620	8314	99
H(37A)	13740	14827	8545	108
H(38A)	15196	14834	7758	102
H(39A)	14362	13947	6711	115
H(1B)	9277	7241	992	89
H(2B)	8996	6360	293	89
H(3B)	10341	5088	1018	152
H(4B)	8864	4252	765	152
H(5B)	9136	5132	1467	152
H(6B)	7584	6544	2254	76
H(7B)	9099	6957	3220	82
H(8B)	10556	9172	3423	87
H(9B)	10497	10604	2624	80
H(10B)	8817	10158	1748	66
H(11B)	5293	5749	1685	63
H(12B)	3058	5427	2037	72
H(13B)	1421	7240	1964	65
H(14B)	2099	9199	1523	77
H(15B)	4264	9456	1157	65
H(16B)	3320	4205	173	73
H(17B)	1089	4874	-306	103
H(18B)	850	7045	-592	107
H(19B)	2865	8573	-596	88
H(20B)	5079	7814	-264	63
H(21B)	6979	2816	-577	83
H(22B)	7789	2487	-1587	118
H(23B)	8538	4236	-2044	80
H(24B)	8092	6609	-1636	69
H(25B)	7204	7025	-665	62
H(26B)	4385	12448	1406	133
H(27B)	3920	13053	2589	145
H(28B)	5620	14117	3458	83
H(29B)	7906	14354	3932	139
H(30B)	9732	14156	3352	136
H(31B)	9291	13117	2262	118
H(32B)	6939	12722	1759	99
H(33B)	2731	11765	581	145

Table 2.26 / Cont.

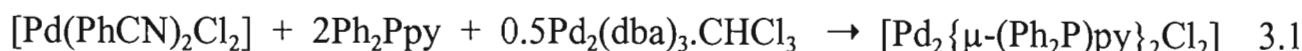
H(34B)	95	11286	51	130
H(35B)	-1663	10202	-52	84
H(36B)	-2450	9460	-1166	121
H(37B)	-939	9571	-1920	107
H(38B)	1376	10383	-1609	100
H(39B)	2103	11445	-563	100

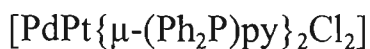
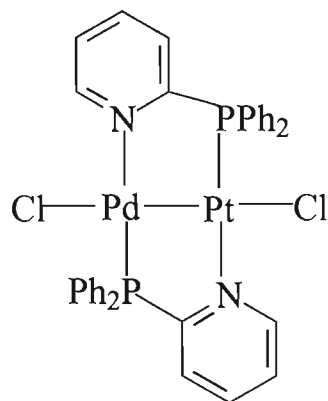
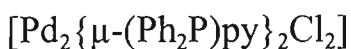
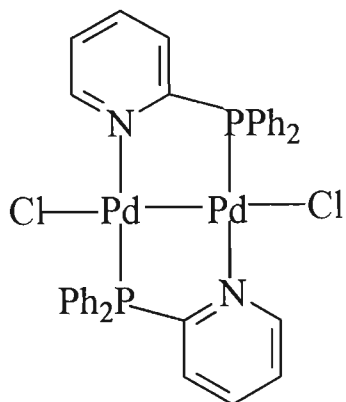
CHAPTER 3

PALLADIUM(II) AND DIPALLADIUM(I) COMPLEXES OF THE PHENYLBIS(2-PYRIDYL)PHOSPHINE LIGAND

3.1 INTRODUCTION

The phenylbis(2-pyridyl)phosphine ligand, $\text{PhP}(\text{py})_2$, is a convenient building block for the construction of mononuclear and dinuclear transition metal complexes⁽⁴¹⁾. Many transition metals preferentially bind through the phosphorus atom to give mononuclear complexes, that are similar in physical properties to their well-known triphenylphosphine analogues. These mononuclear complexes may be employed as metal-containing ligands, that bond to a second metal atom through a pyridine nitrogen, with the concomitant formation of a metal-metal bond. Balch and co-workers have utilized the closely-related 2-(diphenylphosphino)pyridine (Ph_2Ppy) ligand in this approach to the preparation of both homodinuclear and heterodinuclear Pd(I) and Pt(I) complexes. Thus, $[\text{Pd}(\text{PhCN})_2\text{Cl}_2]$ was reacted with 2 moles of Ph_2Ppy to form $[\text{Pd}\{\eta^1\text{-}(\text{Ph}_2\text{P})\text{py}\}_2\text{Cl}_2]$. This complex is further reacted with the zero-valent palladium complex $\text{Pd}_2(\text{dba})_3 \cdot \text{CHCl}_3$ ($\text{dba} = \text{dibenzylideneacetone}$) to afford the dimeric complex $[\text{Pd}_2\{\mu\text{-}(\text{Ph}_2\text{P})\text{py}\}_2\text{Cl}_2]$ as shown in equation 3.1⁽⁴²⁾. Similarly $[\text{Pd}\{\eta^1\text{-}(\text{Ph}_2\text{P})\text{py}\}_2\text{Cl}_2]$ was shown to react with $\text{Pt}_2(\text{dba})_3$ to form $[\text{PdPt}\{\mu\text{-}(\text{Ph}_2\text{P})\text{py}\}_2\text{Cl}_2]$ as shown in equation 3.2.

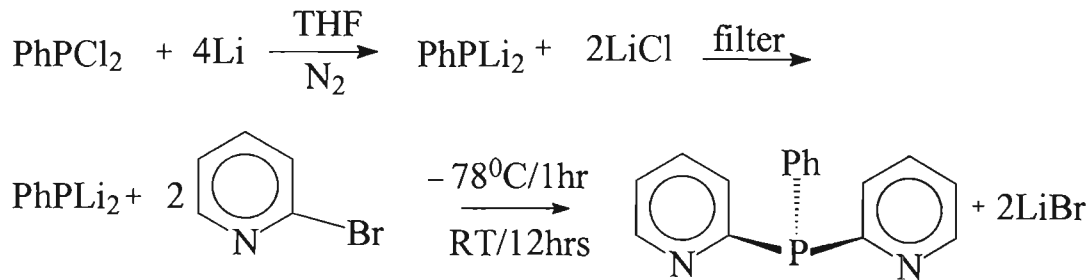




3.2 Results and Discussion

3.2.1 Synthesis of Phenylbis(2-pyridyl)phosphine

The synthesis of the $\text{PhP}(\text{py})_2$ was based on the method used by Newkome⁽⁴³⁾ *et al.* and is outlined in **Scheme 3.1**. There are no reports in the literature of the $\text{PhP}(\text{py})_2$ ligand being previously synthesised using this modified procedure.



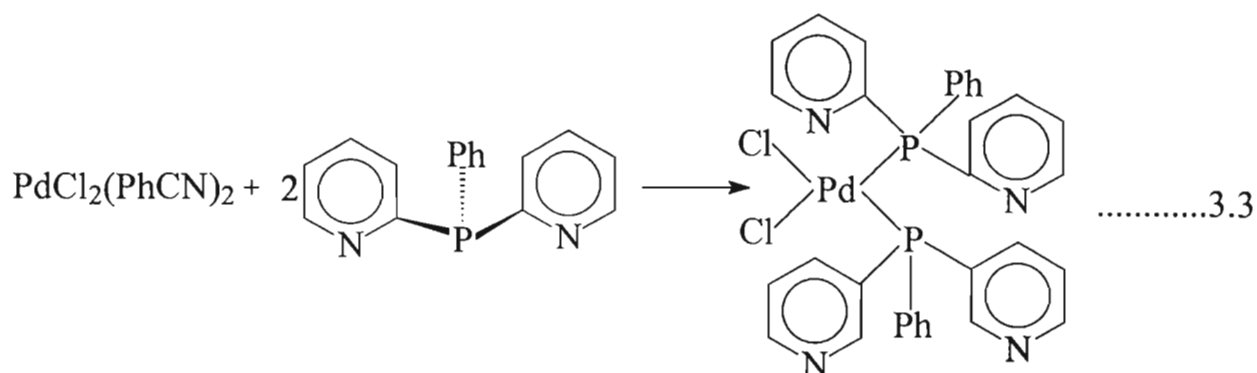
Scheme 3.1: Synthesis of the $\text{PhP}(\text{py})_2$ ligand.

The synthesis of the ligand was performed under an atmosphere of nitrogen, and a white air-sensitive crystalline solid was isolated.

Data obtained from the characterisation of the ligand were in good agreement with that reported in the literature^(43,44) (see **Table 3.2**). The solid state infrared spectrum is, as expected, dominated by modes resulting from vibrations associated with the phenyl moieties and P-C bond vibrations. The ¹H NMR spectrum consists of a broad series of multiplets in the aromatic region ranging from δ 8.6 - 7.2. The ³¹P{¹H} NMR spectrum of PhP(py)₂ shows a sharp singlet at δ -2.0, which is characteristic of these types of ligands^(44,45,46). Elemental analysis is in good agreement with the ligand's formulation (see **Table 3.2**).

3.2.2 Reaction of PhP(py)₂ with [Pd(PhCN)₂Cl₂]

Reaction of [Pd(PhCN)₂Cl₂] with a twice molar amount of PhP(py)₂ in acetonitrile at room temperature for 24 hours was found to afford a product characterised as *cis*-[PdCl₂{ η^1 -PhP(py)₂}] **6** reaction equation 3.3.



This product was isolated as an air-stable light-yellow crystalline compound. The maximum yield (65%) was obtained when the solvent used was acetonitrile and the reaction time was 24 hours. Compound **6** was precipitated by addition of diethylether.

The microanalytical data and spectroscopic data for compound **6** are listed in **Table 3.2**. The solid state infrared spectrum (KBr disc) of *cis*-[PdCl₂{η¹-PhP(py)₂}₂] **6** exhibits the characteristic PhP(py)₂ ligand peaks. The broad peak at δ 29.0 in the ³¹P{¹H} NMR spectrum of **6** is shifted downfield relative to its position in the free ligand, where it is observed as sharp singlet at δ -2.0. This indicates that coordination through the P atom has occurred. The ¹H NMR spectrum of **6** shows a broad series of multiplets ranging from δ 8.3 to 7.1.

Single crystals of **6** were grown by the slow solvent diffusion of diethylether into a dichloromethane solution of the compound, and an X-ray crystal structure analysis confirmed that the structure is indeed *cis*-[PdCl₂{η¹-PhP(py)₂}₂] with the ligand bonded in the monodentate mode (η¹-) through the P-atom. An ORTEP generated representation of the structure is illustrated in **Fig 3.1**. A full list of interatomic distances and angles is given in **Tables 3.5** and **3.6** at the end of this Chapter.

The geometry around the Pd atom is approximately square-planar with the P(1)-Pd-P(2) angle of 100.44(5)° being significantly larger than 90° and the Cl(1)-Pd-Cl(2) angle of 91.92(6)° being close to 90°. The larger P(1)-Pd-P(2) angle is ascribed to steric repulsions between the bulky PhP(py)₂ ligands. The coordination sphere of the palladium in **6** consists of Pd-Cl and Pd-P distances within the normal

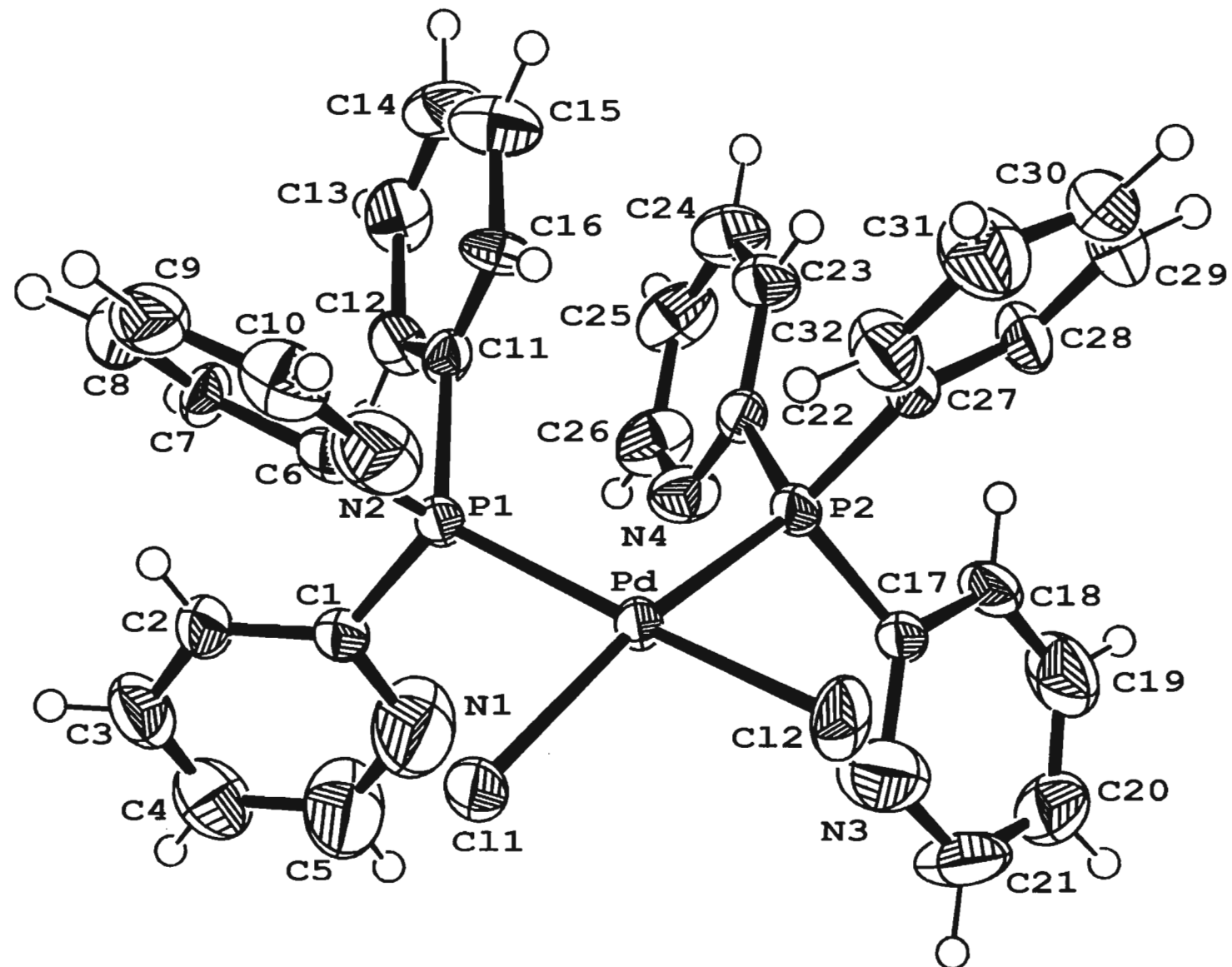


Fig. 3.1: Molecular Structure of *cis*-[PdCl₂{ η^1 -PhP(py)₂}₂] 6

ranges for bonds to palladium (Pd-Cl, 2.356(19) and 2.349(14)Å; Pd-P, 2.248(13) and 2.259(18)Å and are similar to those reported for *cis*-(Ph₃P)₂PtCl₂ (Pt-Cl, 2.333 and 2.355Å; Pt-P, 2.250 and 2.264Å)⁽⁴⁷⁾. The PdCl₂ plane forms a dihedral angle of 14.6° with the PdP₂ plane, indicating a distortion towards tetrahedral geometry.

Compound **6** has been independently synthesised by Newkome *et al*⁽⁴⁸⁾. The IR and NMR spectroscopic results obtained in this work are similar to those reported in the literature⁽⁴⁸⁾. A comparison of the bond lengths and angles between this work and the literature is given in **Table 3.1**. As showed in **Table 3.1** the agreement is excellent.

Table. 3.1 Comparison of selected bond lengths and angles of complex **6** and the literature data of this structure.

Angles(°)	This work	Literature ⁽⁴⁸⁾
Cl(1)-Pd-Cl(2)	91.92(6)	91.86(6)
Cl(1)-Pd-P(1)	83.95(5)	83.91(6)
Cl(2)-Pd-P(2)	85.62(5)	85.82(6)
P(1)-Pd-P(2)	100.44(5)	100.46(6)
Bond lengths(Å)		
Pd-Cl(1)	2.356(19)	2.357(14)
Pd-Cl(2)	2.349(14)	2.348(22)
Pd-P(1)	2.248(13)	2.246(18)
Pd-P(2)	2.259(18)	2.256(13)

3.2.3 Reaction of *cis*-[PdCl₂{η¹-PhP(py)₂}₂] **6** with Pd₂(dba)₃

The reaction of *cis*-[PdCl₂{η¹-PhP(py)₂}₂] with an equimolar amount of Pd₂(dba)₃.CHCl₃ in acetonitrile at room temperature for 24 hours afforded a red product characterised as the dinuclear complex [Pd₂Cl₂{μ-PhP(py)₂}₂] **7**. Compound **7** is precipitated from acetonitrile by addition of diethylether. This product was recrystallised from acetonitrile as an air stable red crystalline compound, soluble in most organic solvents, but insoluble in diethylether and hexane.

Table 3.2 lists the microanalytical data and spectroscopic data for the complex. The phosphorus atom of the ligand is indicated by a ³¹P{¹H} NMR spectrum which gives a broad peak at δ 4.5, which has shifted downfield from its position in the free ligand, where it occurs as a sharp singlet at δ -2.0. The ¹H NMR spectrum of **7** shows multiplets in the region from δ 7.7 to 7.0 for the phenyl ring and pyridine hydrogens. The solid state (KBr disk) infrared spectrum exhibits the characteristic PhP(py)₂ ligand peaks.

In order to determine the exact structure of the dimer complex **7** single crystals suitable for X-ray crystallography were grown by the slow solvent diffusion of diethylether into a dichloromethane solution of **7**. An ORTEP generated representation of the structure is illustrated in **Fig. 3.2** along with the atom numbering scheme. A full list of the interatomic distances and angles is given in **Tables 3.11** and **3.12** respectively, at the end of this Chapter.

As shown in **Fig. 3.2**, the coordination around each Pd atom is completed by phosphorus and nitrogen atoms of PhP(py)₂ ligands *trans*- to each other, as well

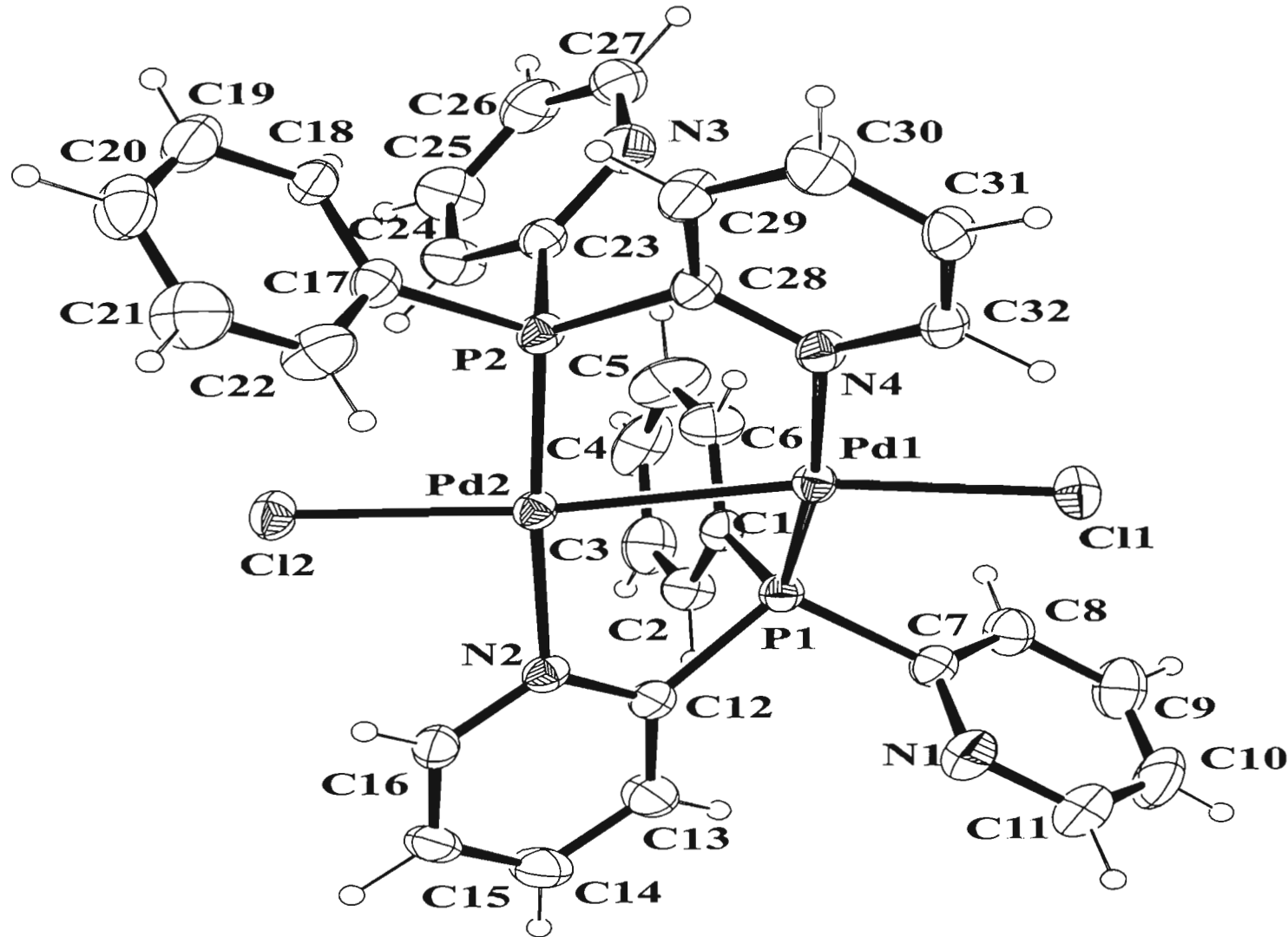


Fig. 3.2: Molecular Structure of $[Pd_2Cl_2\{\mu\text{-PhP}(py)_2\}_2] \ 7$

as by a Cl-atom and the second Pd-atom. The geometry at each Pd atom is approximately square-planar the angles subtended at the Pd atoms by *cis*-disposed atoms ranging from 79.42(4) [P(1)-Pd(1)-Pd(2)] to 95.03(6) $^{\circ}$ [P(1)-Pd(1)-Cl(1)]. The N(4)-Pd(1)-P(1) and N(2)-Pd(2)-P(2) angles of 170.86(12) and 175.29(12) $^{\circ}$ show significant deviations from linearity. Given the short Pd(1)-Pd(2) bond of 2.586(1) \AA , there must be significant non-bonded repulsions within the complex that lead to the non-regular coordination geometry at each Pd-atom. Further evidence for steric effects is the twist around the Pd(1)-Pd(2) bond, as reflected in a N(2)-Pd(2)-Pd(1)-P(1) torsion angle of 33.4 $^{\circ}$ and a N(4)-Pd(1)-Pd(2)-P(2) torsion angle of 28.3 $^{\circ}$. The metal-metal distance of 2.586(7) \AA observed in **7** is comparable to that found for $[\text{Pd}_2(\mu\text{-Ph}_2\text{Ppy})_2\text{Cl}_2]$ [2.594(1) \AA]⁽⁴⁹⁾, and is indicative of a single Pd-Pd bond⁽⁵⁰⁾. The Pd(1)-P(1) and Pd(2)-P(2) distances are 2.2031(15) and 2.186(15) \AA comparable to those reported for $[\text{RhPd}(\mu\text{-Ph}_2\text{Ppy})_2(\text{CO})\text{Cl}_3]$ [Pd-P(1), 2.220(4) and Rh-P(2), 2.243(3)]⁽⁴¹⁾. The Pd(1)-N(4) distance is 2.14(4) \AA and the Pd(2)-N(2) distance is 2.11(4) \AA again distances which are close to literature values^(49,50,51).

3.3 Conclusion

The isolation of compounds **6** and **7** clearly demonstrates that the phenylbis(2-pyridyl)phosphine ligand can coordinate in the monodentate mode (η^1 -) and in the bridging mode (μ -) to the Pd metal atom. Compound **7** is the first example reported of PhP(py)₂ coordinating to Pd in the bridging mode and so stabilising a dinuclear species. As such it extends the type of known modes of coordination that the PhP(py)₂ ligand may adopt when reacted with this transition metal.

3.4 Experimental

3.4.1 Synthesis

General experimental methods are outlined in Appendices A1 and A2. Sources of commercially available chemicals are given in Appendix B.

3.4.1.1: Synthesis of phenylbis(2-pyridyl)phosphine, PhP(py)₂⁽⁴³⁾

To a stirred mixture of lithium Li, (1.40gm; 200 mmol) in anhydrous THF (50 ml) under nitrogen, a solution of freshly distilled dichlorophenylphosphine PhPCl₂, (4ml; 25 mmol) in dry THF (30 ml) was added dropwise over an hour. After the addition was completed and the appearance of a dark red colouration, the solution was refluxed for an additional 2 hours. After cooling to room temperature the solution was filtered. The filtrate was brought to reflux under nitrogen, then a solution of 2-bromopyridine (8.06gm; 50 mmol) in dry THF (20-30 ml) was added dropwise over a 30-minute period, followed by an additional hour of reflux. After cooling to room temperature, the solution was concentrated *in vacuo* and aqueous hydrochloric acid (3N, 50 ml) was added and the mixture then extracted with chloroform. The aqueous layer was neutralised with a dilute sodium carbonate solution. The resultant precipitate was filtered off and recrystallised from petroleum ether (bp 30-60 °C) to afford phenylbis(2-pyridyl)phosphine. Yield: 3.0g (81%).

3.4.1.2: Synthesis of *cis*-[PdCl₂{ η^1 -PhP(py)₂}₂] 6

A solution of the ligand phenylbis(2-pyridyl)phosphine (34 mg; 0.129 mmol) in

acetonitrile (6 ml) was added dropwise to a stirred solution of $[\text{Pd}(\text{PhCN})_2\text{Cl}_2]$ (25 mg; 0.065 mmol) in acetonitrile (6 ml). The resultant mixture was stirred for 24 hours. The colour of the solution changed from orange yellow to light yellow. The volume of acetonitrile was then decreased to *ca.* 2 ml under reduced pressure. Upon addition of diethylether (5 ml) a light yellow crystalline precipitate was obtained. This was filtered, washed with diethylether and dried *in vacuo*. Yield: 30mg (65%).

3.4.1.2: Synthesis of $[\text{Pd}_2\text{Cl}_2\{\mu\text{-PhP(py)}_2\}_2]$ 7

The zero-valent palladium complex $\text{Pd}_2(\text{dba})_3\text{CHCl}_3$ (26 mg; 0.0284 mmol) was added as a solid to a stirred solution of *cis*- $[\text{PdCl}_2\{\eta^1\text{-PhP(py)}_2\}_2]$ 7 (20 mg; 0.0285 mmol) in acetonitrile (15 ml). The mixture was stirred for 24 hours. During the reaction time, the colour of the solution changed from light yellow to red. The volume of acetonitrile was then decreased to *ca.* 5 ml under reduced pressure and the black precipitate (presumably palladium metal) was removed by filtration. A red crystalline precipitate was obtained upon addition of diethylether (10 ml) to the filtrate. This precipitate was filtered, washed with diethylether and dried *in vacuo*. Yield: 20mg (86%).

Table. 3.2 NMR Spectroscopic and microanalytical data for PhP(py)₂ and its complexes

Complex	Infrared Spectrum Data ^a cm ⁻¹	¹ H NMR ^b δ	³¹ P{ ¹ H} NMR ^c δ	Analysis: Found(Calculated)		
				%C	%H	%N
PhP(py) ₂	[1568(m),1560(s)] v(C-Npy) 1476(m),1435(m)] v(P-Cpy,Ph)	8.6-7.2 (m,13H)	-2.0(s)	72.89 (73.00)	4.68 (4.90)	10.21 (10.00)
<i>cis</i> -[PdCl ₂ { η^1 -PhP(py) ₂ } ₂] 6	[1569(m),1541(w)] [1446(m),1423(s)]	8.3-7.1 (m,26H)	29.0(b)	53.92 (54.56)	4.03 (3.69)	7.15 (7.95)
[Pd ₂ Cl ₂ { μ -PhP(py) ₂ } ₂] 7	[1591(m),1519(w)] [14489m],1421(w)]	7.7-7.0 (m,26H)	4.5(s)	47.94 (47.40)	3.37 (3.21)	6.14 (6.91)

a. All spectra run as KBr discs. W = weak, m = medium, s = strong

b. All measured in CDCl₃, m = multiplet

c. All measured in CDCl₃, b = broad, s = singlet

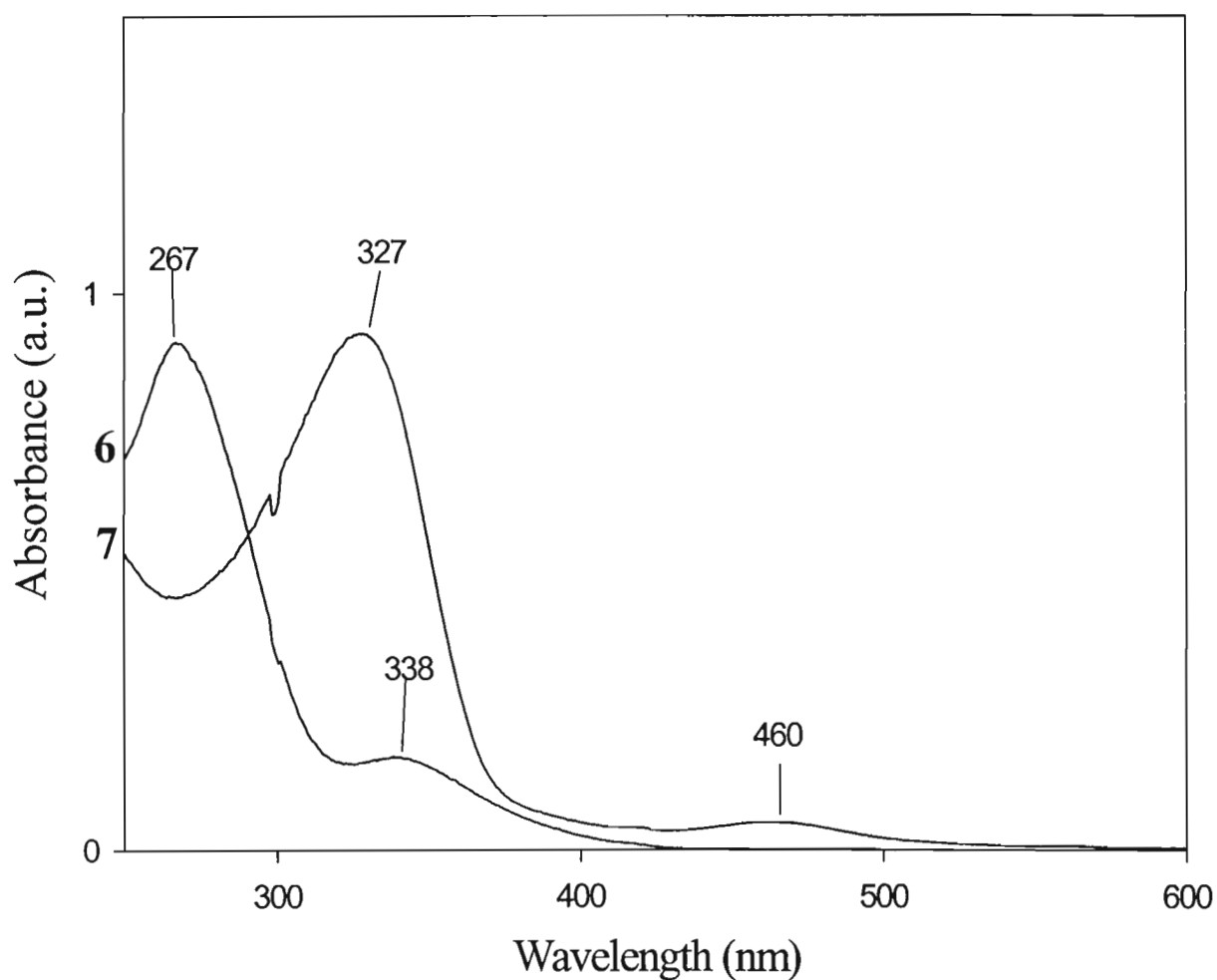


Fig. 3.3: UV/Vis spectra for complexes **6** and **7**

3.4.2. Crystal Structure Determinations

3.4.2.1: X-ray diffraction study of *cis*-[PdCl₂{η¹-PhP(py)₂}₂] 6

Light yellow single crystals 6 were grown by slow vapour diffusion of diethylether into a concentrated solution of 6 in dichloromethane. The general approach used for the intensity data collection and structure solution is described in Appendix A. The crystallographic data are given in Table 3.3, the atomic coordinates in Table 3.4, the anisotropic thermal parameters in Table 3.7, the interatomic distances in Table 3.5 and the interatomic angles in Table 3.6. The hydrogen atom coordinates and isotropic displacement parameters are given in Table 3.8. A list of the observed and calculated structure factors is available on request⁽⁴⁰⁾.

3.4.2.2: X-ray diffraction study of [Pd₂Cl₂{μ-PhP(py)₂}₂] 7

Red rectangular shaped single crystals 7 were grown by slow vapor diffusion of diethyether into a concentrated solution of 7 in dichloromethane. The general approach used for the intensity data collection and structure solution is described in Appendix A. The crystallographic data are given in Table 3.9, the atomic coordinates are given in Table 3.10, the anisotropic thermal parameters in Table 3.13, the interatomic distances in Table 3.11 and the interatomic angles in Table 3.12. The hydrogen atom and isotropic displacement parameters are given in Table 3.14. A list of the observed and calculated structure factors is available on request⁽⁴⁰⁾.

Table 3.3
Crystal Data and Details of the Crystallographic Analysis for
[PdCl₂{η¹-PhP(py)₂}₂] 6

Empirical formula	C ₃₂ H ₂₆ Cl ₂ N ₄ P ₂ Pd
Formula weight	705.81
Temperature	293(2) K
Wavelength	0.71073 Å
Crystal system	Triclinic
Space group	<i>P</i> ī
a(Å)	10.460(4)
b(Å)	11.156(4)
c(Å)	14.647(2)
α(°)	96.24(2)
β(°)	90.39(3)
γ(°)	115.38(4)
V(Å ³)	1532.8(8)
Z	2
Calculated density	1.529 Mg/m ³
Absorption coefficient	0.913 mm ⁻¹
F(000)	712
Crystal size	0.65 x 0.43 x 0.35 mm
Theta range for data collection	2.04 to 22.97 deg.
Index ranges	-11<=h<=11, -12<=k<=12, -2<=l<=16
Reflections collected / unique	5420 / 4248 [R(int) = 0.0126]
Completeness to 2θ = 22.97	100.0%
Max. and min. transmission	0.7405 and 0.5883
Refinement method	Full-matrix least-squares on F ²
Data / restraints / parameters	4248 / 0 / 370
Goodness-of-fit on F ²	1.086
Final R indices [I>2σ(I)]	R1 = 0.0477, wR2 = 0.1301
R indices (all data)	R1 = 0.0530, wR2 = 0.1335
Largest diff. peak and hole	1.423 and -1.042 e.Å ⁻³

**Table 3.4 Atomic coordinates ($\times 10^4$) and equivalent isotropic displacement parameters ($\text{\AA}^2 \times 10^3$) for $[\text{PdCl}_2\{\eta^1\text{-PhP(py)}_2\}]$ 6.
U(eq) is defined as one third of the trace of the orthogonalized
Uij tensor**

	x	y	z	U(eq)
Pd	1502(1)	4348(1)	2402(1)	29(1)
P(1)	2475(1)	2940(1)	1979(1)	28(1)
P(2)	3464(1)	6221(1)	2917(1)	29(1)
Cl(1)	-652(1)	2400(1)	2165(1)	50(1)
Cl(2)	317(1)	5728(1)	2530(1)	53(1)
N(2)	1029(5)	2561(6)	251(4)	64(1)
N(3)	1971(6)	6214(6)	4519(4)	78(2)
N(4)	5075(4)	5435(5)	3847(3)	46(1)
N(1)	2019(9)	2047(7)	3678(4)	101(2)
C(1)	2121(5)	1681(5)	2752(3)	34(1)
C(2)	2001(5)	425(5)	2463(4)	42(1)
C(3)	1763(6)	-476(6)	3087(5)	60(2)
C(4)	1654(8)	-133(7)	3995(5)	78(2)
C(5)	1771(11)	1109(8)	4292(5)	102(3)
C(6)	1823(4)	2144(4)	796(3)	34(1)
C(7)	2275(5)	1241(4)	458(3)	32(1)
C(8)	1937(6)	715(6)	-403(4)	55(2)
C(9)	1165(6)	1049(6)	-994(4)	53(2)
C(10)	717(6)	1997(6)	-668(4)	53(1)
C(11)	4365(4)	3563(4)	1773(3)	29(1)
C(12)	5271(5)	3188(5)	2211(4)	39(1)
C(13)	6642(5)	3638(5)	1912(4)	50(1)
C(14)	7011(5)	4398(6)	1227(4)	54(2)
C(15)	6054(6)	4746(6)	834(4)	54(2)
C(16)	4727(4)	4327(5)	1105(3)	31(1)
C(17)	3190(5)	6858(4)	4076(3)	32(1)
C(18)	4278(6)	7953(5)	4506(4)	50(1)
C(19)	4138(8)	8435(6)	5365(5)	76(2)
C(20)	2921(7)	7859(7)	5815(4)	63(2)
C(21)	1859(7)	6748(7)	5392(4)	73(2)
C(22)	5157(4)	6176(4)	3176(3)	31(1)
C(23)	6392(5)	6879(5)	2771(4)	46(1)

Table 3.4 / Cont.

C(24)	7624(6)	6834(6)	3101(4)	56(2)
C(25)	7567(6)	6108(7)	3800(4)	58(2)
C(26)	6269(6)	5411(6)	4149(4)	55(2)
C(27)	3881(5)	7550(4)	2184(3)	34(1)
C(28)	4861(6)	8804(5)	2495(4)	43(1)
C(29)	5136(7)	9802(6)	1952(5)	60(2)
C(30)	4452(7)	9564(6)	1120(4)	59(2)
C(31)	3505(8)	8303(7)	781(5)	71(2)
C(32)	3216(7)	7269(6)	1332(4)	55(2)

Table 3.5 Interatomic Distances (Å) for [PdCl₂{η¹-PhP(py)}₂] 6

Pd-P(1)	2.2482(13)	Pd-P(2)	2.2594(18)
Pd-Cl(2)	2.3495(14)	Pd-Cl(1)	2.3561(19)
P(1)-C(1)	1.817(5)	P(1)-C(11)	1.833(4)
P(1)-C(6)	1.840(5)	P(2)-C(27)	1.828(5)
P(2)-C(22)	1.832(4)	P(2)-C(17)	1.841(5)
N(2)-C(6)	1.395(7)	N(2)-C(10)	1.395(8)
N(3)-C(17)	1.375(7)	N(3)-C(21)	1.378(8)
N(4)-C(22)	1.331(6)	N(4)-C(26)	1.335(7)
N(1)-C(1)	1.392(8)	N(1)-C(5)	1.394(9)
C(1)-C(2)	1.370(7)	C(2)-C(3)	1.376(8)
C(3)-C(4)	1.363(10)	C(4)-C(5)	1.359(10)
C(6)-C(7)	1.337(6)	C(7)-C(8)	1.311(7)
C(8)-C(9)	1.363(9)	C(9)-C(10)	1.373(9)
C(11)-C(16)	1.318(6)	C(11)-C(12)	1.370(6)
C(12)-C(13)	1.392(7)	C(13)-C(14)	1.337(8)
C(14)-C(15)	1.363(8)	C(15)-C(16)	1.339(7)
C(17)-C(18)	1.348(7)	C(18)-C(19)	1.347(8)
C(19)-C(20)	1.367(10)	C(20)-C(21)	1.341(9)
C(22)-C(23)	1.371(7)	C(23)-C(24)	1.397(8)
C(24)-C(25)	1.360(9)	C(25)-C(26)	1.379(8)
C(27)-C(28)	1.357(7)	C(27)-C(32)	1.362(7)
C(28)-C(29)	1.370(8)	C(29)-C(30)	1.350(9)
C(30)-C(31)	1.362(9)	C(31)-C(32)	1.407(8)

Table 3.6 Interatomic Angles ($^{\circ}$) for $[\text{PdCl}_2\{\eta^1\text{-PhP(py)}_2\}_2]$ 6

P(1)-Pd-P(2)	100.44(5)	P(1)-Pd-Cl(2)	168.36(5)
P(2)-Pd-Cl(2)	85.62(5)	P(1)-Pd-Cl(1)	83.95(5)
P(2)-Pd-Cl(1)	168.93(5)	Cl(2)-Pd-Cl(1)	91.92(6)
C(1)-P(1)-C(11)	105.6(2)	C(1)-P(1)-C(6)	110.4(2)
C(11)-P(1)-C(6)	96.2(2)	C(1)-P(1)-Pd	112.82(15)
C(11)-P(1)-Pd	121.29(15)	C(6)-P(1)-Pd	109.14(15)
C(27)-P(2)-C(22)	105.3(2)	C(27)-P(2)-C(17)	108.0(2)
C(22)-P(2)-C(17)	98.3(2)	C(27)-P(2)-Pd	113.17(16)
C(22)-P(2)-Pd	121.72(15)	C(17)-P(2)-Pd	108.84(15)
C(6)-N(2)-C(10)	117.6(5)	C(17)-N(3)-C(21)	118.7(5)
C(22)-N(4)-C(26)	117.7(4)	C(1)-N(1)-C(5)	118.7(6)
C(2)-C(1)-N(1)	119.9(5)	C(2)-C(1)-P(1)	122.8(4)
N(1)-C(1)-P(1)	117.4(4)	C(1)-C(2)-C(3)	120.0(5)
C(4)-C(3)-C(2)	120.8(5)	C(5)-C(4)-C(3)	119.9(6)
C(4)-C(5)-N(1)	120.7(7)	C(7)-C(6)-N(2)	121.7(5)
C(7)-C(6)-P(1)	116.1(4)	N(2)-C(6)-P(1)	121.9(4)
C(8)-C(7)-C(6)	119.0(5)	C(7)-C(8)-C(9)	124.0(5)
C(8)-C(9)-C(10)	118.0(5)	C(9)-C(10)-N(2)	119.7(5)
C(16)-C(11)-C(12)	123.7(4)	C(16)-C(11)-P(1)	112.3(3)
C(12)-C(11)-P(1)	123.7(4)	C(11)-C(12)-C(13)	116.9(5)
C(14)-C(13)-C(12)	119.7(5)	C(13)-C(14)-C(15)	120.0(5)
C(16)-C(15)-C(14)	121.8(5)	C(11)-C(16)-C(15)	117.9(4)
C(18)-C(17)-N(3)	120.4(5)	C(18)-C(17)-P(2)	117.1(4)
N(3)-C(17)-P(2)	122.4(4)	C(19)-C(18)-C(17)	119.2(5)
C(18)-C(19)-C(20)	122.2(6)	C(21)-C(20)-C(19)	118.2(6)
C(20)-C(21)-N(3)	121.2(6)	N(4)-C(22)-C(23)	123.3(4)
N(4)-C(22)-P(2)	112.0(3)	C(23)-C(22)-P(2)	124.5(4)
C(22)-C(23)-C(24)	117.7(5)	C(25)-C(24)-C(23)	119.8(5)
C(24)-C(25)-C(26)	118.2(5)	N(4)-C(26)-C(25)	123.2(6)
C(28)-C(27)-C(32)	120.9(5)	C(28)-C(27)-P(2)	119.4(4)
C(32)-C(27)-P(2)	119.7(4)	C(27)-C(28)-C(29)	118.9(5)
C(30)-C(29)-C(28)	121.4(6)	C(29)-C(30)-C(31)	120.4(6)
C(30)-C(31)-C(32)	118.6(6)	C(27)-C(32)-C(31)	119.6(5)

Table 3.7 Anisotropic displacement parameters ($\text{\AA}^2 \times 10^3$) for**[PdCl₂{η¹-PhP(py)₂}₂] 6.**

The anisotropic displacement factor exponent takes the form:
-2 Π² [h² a*² U11 + ... + 2 h k a* b* U12]

	U11	U22	U33	U23	U13	U12
Pd	16(1)	21(1)	48(1)	1(1)	5(1)	8(1)
P(1)	20(1)	21(1)	43(1)	4(1)	7(1)	9(1)
P(2)	20(1)	22(1)	43(1)	4(1)	5(1)	7(1)
Cl(1)	20(1)	31(1)	88(1)	-6(1)	12(1)	3(1)
Cl(2)	30(1)	38(1)	97(1)	-5(1)	-2(1)	23(1)
N(2)	48(3)	60(3)	76(4)	12(3)	3(3)	14(3)
N(3)	62(4)	76(4)	75(4)	3(3)	18(3)	12(3)
N(4)	38(2)	58(3)	51(3)	15(2)	11(2)	26(2)
N(1)	168(7)	77(4)	74(4)	26(3)	33(4)	64(5)
C(1)	28(2)	29(2)	45(3)	5(2)	8(2)	11(2)
C(2)	38(3)	32(3)	59(3)	6(2)	9(2)	17(2)
C(3)	51(3)	35(3)	97(5)	19(3)	12(3)	19(3)
C(4)	97(5)	55(4)	89(5)	39(4)	27(4)	33(4)
C(5)	183(10)	71(5)	60(4)	28(4)	37(5)	58(6)
C(6)	15(2)	29(2)	51(3)	4(2)	5(2)	2(2)
C(7)	30(2)	30(2)	41(3)	-3(2)	3(2)	20(2)
C(8)	50(3)	41(3)	69(4)	-3(3)	15(3)	17(3)
C(9)	43(3)	49(3)	48(3)	-3(3)	8(3)	3(3)
C(10)	43(3)	58(4)	46(3)	8(3)	-7(2)	10(3)
C(11)	21(2)	26(2)	41(3)	-3(2)	3(2)	11(2)
C(12)	25(2)	31(2)	64(3)	10(2)	3(2)	13(2)
C(13)	26(3)	49(3)	81(4)	5(3)	-1(3)	23(2)
C(14)	26(3)	71(4)	57(3)	4(3)	12(2)	15(3)
C(15)	35(3)	74(4)	44(3)	17(3)	4(2)	11(3)
C(16)	12(2)	45(3)	36(2)	18(2)	4(2)	10(2)
C(17)	23(2)	25(2)	49(3)	6(2)	9(2)	10(2)
C(18)	49(3)	30(3)	46(3)	-4(2)	16(2)	-4(2)
C(19)	90(5)	40(3)	68(4)	-9(3)	6(4)	3(3)
C(20)	80(5)	65(4)	46(3)	3(3)	16(3)	36(4)
C(21)	51(4)	91(5)	57(4)	-2(4)	27(3)	14(4)
C(22)	22(2)	26(2)	40(3)	-3(2)	2(2)	8(2)

Table 3.7. / Cont.

C(23)	30(3)	43(3)	64(3)	12(3)	14(2)	14(2)
C(24)	26(3)	66(4)	74(4)	11(3)	10(3)	18(3)
C(25)	32(3)	84(4)	59(4)	-7(3)	-4(3)	30(3)
C(26)	55(4)	77(4)	51(3)	15(3)	6(3)	43(3)
C(27)	31(2)	27(2)	45(3)	6(2)	11(2)	14(2)
C(28)	46(3)	25(3)	51(3)	6(2)	2(2)	9(2)
C(29)	71(4)	31(3)	75(4)	13(3)	18(3)	18(3)
C(30)	77(4)	46(3)	63(4)	24(3)	30(3)	31(3)
C(31)	89(5)	68(4)	55(4)	19(3)	1(3)	29(4)
C(32)	71(4)	41(3)	46(3)	8(3)	4(3)	17(3)

Table 3.8 Hydrogen atom Coordinates ($\times 10^4$) and isotropic displacement Parameters ($\text{\AA}^2 \times 10^3$) for $[\text{PdCl}_2\{\eta^1\text{-PhP(Py)}_2\}_2]$ 6.

	x	y	z	U(iso)
H(2)	2081	181	1846	50
H(3)	1676	-1329	2886	72
H(4)	1499	-747	4411	93
H(5)	1684	1336	4911	122
H(7)	2820	990	829	38
H(8)	2243	75	-625	66
H(9)	948	646	-1600	64
H(10)	208	2262	-1058	63
H(12)	4985	2657	2686	47
H(13)	7297	3412	2188	60
H(14)	7920	4689	1018	65
H(15)	6330	5289	365	65
H(16)	4082	4568	830	37
H(18)	5114	8371	4214	60
H(19)	4895	9185	5662	91
H(20)	2832	8227	6398	75
H(21)	1032	6330	5693	87
H(23)	6408	7370	2293	55
H(24)	8482	7299	2842	67
H(25)	8381	6082	4036	69
H(26)	6224	4898	4619	66
H(28)	5338	8982	3068	51
H(29)	5808	10663	2161	72
H(30)	4629	10266	776	71
H(31)	3060	8128	198	85
H(32)	2574	6399	1116	66

Table 3.9
Crystal Data and Details of the Crystallographic Analysis for
[Pd₂Cl₂{μ-PhP(py)₂}₂] 7

Empirical formula	C16.50 H14 Cl2 N2 P Pd
Formula weight	448.57
Temperature	293(2) K
Wavelength	0.71069 Å
Crystal system	Triclinic
Space group	<i>P</i> ̄1
a(Å)	9.7783(17)
b(Å)	12.783(3)
c(Å)	15.267(3)
α(°)	107.836(15)
β(°)	100.511(15)
γ(°)	100.569(16)
V(Å ³)	1726.8(6)
Z	2
Calculated density	0.863 Mg/m ³
Absorption coefficient	0.737 mm ⁻¹
F(000)	444
Crystal size	0.50 x 0.20 x 0.15 mm
Theta range for data collection	2.19 to 22.97 deg.
Index ranges	-10<=h<=10, -14<=k<=13, -2<=l<=16
Reflections collected / unique	6092 / 4783 [R(int) = 0.0167]
Completeness to 2θ = 22.97	99.9%
Absorption correction	Semi-empirical
Max. and min. transmission	0.999 and 0.789
Refinement method	Full-matrix least-squares on F ²
Data / restraints / parameters	4783 / 0 / 432
Goodness-of-fit on F ²	1.006
Final R indices [I>2sigma(I)]	R1 = 0.0412, wR2 = 0.1023
R indices (all data)	R1 = 0.0565, wR2 = 0.1085
Extinction coefficient	No
Largest diff. peak and hole	0.869 and -1.535 e.Å ⁻³

**Table 3.10 Atomic coordinates ($\times 10^4$) and equivalent isotropic displacement parameters ($\text{\AA}^2 \times 10^3$) for $[\text{Pd}_2\text{Cl}_2\{\mu\text{-PhP(Py)}_2\}_2]$ 7
U(eq) is defined as one third of the trace of the orthogonalized
 U_{ij} tensor.**

	x	y	z	U(eq)
Pd(1)	3451(1)	1793(1)	3988(1)	34(1)
Pd(2)	4420(1)	169(1)	3038(1)	34(1)
Cl(1)	2745(2)	3249(1)	5123(1)	55(1)
Cl(2)	5224(2)	-1310(1)	2009(1)	51(1)
P(1)	5772(1)	2453(1)	4680(1)	35(1)
P(2)	2688(1)	112(1)	1880(1)	37(1)
N(1)	6095(6)	3124(5)	6576(4)	60(1)
N(2)	6100(4)	366(4)	4209(3)	35(1)
N(3)	2281(6)	1646(5)	975(4)	59(1)
N(4)	1289(4)	1116(4)	3104(3)	38(1)
C(1)	6856(6)	3121(4)	4048(4)	40(1)
C(2)	8305(6)	3436(5)	4368(4)	49(2)
C(3)	9124(8)	3942(6)	3909(6)	70(2)
C(4)	8481(10)	4135(6)	3114(6)	81(3)
C(5)	7044(11)	3803(7)	2772(6)	87(3)
C(6)	6200(8)	3285(6)	3245(5)	60(2)
C(7)	6267(6)	3533(5)	5868(4)	41(1)
C(8)	6688(7)	4671(5)	6028(5)	53(2)
C(9)	7010(9)	5424(6)	6938(6)	75(2)
C(10)	6888(9)	5034(8)	7671(6)	85(3)
C(11)	6410(8)	3883(7)	7466(5)	72(2)
C(12)	6695(5)	1401(4)	4872(4)	36(1)
C(13)	7927(6)	1598(5)	5568(5)	53(2)
C(14)	8566(7)	729(6)	5592(5)	58(2)
C(15)	7938(6)	-317(6)	4930(4)	49(2)
C(16)	6723(6)	-482(5)	4254(4)	44(1)
C(17)	1943(6)	-1295(5)	927(4)	44(1)
C(18)	1631(6)	-1386(5)	19(4)	47(2)
C(19)	1098(8)	-2412(7)	-667(5)	71(2)
C(20)	842(8)	-3382(7)	-457(6)	76(2)
C(21)	1154(9)	-3293(7)	476(7)	87(3)

Table 3.10 / Cont.

C(22)	1700(8)	-2248(6)	1171(5)	69(2)
C(23)	3177(6)	1041(5)	1237(4)	39(1)
C(24)	4483(7)	1095(6)	993(5)	60(2)
C(25)	4867(8)	1751(7)	474(5)	69(2)
C(26)	3956(8)	2344(6)	200(5)	67(2)
C(27)	2689(8)	2298(5)	449(5)	59(2)
C(28)	1046(5)	415(5)	2201(4)	38(1)
C(29)	-279(6)	-42(6)	1597(5)	55(2)
C(30)	-1472(7)	208(6)	1919(5)	64(2)
C(31)	-1236(6)	910(5)	2830(4)	52(2)
C(32)	140(6)	1358(5)	3399(4)	47(1)
C(33)	2821(9)	3450(7)	7773(7)	93(3)
Cl(3)	1035(4)	3027(4)	7649(3)	193(2)
Cl(4)	3648(3)	4534(2)	8857(2)	113(1)

Table 3.11 Interatomic distances [Å] for $[\text{Pd}_2\text{Cl}_2\{\mu\text{-PhP(Py)}_2\}_2]$ 7

Pd(1)-N(4)	2.147(4)	Pd(1)-P(1)	2.2032(15)
Pd(1)-Cl(1)	2.4241(15)	Pd(1)-Pd(2)	2.5863(7)
Pd(2)-N(2)	2.112(4)	Pd(2)-P(2)	2.1862(15)
Pd(2)-Cl(2)	2.4161(15)	P(1)-C(12)	1.817(5)
P(1)-C(1)	1.825(5)	P(1)-C(7)	1.825(6)
P(2)-C(23)	1.811(6)	P(2)-C(28)	1.834(5)
P(2)-C(17)	1.847(6)	N(1)-C(11)	1.346(9)
N(1)-C(7)	1.361(8)	N(2)-C(12)	1.340(7)
N(2)-C(16)	1.350(7)	N(3)-C(23)	1.355(7)
N(3)-C(27)	1.380(9)	N(4)-C(32)	1.337(7)
N(4)-C(28)	1.345(7)	C(1)-C(2)	1.351(8)
C(1)-C(6)	1.371(8)	C(2)-C(3)	1.359(9)
C(3)-C(4)	1.375(11)	C(4)-C(5)	1.344(12)
C(5)-C(6)	1.397(10)	C(7)-C(8)	1.367(8)
C(8)-C(9)	1.366(10)	C(9)-C(10)	1.372(12)
C(10)-C(11)	1.376(11)	C(12)-C(13)	1.378(8)
C(13)-C(14)	1.377(8)	C(14)-C(15)	1.353(9)
C(15)-C(16)	1.360(8)	C(17)-C(18)	1.328(8)
C(17)-C(22)	1.372(9)	C(18)-C(19)	1.340(9)
C(19)-C(20)	1.365(11)	C(20)-C(21)	1.365(12)
C(21)-C(22)	1.364(10)	C(23)-C(24)	1.390(8)
C(24)-C(25)	1.368(9)	C(25)-C(26)	1.361(10)
C(26)-C(27)	1.357(10)	C(28)-C(29)	1.352(8)
C(29)-C(30)	1.398(8)	C(30)-C(31)	1.354(9)
C(31)-C(32)	1.371(8)	C(33)-Cl(3)	1.687(9)
C(33)-Cl(4)	1.734(9)		

Table 3.12 Interatomic Angles ($^{\circ}$) for $[\text{Pd}_2\text{Cl}_2\{\mu\text{-PhP(py)}_2\}_2]$ 7

N(4)-Pd(1)-P(1)	170.86(12)	N(4)-Pd(1)-Cl(1)	91.62(12)
P(1)-Pd(1)-Cl(1)	95.03(6)	N(4)-Pd(1)-Pd(2)	94.89(12)
P(1)-Pd(1)-Pd(2)	79.42(4)	Cl(1)-Pd(1)-Pd(2)	169.85(4)
N(2)-Pd(2)-P(2)	175.29(12)	N(2)-Pd(2)-Cl(2)	91.00(12)
P(2)-Pd(2)-Cl(2)	93.10(6)	N(2)-Pd(2)-Pd(1)	94.15(11)
P(2)-Pd(2)-Pd(1)	81.65(4)	Cl(2)-Pd(2)-Pd(1)	174.21(4)
C(12)-P(1)-C(1)	102.6(2)	C(12)-P(1)-C(7)	102.2(3)
C(1)-P(1)-C(7)	102.7(3)	C(12)-P(1)-Pd(1)	115.27(18)
C(1)-P(1)-Pd(1)	115.90(19)	C(7)-P(1)-Pd(1)	116.13(18)
C(23)-P(2)-C(28)	105.1(3)	C(23)-P(2)-C(17)	103.0(3)
C(28)-P(2)-C(17)	100.8(2)	C(23)-P(2)-Pd(2)	115.19(18)
C(28)-P(2)-Pd(2)	116.34(18)	C(17)-P(2)-Pd(2)	114.53(19)
C(11)-N(1)-C(7)	117.6(6)	C(12)-N(2)-C(16)	118.1(5)
C(12)-N(2)-Pd(2)	119.2(3)	C(16)-N(2)-Pd(2)	122.2(4)
C(23)-N(3)-C(27)	118.3(5)	C(32)-N(4)-C(28)	116.8(5)
C(32)-N(4)-Pd(1)	123.6(4)	C(28)-N(4)-Pd(1)	119.6(3)
C(2)-C(1)-C(6)	120.4(5)	C(2)-C(1)-P(1)	119.6(4)
C(6)-C(1)-P(1)	119.9(5)	C(1)-C(2)-C(3)	120.2(6)
C(2)-C(3)-C(4)	120.0(7)	C(5)-C(4)-C(3)	120.6(7)
C(4)-C(5)-C(6)	119.4(8)	C(1)-C(6)-C(5)	119.3(7)
N(1)-C(7)-C(8)	122.4(6)	N(1)-C(7)-P(1)	114.8(4)
C(8)-C(7)-P(1)	122.7(5)	C(9)-C(8)-C(7)	118.9(7)
C(8)-C(9)-C(10)	119.9(7)	C(9)-C(10)-C(11)	118.8(7)
N(1)-C(11)-C(10)	122.3(8)	N(2)-C(12)-C(13)	120.8(5)
N(2)-C(12)-P(1)	112.5(4)	C(13)-C(12)-P(1)	126.5(4)
C(14)-C(13)-C(12)	120.3(6)	C(15)-C(14)-C(13)	118.3(6)
C(14)-C(15)-C(16)	119.8(6)	N(2)-C(16)-C(15)	122.5(6)
C(18)-C(17)-C(22)	120.3(6)	C(18)-C(17)-P(2)	120.7(5)
C(22)-C(17)-P(2)	119.0(5)	C(17)-C(18)-C(19)	120.2(7)
C(18)-C(19)-C(20)	121.5(7)	C(19)-C(20)-C(21)	118.6(7)
C(22)-C(21)-C(20)	119.7(8)	C(21)-C(22)-C(17)	119.7(8)
N(3)-C(23)-C(24)	120.5(6)	N(3)-C(23)-P(2)	121.2(4)
C(24)-C(23)-P(2)	118.3(5)	C(25)-C(24)-C(23)	120.1(6)
C(26)-C(25)-C(24)	119.2(7)	C(27)-C(26)-C(25)	120.4(7)
C(26)-C(27)-N(3)	121.4(7)	N(4)-C(28)-C(29)	123.3(5)
N(4)-C(28)-P(2)	113.2(4)	C(29)-C(28)-P(2)	123.4(4)
C(28)-C(29)-C(30)	119.2(6)	C(31)-C(30)-C(29)	117.9(6)

Table 3.12 / Cont.

C(30)-C(31)-C(32)	119.9(6)	N(4)-C(32)-C(31)	122.9(6)
Cl(3)-C(33)-Cl(4)	110.8(5)		

**Table 3.13 Anisotropic displacement parameters ($\text{\AA}^2 \times 10^3$) for
[Pd₂Cl₂{μ-PhP(py)₂}₂] 7.**

The anisotropic displacement factor exponent takes the form:
 $-2 \Pi^2 [h^2 a^{*2} U_{11} + \dots + 2 h k a^* b^* U_{12}]$

	U11	U22	U33	U23	U13	U12
Pd(1)	33(1)	38(1)	35(1)	11(1)	14(1)	11(1)
Pd(2)	32(1)	38(1)	32(1)	10(1)	14(1)	11(1)
Cl(1)	58(1)	45(1)	60(1)	6(1)	23(1)	21(1)
Cl(2)	54(1)	54(1)	47(1)	10(1)	24(1)	21(1)
P(1)	35(1)	36(1)	36(1)	13(1)	14(1)	9(1)
P(2)	31(1)	48(1)	32(1)	11(1)	15(1)	11(1)
N(1)	69(4)	63(3)	49(3)	15(3)	25(3)	15(3)
N(2)	35(2)	41(3)	31(2)	14(2)	15(2)	10(2)
N(3)	59(3)	61(3)	55(3)	13(3)	16(3)	19(3)
N(4)	32(2)	49(3)	38(3)	16(2)	18(2)	11(2)
C(1)	50(3)	33(3)	41(3)	14(3)	23(3)	10(2)
C(2)	40(3)	56(4)	55(4)	24(3)	20(3)	9(3)
C(3)	58(4)	67(5)	81(6)	14(4)	36(4)	9(4)
C(4)	107(7)	64(5)	68(5)	15(4)	55(5)	-9(5)
C(5)	112(7)	84(6)	69(5)	47(5)	26(5)	-3(5)
C(6)	62(4)	65(4)	60(4)	32(4)	18(3)	11(3)
C(7)	36(3)	45(3)	41(3)	13(3)	13(3)	8(3)
C(8)	60(4)	38(3)	56(4)	11(3)	18(3)	10(3)
C(9)	88(6)	43(4)	77(6)	-4(4)	27(4)	10(4)
C(10)	88(6)	85(6)	50(5)	-18(5)	15(4)	21(5)
C(11)	87(5)	80(6)	48(4)	13(4)	25(4)	23(4)
C(12)	35(3)	40(3)	36(3)	15(3)	15(3)	8(2)
C(13)	51(4)	45(3)	52(4)	12(3)	1(3)	10(3)
C(14)	55(4)	62(4)	56(4)	23(4)	1(3)	19(3)
C(15)	54(4)	61(4)	52(4)	35(3)	21(3)	30(3)
C(16)	56(4)	40(3)	40(3)	13(3)	21(3)	17(3)
C(17)	30(3)	55(4)	44(4)	8(3)	17(3)	11(3)
C(18)	49(3)	50(5)	36(4)	6(3)	10(3)	16(3)
C(19)	77(5)	79(6)	47(4)	4(4)	19(4)	23(4)
C(20)	63(5)	60(5)	72(6)	-10(4)	6(4)	9(4)
C(21)	90(6)	53(5)	94(7)	17(5)	7(5)	-7(4)

Table 3.13 / Cont.

C(22)	83(5)	53(4)	56(4)	16(4)	8(4)	-7(4)
C(23)	35(3)	47(3)	37(3)	12(3)	16(2)	10(2)
C(24)	43(3)	88(5)	68(5)	41(4)	33(3)	26(3)
C(25)	54(4)	91(5)	82(5)	45(5)	41(4)	16(4)
C(26)	90(6)	64(4)	50(4)	20(4)	33(4)	10(4)
C(27)	72(5)	47(4)	56(4)	17(3)	14(4)	17(3)
C(28)	26(3)	49(3)	39(3)	12(3)	16(2)	6(2)
C(29)	33(3)	73(4)	43(4)	3(3)	9(3)	7(3)
C(30)	31(3)	81(5)	72(5)	16(4)	18(3)	6(3)
C(31)	38(3)	70(4)	54(4)	16(3)	27(3)	19(3)
C(32)	42(3)	63(4)	42(3)	16(3)	23(3)	22(3)
C(33)	88(6)	89(6)	101(7)	27(5)	28(5)	29(5)
Cl(3)	101(2)	215(4)	191(4)	19(3)	22(2)	-28(2)
Cl(4)	145(2)	90(2)	85(2)	26(1)	4(2)	16(2)

Table 3.14 Hydrogen atom Coordinates ($\times 10^4$) and isotropic displacement Parameters ($\text{\AA}^2 \times 10^3$) for $[\text{Pd}_2\text{Cl}_2\{\mu\text{-PhP(Py)}_2\}_2]$ 7.

	x	y	z	U(iso)
H(1)	8742	3305	4905	58
H(2)	10240(8)	4183(18)	4158(19)	84
H(3)	8970(5)	4450(4)	2850(3)	97
H(4)	6610(4)	3918(13)	2220(5)	105
H(5)	5170(7)	3047(18)	3010(17)	72
H(6)	6753(8)	4920(2)	5540(4)	63
H(7)	7330(3)	6240(7)	7067(12)	90
H(8)	7090(2)	5460(5)	8200(6)	102
H(9)	6292(12)	3600(2)	8000(4)	87
H(10)	8310(3)	2280(5)	6000(3)	63
H(11)	9380(6)	854(11)	6030(3)	70
H(12)	8360(3)	-950(4)	4939(4)	59
H(13)	6340(3)	-1150(5)	3840(3)	53
H(14)	1693(16)	-1120(6)	-47(16)	56
H(15)	916(18)	-2458(8)	-1240(5)	85
H(16)	430(3)	-4160(6)	-990(4)	91
H(17)	1003(17)	-3910(6)	628(17)	104
H(18)	1896(19)	-2184(8)	1780(5)	83
H(19)	5100(5)	680(3)	1182(15)	72
H(20)	5860(7)	1797(7)	288(14)	83
H(21)	4190(2)	2770(4)	-150(3)	81
H(22)	2040(5)	2750(3)	247(15)	70
H(23)	-396(11)	-520(4)	980(5)	66
H(24)	-2430(7)	-110(3)	1510(3)	77
H(25)	-1970(6)	1080(14)	3057(18)	63
H(26)	295(11)	1900(3)	4080(4)	56
H(27)	2990(14)	3724(16)	7240(3)	112
H(28)	3250(3)	2790(4)	7730(7)	112

CHAPTER 4

2,5-BIS(DIPHENYLPHOSPHINO)THIOPHENE AS A BRIDGING LIGAND IN PLANAR COMPLEXES OF PALLADIUM(II)

4.1 INTRODUCTION

The study of the binding of small molecules to the cavity between the two metals in dinuclear complexes continues to attract attention⁽⁵²⁾. Bidentate phosphines have proven to be useful in constructing dinuclear complexes that can have a variety of interactions between the two metal centres. The face-to-face structure of some of these dinuclear complexes is representative of molecules containing two square-planar metal ions. With a ligand such as 2,6-bis(diphenylphosphino)pyridine, $(\text{Ph}_2\text{P})_2\text{py}$, the formation of such a structure would produce a cavity between the two metal atoms⁽⁵²⁾. The reaction of $(\text{Ph}_2\text{P})_2\text{py}$ with $\text{PdCl}_2(\text{cod})$ ($\text{cod} = \text{cyclooctadiene}$) gives the trinuclear complex as shown in Fig. 4.1⁽⁵³⁾.

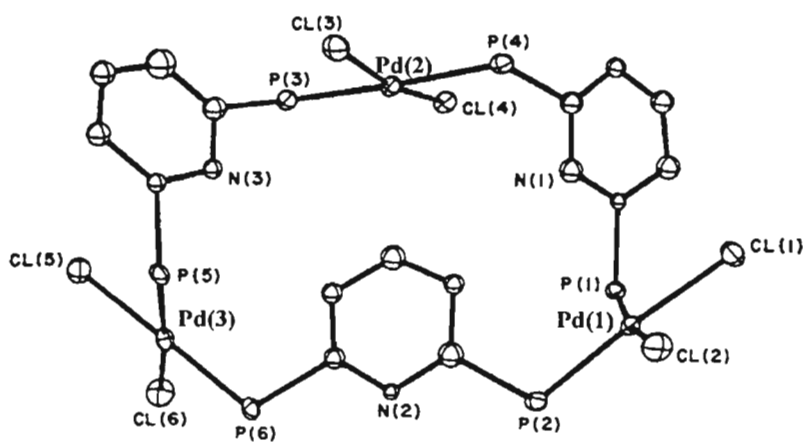


Fig. 4.1 Structure of $[\text{Pd}_3\text{Cl}_6\{\mu-(\text{Ph}_2\text{P})_2\text{py}\}_3]$

In addition $(\text{Ph}_2\text{P})_2\text{py}$ reacts with $\text{PtCl}_2(\text{cod})$ to yield the dimer $[\text{Pt}_2\{\mu-(\text{Ph}_2\text{P})_2\text{py}\}_2\text{Cl}_4]^{(54)}$, with a central 12-membered ring as shown in **Fig. 4.2**. The platinum atoms have square-planar coordination. The nonbonded $\text{Pt} \dots \text{Pt}$ separation is 8.2\AA . The P-py-P portions of the ring are planar and parallel to each other, the perpendicular separation between the planes being 3.01\AA .

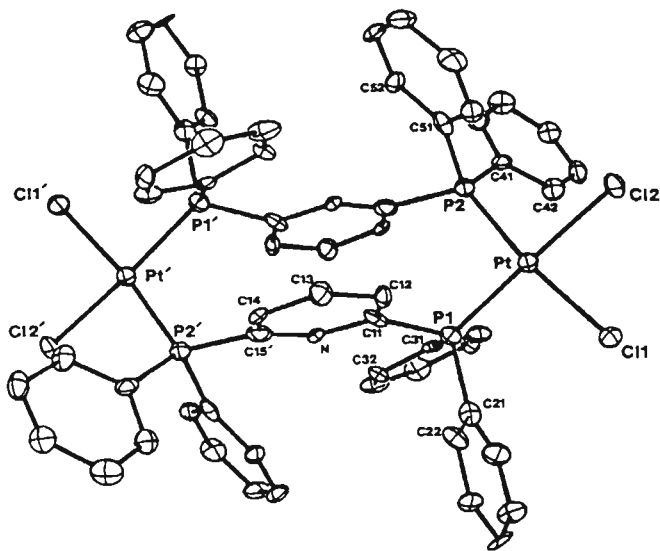


Fig. 4.2: Structure of $[\text{Pt}_2\text{Cl}_4\{\mu-(\text{Ph}_2\text{P})_2\text{py}\}_2]$

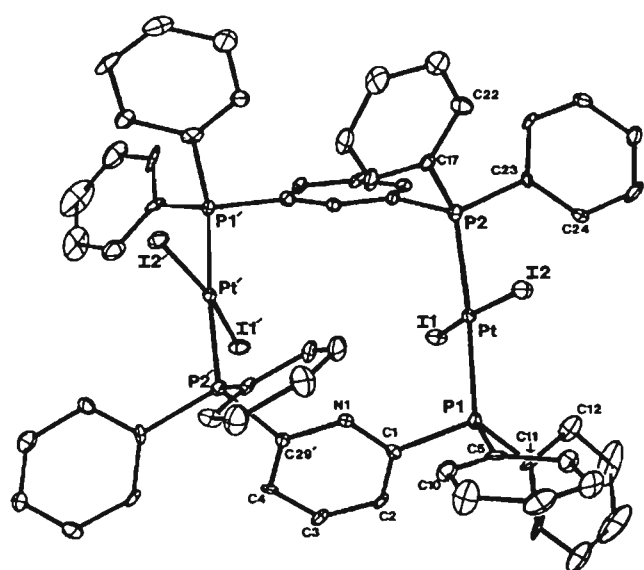
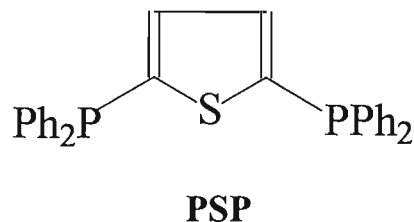


Fig. 4.3 Structure of $[\text{Pt}_2\text{I}_4\{\mu-(\text{Ph}_2\text{P})_2\text{py}\}_2]$

Similarly, the $(\text{Ph}_2\text{P})_2\text{py}$ ligand reacts with $\text{PtI}_2(\text{cod})$ also to afford a dimer, $[\text{Pd}_2\text{I}_4\{\mu-(\text{Ph}_2\text{P})_2\text{py}\}]_2^{(54)}$, with a central 12-membered ring as shown in **Fig. 4.3**. The iodo- complex differs from the chloro-species in that the planar Pt-centres adopt a face-to-face geometry.. The Pt-P distances are longer than in the chloro complex and this is a consequence of the greater *trans*-influence of a phosphino- as compared to a chloro-group; thus the Pt-P bond distances *trans* to phosphorus in $[\text{Pt}_2\text{I}_4\{\mu-(\text{Ph}_2\text{P})_2\text{py}\}]$ [Pt-P(1) 2.307(4) and Pt-P(2) 2.306(5) \AA] are longer than the Pt-P bond distance when it is *trans* to Cl in $[\text{Pt}_2\text{Cl}_4\{\mu-(\text{Ph}_2\text{P})_2\text{py}\}]$ [Pt-P(1) 2.252(7) and Pt-P(2) 2.278(7) \AA]. The Pt...Pt separation is 5.33 \AA . The P-py-P units are planar and the two pyridyl planes are inclined at an angle of 71.9°. A fairly open cavity exists in the centre of the molecule.

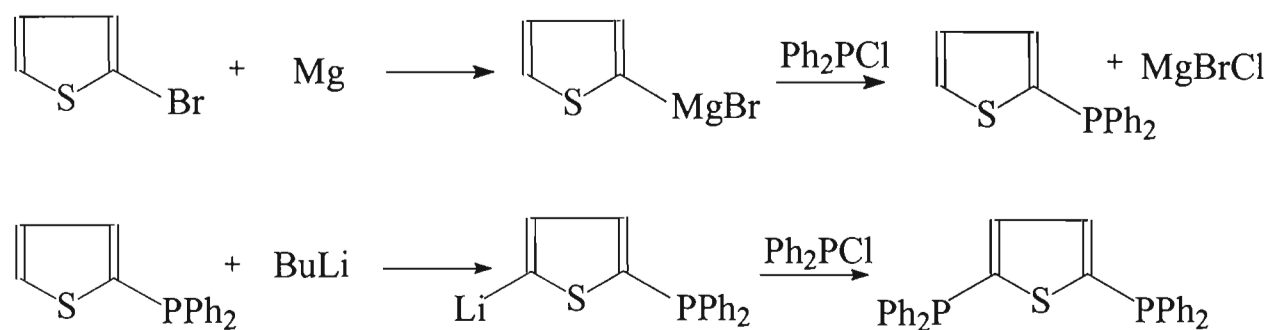
The aim of this part of the work was to produce a PSP ligand-bridged dipalladium(II) complex, hopefully with a face-to-face structure. This expectation is based on the fact that the rigidity of the PCSCP backbone of the ligand prevents it from bonding to a metal in the chelating mode. Thus, this ligand, like $(\text{PPh}_2)\text{py}$, is likely to bridge two well-separated metal centres in this case two square-planar Pd(II) centres.



4.2 Results and Discussion

4.2.1 Synthesis of 2,5-bis(diphenylphosphino)thiophene (PSP)

The synthesis of the $\text{Ph}_2\text{P}(\text{C}_4\text{H}_2\text{S})\text{PPh}_2$, (PSP) was carried out using a method developed by E.Lakoba⁽⁵⁵⁾ and is outlined in **Scheme 4.1**. The PSP ligand was



Scheme 4.1: Synthesis of the $\text{Ph}_2\text{P}(\text{C}_4\text{H}_2\text{S})\text{PPh}_2$ ligand.

synthesised in a two-step procedure. The first step involved the reaction of Mg with 2-bromothiophene and Ph_2PCl to afford 2-diphenylphosphinothiophene (PS). This step proceeded with good yields. In the second step the PS ligand was reacted with BuLi and Ph_2PCl to afford the PSP ligand. There are no reports in the literature of the $\text{Ph}_2\text{P}(\text{C}_4\text{H}_2\text{S})\text{PPh}_2$ being synthesised in this way.

The synthesis of the ligand was performed under an atmosphere of nitrogen, and a white crystalline solid was isolated. The $^{31}\text{P}\{\text{H}\}$ NMR spectrum of $\text{Ph}_2\text{P}(\text{C}_4\text{H}_2\text{S})\text{PPh}_2$ shows a sharp singlet at $\delta = 17.0$. Elemental analysis is in good agreement with the ligand's formulation (see **Section 4.3.1.2**). The spectroscopic data are given in **Table 4.1**.

4.2.2 Reaction of $\text{Ph}_2\text{P}(\text{C}_4\text{H}_2\text{S})\text{PPh}_2$ with $[\text{Pd}(\text{PhCN})_2\text{Cl}_2]$

A twice molar amount of $\text{Ph}_2\text{P}(\text{C}_4\text{H}_2\text{S})\text{PPh}_2$ in dichloromethane was added dropwise to a stirred solution of $[\text{PdCl}_2(\text{PhCN})_2]$ in dichloromethane and the resultant solution heated under reflux for 45 minutes producing an yellow solution. The complex formed was precipitated by the addition of hexane. It is stable to air both in the solid state and in solution. The product was characterised as $[\text{Pd}_2\text{Cl}_4\{\mu\text{-}\text{Ph}_2\text{P}(\text{C}_4\text{H}_2\text{S})\text{PPh}_2\}_2]$ 8 (see below).

The solid state infrared spectrum of 8 indicates the presence of the ligand (PSP) (see **Table 4.1**). Typically bands are observed in the fingerprint region from 500-1600 cm^{-1} . The ^1H NMR spectrum of 8 in CDCl_3 exhibits resonances between δ 7.7 - 7.2 associated with the aromatic rings of the PSP ligand. The $^{31}\text{P}\{^1\text{H}\}$ NMR spectrum of 8 exhibits a broad peak centered at δ 12.7, which is shifted downfield from its position in the free ligand, which shows a sharp singlet at δ -17.0. Such a downfield shift is consistent with the bidentate phosphine ligand adopting a

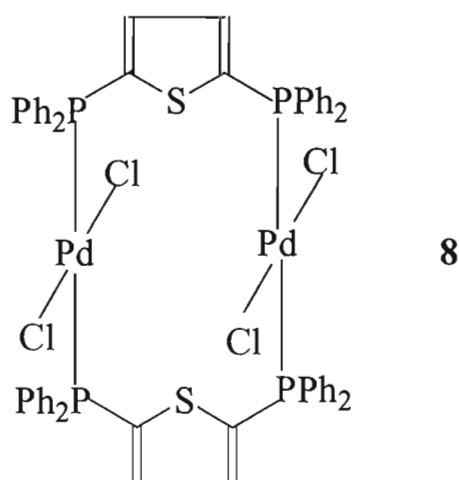


Fig. 4.4: Proposed structure of $[\text{Pd}_2\text{Cl}_4\{\mu\text{-}\text{Ph}_2\text{P}(\text{C}_4\text{H}_2\text{S})\text{PPh}_2\}_2]$ 8

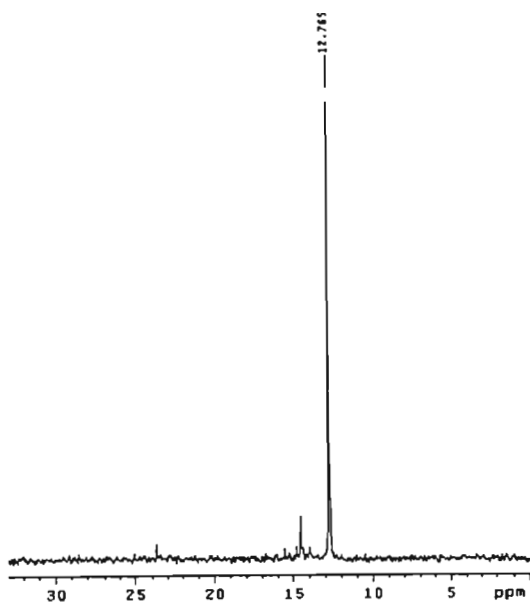


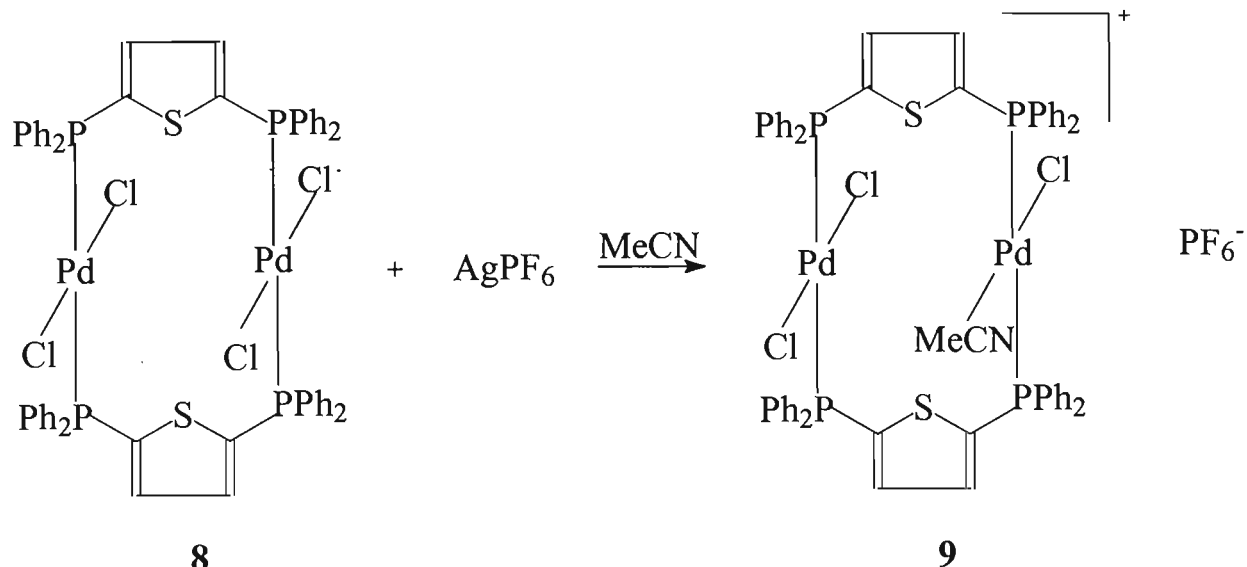
Fig. 4.5: $^{31}\text{P}\{\text{H}\}$ NMR spectrum of $[\text{Pd}_2\text{Cl}_4\{\mu\text{-Ph}_2\text{P}(\text{C}_4\text{H}_2\text{S})\text{PPh}_2\}_2]$ **8**

bridging coordination mode. Elemental analysis for %C, %H, is consistent with the proposed structure for **8**. The proposed structure of **8** is shown in **Figure 4.4**. Unfortunately, repeated attempts to grow single crystals of **8** proved unsuccessful. However, as noted, the PSP ligand is very likely to bridge two well-separated Pd-centres, and thus there is a measure of confidence that the proposed structure is the correct one.

4.2.3 Reaction of $[\text{Pd}_2\text{Cl}_4\{\mu\text{-Ph}_2\text{P}(\text{C}_4\text{H}_2\text{S})\text{PPh}_2\}_2]$ **8** with AgPF_6

The reaction of $[\text{Pd}_2\text{Cl}_4\{\mu\text{-Ph}_2\text{P}(\text{C}_4\text{H}_2\text{S})\text{PPh}_2\}_2]$ **8** with equimolar amount of AgPF_6 in acetonitrile at room temperature for 24 hours produced an orange solution. A orange solid was precipitated by addition of diethylether. This is an air-stable material, soluble in CH_3CN and CH_2Cl_2 . But this solid material decomposes in

light. The proposed formulation of the product is $[\text{Pd}_2\text{Cl}_3(\text{MeCN})\{\mu-\text{Ph}_2\text{P}(\text{C}_4\text{H}_2\text{S})\text{PPh}_2\}_2](\text{PF}_6^-)$ **9** *i.e.*, the reaction is believed to proceed according to the equation shown in **Scheme 4.2**.



Scheme 4.2: Synthesis of $[\text{Pd}_2\text{Cl}_3\{\mu\text{-Ph}_2\text{P}(\text{C}_4\text{H}_2\text{S})\text{PPh}_2\}_2(\text{MeCN})]\text{PF}_6^-$

The solid state infrared spectrum of **9** exhibits a pattern of peaks in the fingerprint region ($500 - 1600 \text{ cm}^{-1}$) indicative of the presence of the PSP ligand; also evident is a strong band at 839 cm^{-1} readily assigned to the anionic PF_6^- group. The $^{31}\text{P}\{\text{H}\}$ NMR spectrum of **9** consists of two single peaks at δ 21.0 and 21.1. The closeness of these two peaks indicates the presence of two phosphorus atoms in the product complex in very similar chemical environments. This is consistent with the structure proposed in **Scheme 4.2**. It is noted that the 4-bond separation between the two chemically distinct P-atoms precludes any coupling between these nuclei. The downfield shift relative to the free ligand is, as noted above, consistent with the bridging mode of coordination for the PSP ligand. The ^1H NMR spectrum of **9** exhibited resonances between δ 7.7 and 7.4 associated with the phenyl rings of the ligand, together with a sharp singlet at δ 2.3 assigned to the methyl group

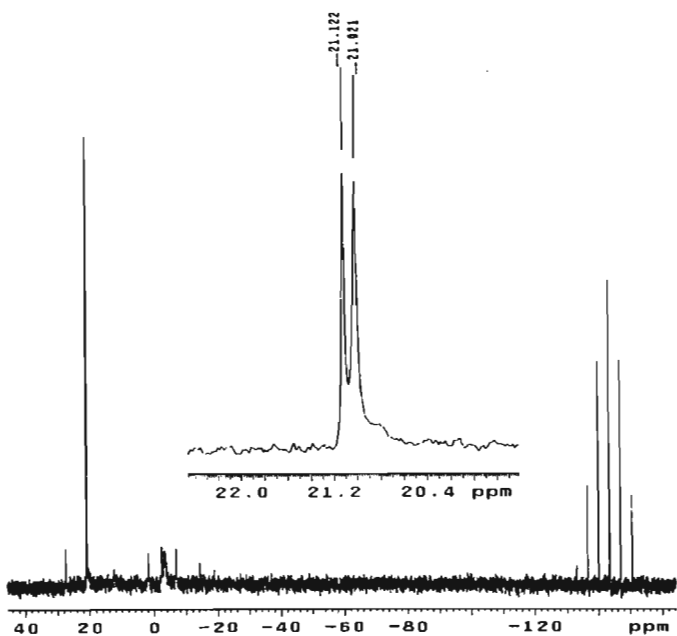


Fig. 4.6: $^{31}\text{P}\{\text{H}\}$ NMR spectrum for $[\text{Pd}_2\text{Cl}_3(\text{MeCN})\{\mu\text{-Ph}_2\text{P}(\text{C}_4\text{H}_2\text{S})\text{PPh}_2\}_2](\text{PF}_6)$ **9**

of the acetonitrile. Unfortunately, the elemental analysis for %C, %H and %N is not entirely consistent with the proposed formula for **9** (see Section 4.3.1.4). However, we favour the proposed structure on the basis of the spectroscopic results. Despite repeated attempts single crystals could not be grown and therefore it was not possible to confirm the above structure by means of a X-ray diffraction study.

4.3 Experimental

4.3.1 Synthesis

General experimental methods are outlined in Appendices A1 and A2. Sources of commercially available chemicals are given in Appendix B.

4.3.1.1: Synthesis of Ph₂P(C₄H₂S), PS⁽⁵⁵⁾

A solution of 2-bromothiophene (8.15g; 50 mmol) in dry ether (60 ml) was added dropwise to a stirred solution of Mg (1.25g; 50 mmol) in dry ether (10 ml). The first 10 ml was added quickly to initiate the reaction. After all the 2-bromothiophene was added, the mixture was gently heated to reflux and left refluxing for about 1.5 hours. The reaction mixture was then cooled down to 0° (ice-water bath). Freshly distilled Ph₂PCl (9ml; 50 mmol) in dry ether (50 ml) was added dropwise into the reaction mixture. The mixture was extracted with ether. The ether extracts were dried over MgSO₄, filtered and evaporated to dryness. An oil was obtained and MeOH (50 ml) was added and the mixture left to solidify. White crystals were filtered off, washed with cold MeOH and dried. These were used without further characterisation.

4.3.1.2: Synthesis of Ph₂P(C₄H₂S)PPh₂, PSP ligand⁽⁵⁵⁾

BuLi (1.1mL; 20 mmol) was added dropwise to a solution of PS (5.36g; 0.020 mmol) in dry THF (40 ml) at 0°C. The mixture was left to stir at room temperature for 2 hours. Freshly distilled Ph₂PCl (3.7mL; 21 mmol) in dry THF (40 ml) was added to the BuLi solution. The addition of Ph₂PCl was carried at 0°C for 30-40 minutes. Stirring was continued for 24 hours. The volume of the THF solution was reduced under vacuum. Dry ether was added and the ether extracts dried over MgSO₄, filtered and evaporated to dryness. A viscous oil was obtained. This was dissolved in acetonitrile and placed in a freezer. White coloured PSP was precipitated out slowly over a period of one month. Calcd for P₂SC₂₈H₂₃: C, 74.20; H, 5.07%. Found: C, 73.68; H, 5.21%.

4.3.1.3: Synthesis of $[\text{Pd}_2\text{Cl}_4\{\mu\text{-Ph}_2\text{P}(\text{C}_4\text{H}_2\text{S})\text{PPh}_2\}_2]$ **8**

A solution of 2,5-bis(diphenylphosphino)thiophene (59.02 mg; 0.130 mmol) in dichloromethane (10 ml) was added dropwise to a stirred solution of $[\text{Pd}(\text{PhCN})\text{Cl}_2]$ (25 mg; 0.065 mmol) in dichloromethane (10 ml). The resultant solution was refluxed at 40–50°C for 45 minutes. After cooling this solution the volume of dichloromethane was decreased to *ca.* 5 ml under reduced pressure. A yellow precipitate was obtained upon addition of hexane (15 ml). This precipitate was filtered, washed with hexane and dried *in vacuo* to give an analytically pure sample. Calcd for $\text{Pd}_2\text{S}_2\text{Cl}_4\text{P}_4\text{C}_{56}\text{H}_{44}$: C, 53.54; H, 3.5%. Found: C, 53.72; H, 3.72%. Yield: 50mg (61%)

4.3.1.4: Synthesis of $[\text{Pd}_2\text{Cl}_3\{\mu\text{-Ph}_2\text{P}(\text{C}_4\text{H}_2\text{S})\text{PPh}_2\}_2(\text{MeCN})](\text{PF}_6)_2$ **9**

A solution of AgPF_6 (50 mg; 0.039 mmol) in acetonitrile (6 ml) was added dropwise to a stirred solution of $[\text{Pd}_2\text{Cl}_4\{\mu\text{-Ph}_2\text{P}(\text{C}_4\text{H}_2\text{S})\text{PPh}_2\}_2]$ **8** (10 mg; 0.039 mmol) in acetonitrile (6 ml). The solution changed from cloudy yellow to a clear orange yellow colour. The mixture was stirred for 24 hours, and the white precipitate of the AgCl filtered off. The volume of acetonitrile was decreased to *ca.* 4 ml under reduced pressure. An orange yellow precipitate was isolated and recrystallised from acetonitrile/ether solution to afford a yellow crystalline product. The precipitate was then washed with diethyl ether and dried *in vacuo*. Calcd for $\text{Pd}_2\text{Cl}_2\text{N}_6\text{P}_5\text{F}_6\text{S}_2\text{C}_{68}\text{H}_{62}$ (complex **9** with PF_6^- as counterion and $5\text{CH}_3\text{CN}$): C, 51.01; H, 3.87; N, 4.37%. Found: C, 51.92; H, 4.92; N%, 1.0. Yield: 10mg (39%)

Table 4.1: Infrared and NMR data for $\text{Ph}_2\text{P}(\text{C}_4\text{H}_2\text{S})\text{PPh}_2$ and its complexes

Complex	Infrared Spectroscopic Data ^a cm^{-1}	^1H NMR ^b δ	$^{31}\text{P}\{^1\text{H}\}$ NMR δ
$\text{Ph}_2\text{P}(\text{C}_4\text{H}_2\text{S})\text{PPh}_2$	534(m),699(vs), 744(vs),819(s),964(w), 1433(s),1475(s) 1583(m)	7.7-7.1 (m,22H)	-17.0(s)
$[\text{Pd}_2\text{Cl}_4\{\mu\text{-}\text{Ph}_2\text{P}(\text{C}_4\text{H}_2\text{S})\text{PPh}_2\}]$ 8	533(m),690(vs), 813(w),1014(s) 1097(s),1184(w), 1434(vs),1481(m)	7.7-7.2 (m,22H)	12.7(s)
$[\text{Pd}_2\text{Cl}_3\{\mu\text{-}\text{Ph}_2\text{P}(\text{C}_4\text{H}_2\text{S})\text{PPh}_2\}_2]\text{.MeCN}(\text{PF}_6)_2$ 9	557(s),692(vs), 1384(vs),1437(m) [839(vs) $\nu(\text{P-F})$]	7.7-7.4 (m,44H) 2.3(s,3H)	21.0(s),21.1(s)

a. All infrared spectra run as discs. W = weak, m = medium, s = strong, vs = verystrong

b. $\text{Ph}_2\text{P}(\text{S})\text{PPh}_2$ and **8** run in CDCl_3 , **9** run in CD_3CN , m = multiplet, s = singlet

c. $\text{Ph}_2\text{P}(\text{S})\text{PPh}_2$ and **8** run in CDCl_3 **9** run in CD_3CN , s = singlet

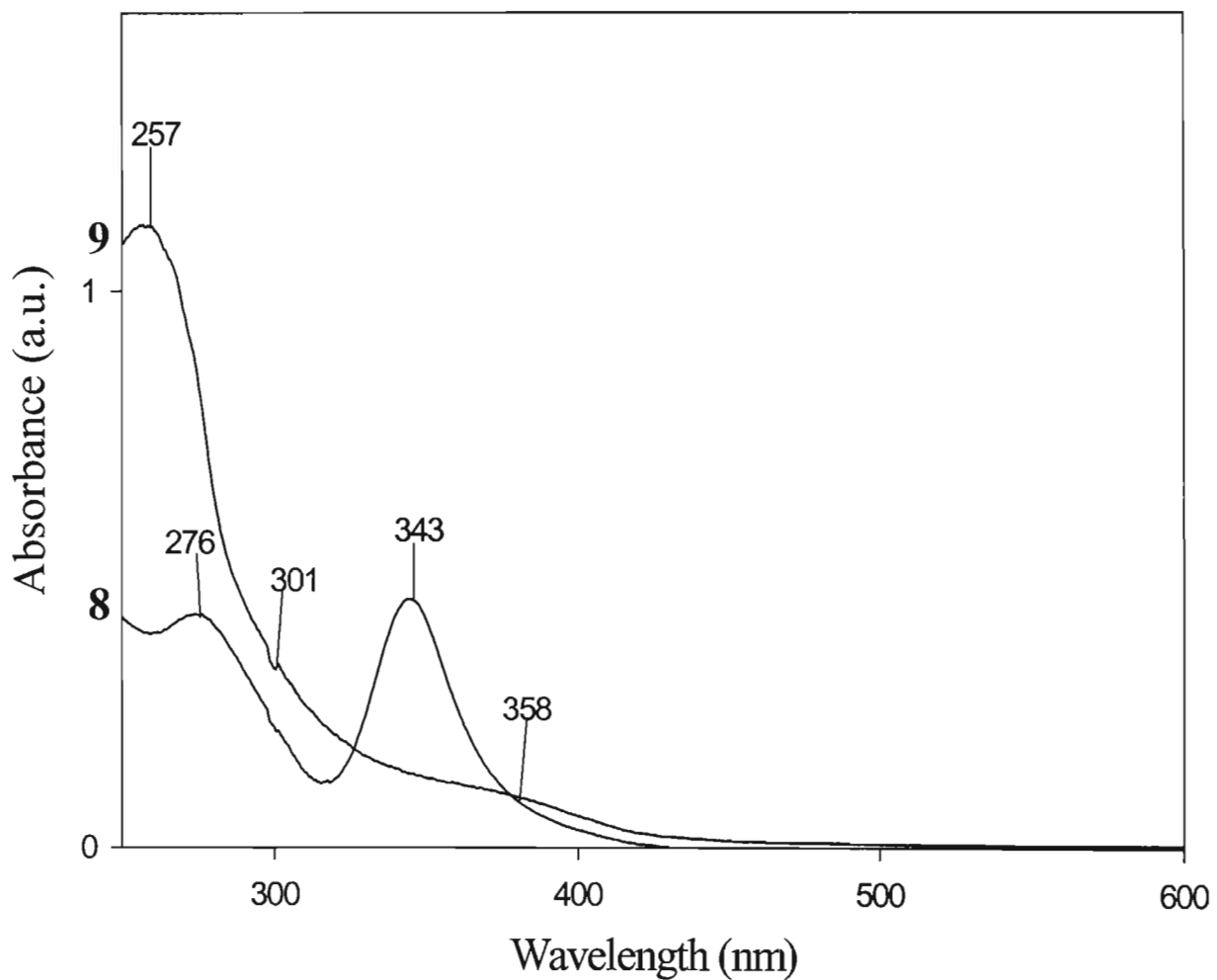


Fig. 4.7 UV/Vis spectra for complexes **8** and **9**

APPENDIX A

General Experimental Details

A.1. INSTRUMENTATION

Carbon, hydrogen and nitrogen analyses were performed by the Microanalytical Laboratory of the Department of Chemistry and Chemical Technology at the University of Natal (Pietermaritzburg) and by Galbraith Laboratories, Knoxville, Tennessee, U.S.A.

$^{31}\text{P}\{\text{H}\}$ NMR and ^1H NMR spectra were recorded on either a Varian Gemini, Varion Unity Inova or Varian FT-80 spectrometer.

Deuterated solvents were employed in all cases.

Mass spectra were recorded on a Hewlett-Packard HP5988A gas chromatographic mass spectrometer.

Infrared spectra were recorded as KBr disks using a Shimadzu Fourier Transform IR 1400 spectrometer.

A.2. EXPERIMENTAL TECHNIQUES

All reactions unless otherwise stated, were performed under an atmosphere of nitrogen using standard Schlenk techniques. All solvents were freshly distilled and dried before use using standard procedures⁽⁵⁶⁾.

A.3. Crystal Structure Determinations

A.3.1 DATA COLLECTION

The intensities of the reflections were measured at 22°C with an Enraf-Nonius CAD-4 Diffractometer utilising graphite monochromated Mo-K_α radiation.

Cell constants were obtained by fitting the setting angles of 25 high-order reflections ($\theta > 12^\circ$). Three standard reflections were measured every hour to check on any possible decomposition of the crystal. An ω -2θ scan with a variable speed up to a maximum of 5.49°.min⁻¹ was used. The ω angle changed as $a_\omega + b_\omega \tan\theta$ (°) and the horizontal aperture as $a_h + b_h \tan\theta$ (mm), but was limited to the range 1.3 to 5.9 mm. The vertical slit was fixed at 4 mm. Optimum values of a_ω , b_ω , a_h and b_h were determined for each crystal by a critical evaluation of the peak shape for several reflections with different values of θ using the program OTPLOT (Omega-Theta plot; Enraf-Nonius diffractometer control program, 1988). Where applicable, a linear decay correction was applied using the mean value linear curves fitted through three intensity control reflections, measured at regular time intervals. Data were corrected for Lorentz and polarization effects, and where possible for absorption by the psi-scan (Semi-empirical) method⁽⁵⁷⁾.

A.3.2 STRUCTURE SOLUTION AND REFINEMENT

The phase problem was solved by utilising direct methods or the Patterson function. Once a suitable phasing model was found, successive applications of Fourier and difference Fourier techniques allowed the location of the remaining non

hydrogen atoms. All structures were refined using weighted full-matrix least-squares methods; the weighting schemes are defined as follows:

$$R1 = \Sigma |F_o - F_c| / \Sigma F_o$$

$$wR2 = \{ \Sigma [w(F_o^2 - F_c^2)]^2 / \Sigma (wF_o^2)^2 \}^{1/2}$$

$$w = 1.0 / [\sigma^2(F_o^2) + (0.1000^*P)^2 + 0.00^*P]$$

$$\text{where } P = (F_o^2 + 2F_c^2) / 3$$

$$GooF = \{ \Sigma [w(F_o^2 + F_c^2)^2] / (n - P) \}^{1/2}$$

The program OSCAIL, which facilitates the direct use of SHELXS-97⁽⁵⁸⁾, SHELXL-97/2⁽⁵⁹⁾ and ORTEX⁽⁶⁰⁾, was used for structure solution, structure refinement and in labelling atoms in a three dimensional peak plot (generated by ORTEX) respectively for a paperless structure determination. Hydrogen atoms were placed in calculated positions using a riding model and refined isotropically. Mean plane and torsion angle calculations, and the tabulation of fractional coordinates, thermal parameters, interatomic distances and angles was achieved using SHELX-97⁽⁵⁸⁾. Ortep was used for the plots⁽⁶¹⁾.

APPENDIX B

SOURCES OF CHEMICALS

The following chemicals were all purchased from the indicated supplier and were used without further purification.

Chemical	Source	% (Purity)
AgPF ₆	Fluka	99.5
Br-thiophene	Acros	99.5
n-butyl lithium	Merck	99.5
2-bromopyridine	Aldrich	99.5
chlorodiphenylphosphine	Strem	98
dichlorophenylphosphine	Fluka	98
ethyl amine	Aldrich	99.5
iodine	Saarchem	99.5
Li metal	Saarchem	99.9
Mg	Merck	99
MgSO ₄	Saarchem	99
NH ₄ Cl	Saarchem	99
Pd(PhCN) ₂ Cl ₂	Strem	99
triethyl amine	distilled	Saarchem
		98

The starting materials Pd₂(dba)₃.CHCl₃⁽³⁹⁾ were prepared according to literature procedure.

REFERENCES

1. N. Kuhn and M. Winter, *J. Org. Chem.*, 1982, **229**, C33-C36.
2. O. J. Scherer, R. Walter and W. S. Sheldrick., *Angew. Chem. Int. Ed. Engl.*, 1985, **24**, No. 6, 525.
3. H. Schmidbaur, S. Lauteschläger and B. Milewski-Mahrla, *J. Org. Chem.*, 1983, **254**, 59-68.
4. M. Gómez, G. Muller, J. Sales and Solans, *J. Chem. Soc., Dalton Trans.*, 1993, 221.
5. C. S. Browning, R. A. Burrow, D. H. Farrar and A. H. Mirza, *Inorganica Chemica Acta*, 1998, **271**, 112-118.
6. N. N. Greenwood and A. Earnshaw, *Chemistry of the Elements*, Pergamon. Oxford, 1984, p. 827.
7. J. Browning, G. W. Bushnell and K. R. Dixon, *J. Org. Chem.*, 1980, **198**, C11.
8. C. S. Browning, D. H. Farrar and D. C. Frankel, *Acta Cryst.*, 1992, **C48**, 806-811.
9. H. Noth and E. Fluch, *Z. Naturforsch. Teil B*, 1984, **39**, 744-753.
10. R. P. Kamalesh Babu, S. S. Krishnamurthy and M. Nethaji, *Polyhedron*, 1996, **15**, 2689-2699.
11. R. P. Kamalesh Babu, S. S. Krishmurthy and M. Nethaji, *Tetrahedron*, 1995, **6**, No. 2, 427-438.
12. Ozawa, F. Kubo, E. Yanagi, K. Moriguchi K., *Organometallics*, 1993, **12**, 4188.
13. R. Uson, J. Fornies, R. Navarro, M. Tomas, C. Fortuño and J. I. Cebollada, *Polyhedron*, 1989, **8**, No. 8, 1045-1052.

14. C. Scott Browning, D. H. Farrar, D. C. Frankel, J. J. Vittal, *Inorganica Chimica Acta.*, 1997, **254**, 329-338.
15. T. E. Krafft, C. I. Hejna and J. S. Smith, *Inorg. Chem.*, 1990, **29**, 2682.
16. P. Espinet, J. Fornies, C. Fortuno, G. Hidalgo, F. Martinez, M. Tomas and A. J. Welch, *J. Org. Chem.*, 1986, **317**, 105.
17. J. R. Boehm, D. J. Doonam and A. L. Balch, *J. Am. Chem. Soc.*, 1976, **98**, 4845.
18. M. S. Balakrishna, S. S. Krishnamurthy, R. Murugaval, M. Nethaji and I. I. Mathews, *J. Chem. Soc., Dalton Trans.*, 1993, 477.
19. M. Bochmann, I. Hawkins, M. B. Hursthouse and R. I. Short, *Polyhedron*, 1987, **6**, 1987.
20. C. S. Browning and D. H. Farrar, *J. Chem. Soc., Dalton Trans.*, 1995, 521.
21. P. Bhattacharyya, R. N. Sheppard, A. M. Z. Slawin, D. J. Williams and J. Derek Woollins, *J. Chem. Soc., Dalton Trans.*, 1993, 2393.
22. J. Ellermann, P. Gabold, C. Schelle, F. A. Knoch, M. Moll and Walter Bauer, *Z. Anorg. Allg. Chem.*, 1995, **621**, 1832-1843.
23. C. Scott Browning and D. H. Farrar, *J. Chem. Soc., Dalton Trans.*, 1995, 2005.
24. D. H. Farrar and N. C. Payne, *J. Org. Chem.*, 1981, **220**, 251-270.
25. J. T. Mague and Zhaiwei Lin, *Organometallics*, 1992, **11**, 4139-4150.
26. J. H. Letcher, and J. R. Van Wazer, *Top. Phosphorus Chem.* 1967, **5**, 1; J. F. Nixon, Personal Communication.
27. D. G. Gorenstein, *J. Am. Chem. Soc.* 1975, **97**, 898.
28. L. S. Benner and A. L. Balch, *J. Am. Chem. Soc.*, 1978, 6099.
29. R. J. Puddephatt, *Chem. Soc. Rev.*, 1983, **12**, 99.
30. M. S. Balakrishna, V. S. Reddy, S. S. Krishnamurthy, J. F. Nixon, J. C. T. R.

- Burckett St. Laurent, *Coord. Chem. Rev.*, 1994, **129**, 1.
31. G. Ewart, A. P. Lane, J. McKechnie and D. S. Payne, *J. Chem. Soc.*, 1964, Part II, 1543.
32. G. Ewart, D. S. Payne, and A. P. Lane, *J. Chem. Soc.*, 1962, 3984.
33. J.A. A. Mokuolu, D. S. Payne, J. C. Speakman, *J. Chem. Soc., Dalton Trans.*, 1973, 1443.
34. D. P. Freyburg, J. L. Robins, K. N. Raymond and J. C. Smart, *J. Am. Chem. Soc.*, 1979, **101**, 892.
35. K. Aparna, S. S. Krishnumurthy and M. Nethaji, *J. Chem. Soc., Dalton Trans.*, 1995, 2991-2997.
36. K. Bokolo, A. Courtois, J. -J. Delpuech, E. Elkaim, J. Protas, D. Rinaldi, L. Rodehäuser and P. R. Rubini, *J. Am. Chem. Soc.*, 1984, **106**, 6333.
37. R. U. Kirss and R. Eisenberg, *Inorg. Chem.*, 1989, **28**, 3372.
38. G. K. Anderson, M. Lin, A. Sen and E. Gretz, *Inorganic Syntheses*, 1990, **28**, 60-62.
39. J. J. Bonnet and James A. Ibers, *J. Org. Chem.*, 1974, **65**, 253-266.
40. J. S. Field, School of Chemical and Physical Sciences, Private Bag X01, Pietermaritzburg, South Africa. E-mail: fieldj@nu.ac.za
41. J. P. Farr, M. M. Olmstead and A. L. Balch, *Inorg. Chem.*, 1983, **22**, 1229-1235.
42. A. Maisonnat, J. P. Farr and A. L. Balch, *Inorg. Chim. Acta.*, 1981, **53**, L217.
43. G. R. Newkome and D. C. Hager, *J. Org. Chem.*, 1978, **43**, 947.
44. I. Mitteil, H. Schmidbaur and Y. Inoguchi, *Z. Naturforsch.*, 1980, **35b**, 1329.
45. R. Ziessel, *Tetrahedron Letters*, 1989, **30**, 493.
46. F. G. Mann and J. Watson, *J. Org. Chem.*, 1948, **13**, 502.
47. T. J. Shapley, Henly, J. R. Rheingold, A. L. Balch, *J. Org. Chem.*, 1986, **310**,

55.

48. G. R. Newkome, W. D. Evans and R. F. Fronczek, *Inorg. Chem.*, 1987, **26**, 3500-3506.
49. A. Maisonet, J. P. Farr, M. M. Olmstead, C. T. Hunt and A. Balch, *Inorg. Chem.*, 1982, **21**, 3961-3967.
50. F. A. Cotton, G. Wilkinson, C. A. Murillo and M. Bochmann, *Advanced Inorg. Chem.*, 1999, 6th Edition.
51. J. P. Farr, F. E. Wood and A. L. Balch, *Inorg. Chem.*, 1983, **22**, 3387-3393.
52. S. Shieh, D. Li, S. Peng and C-M Che, *J. Chem. Soc., Dalton Trans.*, 1993, 195.
53. F. E. Wood, M. M. Olmstead and A. L. Balch, *J. Am. Chem. Soc.*, 1983, **105**, 6332-6334
54. F. E. Wood, Janhvoslef, Håkon Hope and A. L. Balch, *Inorg. Chem.*, 1984, **23**, 4309-4315.
55. E. Lakoba, PhD thesis, University of Natal, 2001
56. W. L. F. Armarego, D. D. Perrin and D. R. Perrin, Purification of Laboratory Chemicals, 2nd ed. Pergamon Press, New York, 1980.
57. F. S. Mathews, A. C. T. North and D. C. Phillips, *Acta Crystallogr., Sect. A.*, 1968, **24**, 351.
58. G. M. Sheidrick, *Acta Cryst. A*, 1990, **46**, 467.
59. G. M. Sheldrick, T. R. Schneider, "SHELXL: High-Resolution Refinement", *Methods in Enzymology*, 1997, **277**, 319.
60. P. McArdle, *J. Appl. Cryst.*, 1995, **28**, 65.
61. C. K. Johnson, M. N. Burnett ORTEPIII, Report ORNL-6895, Oak Ridge National Laboratory, 1996.